Ollscoil na hÉireann, Corcaigh

THE NATIONAL UNIVERSITY OF IRELAND, CORK

Coláiste na hOllscoile,

Corcaigh

UNIVERSITY COLLEGE CORK

Cork Cancer Research Centre

Optimisation of immune effector function within the tumour microenvironment

Thesis presented by

William L Byrne, BPharm., MPSI

Under the supervision of

Dr. Mark Tangney

for the degree of

Doctor of Philosophy

April 2013

Cancer represents a leading of cause of death in the developed world, inflicting tremendous suffering and plundering billions from health budgets. The traditional treatment approaches of surgery, radiotherapy and chemotherapy have achieved little in terms of cure for this deadly disease. Instead, life is prolonged for many, with dubious quality of life, only for disease to reappear with the inevitable fatal outcome. "Blue sky" thinking is required to tackle this disease and improve outcomes. The realisation and acceptance of the intrinsic role of the immune system in cancer pathogenesis, pathophysiology and treatment represented such a "blue sky" thought. Moreover, the embracement of immunotherapy, the concept of targeting immune cells rather than the tumour cells themselves, represents a paradigm shift in the approach to cancer therapy.

The harnessing of immunotherapy demands radical and innovative therapeutic endeavours – endeavours such as gene and cell therapies and RNA interference, which two decades ago existed as mere concepts. This thesis straddles the frontiers of fundamental tumour immunobiology and novel therapeutic discovery, design and delivery. The work undertaken focused on two distinct immune cell populations known to undermine the immune response to cancer – suppressive T cells and macrophages. Novel RNAi mediators were designed, validated and incorporated into clinically relevant gene therapy vectors – involving a traditional lentiviral vector approach, and a novel bacterial vector strategy.

Chapter 2 deals with the design of novel RNAi mediators against FOXP3 – a crucial regulator of the immunosuppressive regulatory T cell population. Two mediators were tested and validated. The superior mediator was taken forward as part of work in chapter 3.

Chapter 3 deals with transposing the RNA sequence from chapter 2 into a DNA-based construct and subsequent incorporation into a lentiviral-based vector system. The lentiviral vector was shown to mediate gene delivery *in vitro* and functional RNAi was achieved against FOXP3. Proof of gene delivery was further confirmed *in vivo* in tumour-bearing animals.

Chapter 4 focuses on a different immune cell population – tumour-associated macrophages. Non-invasive bacteria were explored as a specific means of delivering

gene therapy to this phagocytic cell type. Proof of delivery was shown *in vitro* and *in vivo*. Moreover, *in vivo* delivery of a gene by this method achieved the desired immune response in terms of cytokine profile.

Overall, the data presented here advance exploration within the field of cancer immunotherapy, introduce novel delivery and therapeutic strategies, and demonstrate pre-clinically the potential for such novel anti-cancer therapies.

I hereby declare that I am the sole author of this thesis. This work has not been submitted for another degree, either at University College Cork or elsewhere.

I authorise University College Cork to lend and photocopy this thesis to other institutions or individuals for the purpose of scholarly research.

_____

William Byrne

I would like to take this opportunity to extend my sincere gratitude to Dr. Mark Tangney. Although this project was foisted upon him with little remaining in terms of time and money he played an enormous part in bringing about a successful conclusion.

To all the members of the Cork Cancer Research Centre both within the lab and the development office, both past and present, I extend warm thanks. In particular I would like to acknowledge the substantial contributions of Drs. Tracey O' Donovan, Patrick Forde and Michelle Nyhan who gave generously of their time and expertise throughout this project. Mike Bourke and Marcel de Kruijf were an ever-present repository of scientific and sporting knowledge which greatly enhanced the overall experience. The unwavering support of Dr. Declan Soden is also gratefully acknowledged.

I also wish acknowledge the collective contribution of the PhD Scholars Programme in Cancer Biology which provided a platform for the completion of this work. In particular I would like to thank the members of my thesis committee; Professors Rosemary O'Connor and Tommie McCarthy and Dr. Orla Barry for their continued support and guidance throughout this project. Dr. Kellie Dean also played an invaluable role throughout the duration of the entire programme and for this I am very grateful.

Lastly, but by no means least I applaud my initial supervisor Professor Gerry O' Sullivan (RIP). From the moment he accepted me as a PhD candidate, through all the erratic phone calls at unsociable hours and lengthy discussions on science and sport (including cricket) there was never a harsh word. He brought a light-heartedness and perspective to science that framed even the most disappointing of results in bright lights. I will always have tremendous respect for this man and all that he achieved.

AAV	Adeno-associated virus
ADCC	Antibody-dependent cell-mediated cytotoxicity
ALA	Aminolevulinic Acid
APC	Antigen presenting cell
ARTC1	Antigen recognised by T_{Reg} cells 1
bp	Base pair
B16OVA	B16 melanoma tumour over-expressing the "OVAlbumin" antigen
CDC	Complement-dependent cytotoxicity
CEA	Carcinoembryonic antigen
CFU	Colony forming unit
cm	centimetre
CMV	Cytomegalovirus
COX-2	Cyclooxygenase-2
CTAG2	Cancer/testis antigen 2
CTLA-4	Cytotoxic T-Lymphocyte Antigen 4
DC	Dendritic cell
DMEM	Dulbecco's Modified Eagle Medium
DNA	Deoxyribonucleic Acid
EDTA	Ethylenediaminetetracetic Acid
FACS	Fluoresence-activated cell sorting
FBS	Foetal Bovine Serum
FLuc	Firefly luciferase reporter gene
FOXP3	Forkhead box P3
Gfi-1	Growth factor independent 1
GFP	Green fluorescent protein
h	hour
HER2	Human Epidermal Growth Factor Receptor 2
hFOXP3	Human FOXP3
hsa-miR-31	*Homo sapien* microRNA-31
HSPs	Heat shock proteins
IDO	Indoleamine 2,3-dioxygenase
IFN	Interferon

IGRP	islet-specific glucose-6-phosphatase catalytic subunit related protein
IL	Interleukin
IκB	inhibitor of kappa B
IKKβ /IKK2	inhibitor of kappa B kinase β
IKK2-DN	inhibitor of kappa B kinase β –dominant negative (kinase deficient)
i.p.	Intra-peritoneal
IRF-4	Interferon regulatory factor 4
i.t.	Intra-tumoural
Luc	luciferase
MCS	Multiple cloning site
MDSCs	Myeloid-derived suppressor cells
mFOXP3	Mouse FOXP3
MHC	Major histocampatibility complex
min	Minute
miR-31	Mature microRNA-31
miRNA	microRNA
mKC	Mouse keratinocyte chemoattractant
ml	millilitre
mmu-miR-31	*Mus musculus* microRNA-31
MOI	Multiplicity of infection
mRNA	Messenger RNA
MUC-1	Mucin 1
NFκB	nuclear factor kappa-light-chain-enhancer of activated B cells
NOD	Non-obese diabetic
OD_{600}	Optical density at 600 nanometres
PBS	Phosphate buffered saline
PCR	Polymerase chain reaction
PD-L1	Programmed cell death 1 ligand 1
PE	phycoerythrin
RNA	Ribonucleic acid
RNAi	RNA interference
RPMI	Roswell Park Memorial Institute

s	second
s.c.	Sub cutaneous
SEM	Standard error of the mean
shRNA	Short hairpin RNA
siRNA	Small interfering RNA
TAMs	Tumour-associated macrophages
TCR	T cell receptor
TGF-β	Transforming growth factor β
TLR	Toll-like receptor
T_{Regs}	Regulatory T cells
TU	Transducing unit
VEGF	Vascular endothelial growth factor
UTR	Untranslated region
wt	Wild-type
µl	microlitre
°C	Degrees Celsius

Sections from this chapter have been published as

"Targeting regulatory T cells in cancer". Byrne WL, Mills KH, Lederer JA, O'Sullivan GC. *Cancer Res* Nov 2011: 71; 6915. Review. PMID 22068034

&

"Use of Optical Imaging to advance novel therapies to the clinic". Byrne WL, De Lille A, Kuo C, de Jong JS, van Dam GM, Francis KP, Tangney M. *J Control Release* 2013. *In press*. Review.

The immune system and cancer are inextricably linked. Most tumours develop in the face of normal immune function and anti-tumour responses of varying strength result. A strong immune response against the primary tumour is associated with clearance and induced dormancy of metastatic cancer cells, with a resulting enhanced prognosis. Conversely, global immune deficiencies secondary to disease or therapy are thought to be associated with an increased frequency, earlier recurrence, more rapid progression of tumours and poorer prognosis [1]. Responses to chemotherapy and oncolytic virotherapy may in part be immune-determined and there is persuasive evidence that an intact immune system, specifically determined by $CD4^+$ T cells, is required for sustained tumour regression following oncogene inactivation therapies [2].

Immune evasion is now considered a hallmark of cancer that results from both passive and active tolerising conditions which subvert anti-tumour immune responses [3]. Passive tolerisation may result from down-regulation of MHC Class I expression on the tumour cells and/or low antigenicity secondary to immune editing and selective cell growth. Other tolerising mechanisms involve inhibition of immune cells in the tumour domain by depletion of tryptophan by the enzyme 2, 3 indoleamine dioxygenase (IDO). Active tolerisation involves suppression of anti-tumour cell-mediated responses by tumour infiltrating regulatory T cells (T_{Regs}) and myeloid derived suppressor cells [4].

Surmounting the immune suppression that exists within solid tumours would break the body's immune tolerance of the cancer, and, either alone or in combination with immuno-stimulatory strategies, improve patient outcomes.

1.1.1.1 The rationale for Immune Therapy of Cancer

There is renewed optimism that many cancers can be cured or forestalled by immune-based therapies, used either alone or as part of multimodal programmes.

This originates from an improved understanding of tumour immune interactions and the availability of gene, cell and ligand-based technologies which promote effector anti-tumour responses. The majority of immune therapy strategies for cancer seek to mobilise the adaptive arm of the immune system either directly by manipulating T or B lymphocytes or indirectly by undermining suppressive components within the immune system. The rational for such strategies derives from the adaptive anti-tumour immune responses that result. These responses are both tumour antigen-specific and durable.

Adaptive anti-tumour immune responses are acquired through the integrated intercellular responses of the innate and adaptive immune systems [5] (figure 1.1, centre). Tumour infiltrating T cells, especially $CD8^+$ cytotoxic T lymphocytes (CTLs) and IFNγ-secreting $CD4^+$ (Th1) cells, are central to effective immune containment. Adaptive immune responses are initiated when cells of the innate immune system (NKT, γδ T, NK and macrophages) are recruited to the tumour microenvironment - the continued process of tumour remodelling results in the shedding of cancer cells and debris with a consequent induction of inflammatory signals. The production of IFN-γ (initially from NK and NKT cells) appears critical as it creates a positive feedback loop by inducing some tumour cell death, the further activation of NK cells and macrophages and the production of chemokines and cytokines which are also tumouricidal and anti-angiogenic. Immature dendritic cells (DCs) are activated following uptake of tumour debris/antigens and migrate to the regional lymph nodes where they present the tumour antigens to naive T cells, which can differentiate into Th1, Th2, Th17 or regulatory T cells (T_{Regs}) depending on the cytokine environment. Th1 cells can license DCs to induce tumour-specific CTLs by cross presentation of antigen on MHC class I. Antigen-specific $CD8^+$ T cells traffic to the tumour where cell-mediated killing of tumour cells is augmented by Th1 and Th17 derived cytokines.

However these effector responses can be inhibited by T_{Regs}, and tumour-associated macrophages (TAMs), induced by or recruited to the growing tumour [6]. This thesis review focuses on these two cell types, T_{Regs} and TAMs, which act as mediators of tumour immune suppression.

1.1.1.2 Immune Suppression by T_{Regs}

T_{Regs} are considered to be the most powerful inhibitors of anti-tumour immunity and the greatest barrier to successful immunotherapy [7]. In the early stages of cancer, T_{Regs} are concentrated in the tumour mass, resulting in concomitant immunity, whereby the primary tumour can progress due to local inhibition of effector immune responses, but metastatic cells are eliminated by uninhibited systemic anti-tumour immune responses. In advanced stage disease or for poorly immunogenic cancers there are increased T_{Regs} systemically and absence of concomitant anti-tumour immunity [8]. While a correlation between increased T_{Reg} number and survival, either negative or positive, remains equivocal, the ratio of T_{Reg} to $T_{effector}$ cells in the tumour mass seems to have greater prognostic significance [9].

There are a number of subtypes of T_{Reg} [9], including natural $CD4^+$ T_{Regs} (nT_{Regs}) which originate in the thymus, express CD25, FOXP3, CTLA-4, LAG3 and GITR and suppress innate and adaptive immune cells. Induced $CD4^+$ T_{Regs} (iT_{Regs}) control immune responses to tissue antigens, including tumour antigens and include $CD4^+$ nT_{Reg}-like, Tr1 and Th3 cells that suppress through production of IL-10 and TGF-β. The iT_{Regs} develop in the periphery following engagement of the TCR of naïve T cells and under the influence of innate IL-10 and TGF-β. Their cell-surface markers are often indistinguishable from those of nT_{Regs} and they differ principally in their mechanism of suppression. Although less well characterised, there are also populations of natural and induced $CD8^+$ T_{Regs}.

While the field is still in its infancy, evidence is emerging that inhibition of T_{Regs} may help in tumour containment, especially when combined with appropriate immunotherapies that activate effector T cells. Systemic T_{Reg} depletion in patients induced regression of melanoma metastases [10] and in mice when combined with immunogene stimulation of intra-tumoural immune effector cells resulted in cure of 90% of animals who had large and weakly immunogenic sarcomas [11]. The clinical objective will be to provide sustained reduction of T_{Reg} function, particularly in the tumour environment, allowing enhancement of anti-tumour effector functions and with minimal risk of developing systemic autoimmune diseases.

1.1.2.1 Current approaches to T_{Reg} modulation

Regulatory T cell depletion (figure 1.1 A)

Depletion strategies are not T cell subset-specific but have a selective advantage when the T_{Reg} accumulation provides functional dominance in the tumour environment. T_{Reg} depletion strategies have focused on monoclonal antibodies or ligand-directed toxins targeted to a T_{Reg} cell surface receptor such as CD25 (IL-2 receptor α chain). Daclizumab and basiliximab are anti-CD25 antibodies which invoke cell death by cytokine deprivation (IL-2) and also by triggering antibody-dependent cell-mediated cytotoxicity (ADCC) or complement-dependent cytotoxicity (CDC). Results from an ongoing clinical trial have shown that Daclizumab reduces T_{Regs} and thereby enhances cytotoxic T lymphocyte responses to tumour antigen induced by vaccination[12].

Denileukin diftitox (Ontak®) is a fusion protein of human IL-2 and the enzymatically active and membrane-translocating domains of diphtheria toxin. After binding to CD25 and internalisation, release of the toxin is cytocidal. Clinical data on the use of Ontak® for alternative indications has led to its application for CD25 targeting of T_{Regs} and the emergence of similar CD25-targeted immunotoxins LMB-2 and RFT5-SMPT-dgA. With one exception, Ontak® depleted T_{Reg} numbers, albeit transiently, with T_{Reg} nadirs persisting for less than 3 weeks [12]. The T_{Reg} elimination was mirrored by a concomitant increase in the prevalence of IFN-γ^+CD3^+ T cells in the blood and *de novo* appearance of melanoma antigen-specific $CD8^+$ T cells [10]. However the clinical benefits were modest. Regression of melanoma metastases in five out of sixteen patients represents the most promising outcome [10]. Consistency of response is an issue as two patients who developed antigen-specific T cells failed to show any tumour regression and another study in melanoma patients failed to yield a single objective clinical response [12].

Ontak® is the subject of numerous clinical trials but to date fails to realise its clinical promise. Since CD25 is also expressed on activated $T_{effector}$ cells, Ontak® may also restrain protective anti-tumour immune responses. Ontak® transiently depleted various T subsets including tumour antigen-specific $CD8^+$ T cells [10]. Its indiscriminate effects on $CD4^+CD25^-$cells are difficult to rationalise.

Low-dose oral metronomic cyclophosphamide induced a profound, selective reduction in T_{Regs} and restored T and NK cell function in advanced cancer patients [13]. This invoked temporary disease stabilisation in a number of patients without clinical improvement. The mechanism underpinning its selective toxicity towards T_{Regs} is unexplained. Metronomic cyclophosphamide also has anti-angiogenic and direct cytotoxic effects, which contribute to tumour stabilisation or shrinkage.

Depleting T_{Regs} may have further consequences aside from an unintended treatment-mediated elimination of activated $T_{effector}$ cells [14]. Their depletion leads to an increase in tumour-mediated $T_{effector}$ to T_{Reg} conversion with a diminution in anti-tumour immune responses. This does not seem to occur with the other T_{Reg} modulation approaches.

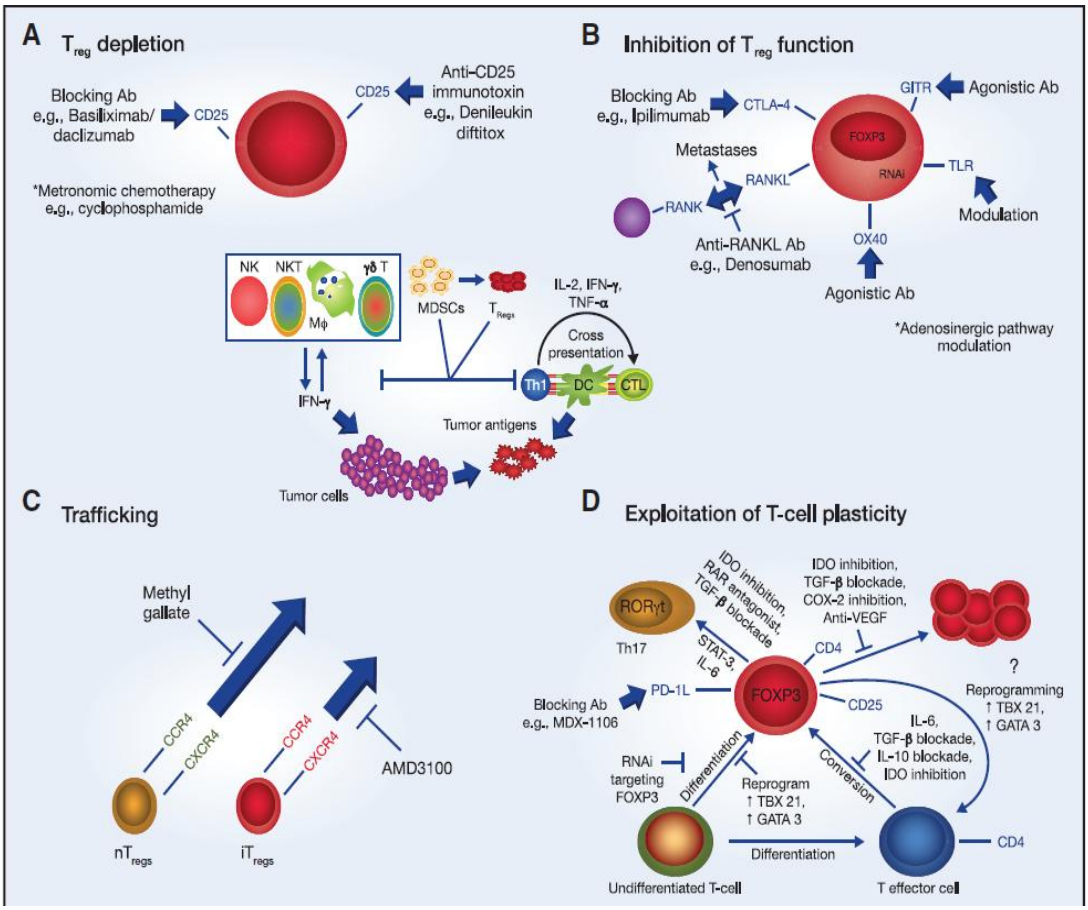

Figure 1.1: Targeting regulatory T cells in cancer. The central schematic depicts the main events involved in mounting an immune response to a tumour. Cells of both the innate and adaptive systems contribute (further details are provided in the text). T_{Regs} offer substantial resistance to this immune assault and thus four different approaches for reducing their immunosuppressive contribution are advanced (A, B, C and D); depletion, inhibition of function, blockade of trafficking and modulation of T cell plasticity. Within each approach numerous existing and novel options for therapeutic manipulation are forwarded. Ab – antibody; DC – dendritic cell; IDO - indoleamine 2,3-dioxygenase; MDSCs – myeloid-derived suppressor cells; T_{Reg} – regulatory T cell. (From [15]).

Suppression of T_{Reg} function (figure 1.1 B)

Similar to CD25, CTLA-4 is not exclusively expressed on T_{Regs} – it is also found on activated $CD4^+$ and $CD8^+$ T cells [9]. CTLA-4 inhibits antigen priming of $T_{effectors}$ by competing with CD28 for the costimulation of CD80/CD86 on APCs. Furthermore, it induces IDO in DCs [16]. The consequent depletion of tryptophan and production of tryptophan metabolites, such as kynurenines and picolinic acid, inhibit $T_{effector}$ proliferation and function. The anti-CTLA-4 antibodies ipilimumab (MDX-010) and tremelimumab (CP-675206) are currently undergoing clinical evaluation. Ipilimumab, as monotherapy or in combination with peptide vaccination improved survival in patients with previously treated metastatic melanoma [17]. Tremelimumab promotes anti-tumour responses but recently these have been shown to result from $T_{effector}$ activation rather than T_{Reg} modulation [18]. This may also be true of Ipilimumab as its clinical mode of action has yet to be fully defined and could be ascribed to direct effects on either $T_{Regs,}$ $T_{effectors}$ or a combination.

The glucocorticoid-induced TNF receptor (GITR) is constitutively expressed on T_{Regs} but also at lower levels on activated $T_{effectors}$. Intra-tumoural injection of an agonistic antibody to GITR (DTA-1) invoked potent anti-tumour immunity and eradicated established tumours in mice [19]. The exact mechanism by which this approach achieves its effects is controversial. One study showed that the benefit of DTA-1 was T_{Reg}-mediated, facilitated by their selective modulation [20]. However a more recent study suggested $T_{effector}$ costimulation as the predominant outcome [21]. Regardless of mechanism of action, GITR approaches have yet to recapitulate these promising findings in humans. Receptor activator of nuclear factor-kβ (RANK) ligand (RANKL) expression on T_{Regs} engages the RANK receptor on cancer cells and promotes metastases [22]. Inhibitors of RANK signalling, such as the anti-RANKL antibody denosumab, already used against osteoclastic-mediated bone resorption, may block direct T_{Reg}-induced metastases of certain cancers.

Targeting FOXP3, the essential transcription factor of T_{Regs}, by RNA interference (RNAi) could also modulate their function. Lentiviral-mediated delivery of miR-31 (a negative regulator of FOXP3) to T_{Regs} abolished their suppressor capability [23]. Translation to clinical application is challenging, as miR-31 would need to be delivered specifically to T_{Regs} because FOXP3 is also transiently expressed on activated human $T_{effectors}$. FOXP3 is also expressed (both mRNA and

protein) in numerous cancer cell lines [24] but the effects of its down-regulation are unknown and could even be counterproductive.

Further options for disrupting T_{Reg} function include Toll-like receptor (TLR) modulation, OX40 stimulation or interference with the adenosinergic pathway. Exposure of T_{Regs} to the TLR8 ligand, poli-G10 abolished their suppressive influence on $CD8^{+}T$ cells, leading to improved anti-tumour immunity [25]. More recently a synthetic TLR1/TLR2 agonist, an analogue of bacterial lipoprotein, mediated a dose-dependent tumour regression and a long-lasting protective response against tumour rechallenge through a reciprocal down-regulation of T_{Regs} and up-regulation of CTL function [26]. These findings suggest that TLR signalling is a worthwhile pursuit but caution is advised as TLR agonists can promote regulatory as well as effector responses [27]. Stimulation of OX40 (a co-stimulatory member of the TNF receptor family) inhibits the suppressive function of T_{Regs} *in vitro* (by down-regulation of FOXP3) and abolishes protection against graft-versus-host disease in mice [14]. The paradoxical stimulatory effects on $T_{effectors}$ make it an enticing target for cancer immunotherapy. Another potential target on T_{Regs} is ectonucleotidase activity which facilitates local generation of adenosine which has immunosuppressive capability. Ectoenzyme inhibitors such as ARL67156 and other modulators of the adenosinergic pathway, such as inhibitors of the A2A adenosine receptor, have been shown to block T_{Reg}-induced immunosuppression [28].

Disrupting Tumoural Homing of Regulatory T Cells (figure 1.1 C)

Chemokine-chemokine receptor and integrin-integrin ligand interactions attract T_{Regs} to the tumour, a phenomenon first observed for the CCL22-CCR4 interaction in ovarian cancer [29]. Importantly CCL22 expression was not confined to tumour cells but also included bystander cells such as tumour-associated macrophages. Further chemokines/integrins have been implicated in the selective recruitment and retention of T_{Regs} at tumour sites including CXCR4, CD103 and CCR2 [9]. Because chemoattraction is ubiquitous in the immune system efforts to block T_{Reg} recruitment to the tumour mass may be limited by the concurrent effects on $T_{effectors}$. Nevertheless, disruption of CCR5/CCL5 signalling blocks T_{Reg} migration to tumours and inhibits pancreatic tumour growth in mice [30]. Methyl gallate has also recently

been shown to inhibit infiltration of T_{Regs} into tumours resulting in reduced tumour growth and prolonged survival rates [31].

Immuno-stimulatory therapies may inadvertently promote tumoural homing of $T_{Regs.}$ Therapy with IL-2 can enhance CCR4 expression on T_{Regs}, which stimulates their migration to the tumour mass and an up-regulation of CXCR4, the receptor for CXCL12, a chemokine linked to development of organ-specific metastases [9]. These findings endorse a more prudent use of IL-2 or perhaps its use in combination with agents such as AMD-3100 which antagonise the CXCR4-CXCL12 interaction.

Exploiting T cell plasticity (figure 1.1 D)

The origins of iT_{Regs} within the tumour microenvironment are diverse as varying degrees of plasticity exist within the helper $CD4^+$ T cell population ($T_{Regs,}$ Th1, Th2, Th17, Tfh) [32]; Pre-differentiated T_{Regs} may migrate under the influence of chemokines [29], T_{Regs} may arise from *de novo* generation via differentiation and expansion or may derive from conversion of $CD4^+CD25^-$ T cells. The plasticity inherent in each of these processes is a potentially exploitable therapeutic niche.

IL-6 is central to T cell plasticity [32]. It helps to convert $FOXP3^+$ T_{Regs} into IL-17 secreting T cells (Th17). It potently abolishes conversion of conventional T cells into iT_{Regs} and in its absence no other cytokine can substitute for this inhibition. Thus, IL-6 merits further investigation as a therapeutic for cancer. TGF-β acts at the axis between T_{Reg} and Th17 differentiation, enhancing the function of FOXP3 and inhibiting the function of RORγt, their essential transcription factors respectively. TGF-β-induced FOXP3 expression is inhibited by proinflammatory cytokines (IL-6 and IL-21 for example) in a Stat-3-dependent manner. Thus Stat-3 may also represent a therapeutic option – indeed forced expression of Stat3 augmented IL-17 production, most likely through increased RORγt expression [32]. Re-directing differentiation towards a Th17 phenotype might also be achieved by direct introduction of RORγt, as this has been shown to induce IL-17 expression upon transduction of naive $CD4^+$ T cells [32]. Conversely, selective methylation at the FOXP3 locus would likely hinder differentiation along a suppressor pathway. Aside from the epigenetic level, targeting FOXP3 at the mRNA and protein levels would also be worthwhile. Other approaches include antagonists for retinoic acid receptors which facilitate differentiation into Th17 cells over T_{Regs} [32]. T_{Reg} differentiation can

be redirected towards lineages other than Th17. Specific inactivation of the transcription factor interferon regulatory factor 4 (IRF-4) elevates Th2 cytokine production while IL-4-driven growth factor independent 1 (Gfi-1) facilitates optimal Th2 differentiation [32].

Blocking T_{Reg} proliferation is an obvious goal. This can be achieved by either direct inhibition of TGF-β, inhibition of indoleamine 2,3-dioxygenase (IDO) directly with 1-methyl-D-tryptophan or indirectly by CTLA-4 blockade. Aside from directly stimulating T_{Reg} expansion, COX-2-derived PGE_2 facilitates tolerogenic APC-led T_{Reg} recruitment and is itself a functional instrument of T_{Regs} in certain tumours [9]. Thus, use of COX-2 inhibitors like celecoxib may be justified. Alternatively, bevacizumab or blockade of PD-L1 on T_{Regs} with MDX-1106 (Phase II) may halt T_{Reg} proliferation.

Inhibiting the peripheral conversion of $CD4^+CD25^-$ T cells into $CD4^+CD25^+$ T_{Regs} may be a useful therapeutic approach. The TGF-β-blocking antibody, 1D11 abolished this conversion and reduced tumour burden in mice. Subsequently other TGF-β-modulators including antibodies, soluble TGF-β receptors and the antisense oligonucleotide AP-12009 have reached Phase I/ II clinical trials. However systemic TGF-β-blockade may carry the risk of developing autoimmune disorders. Furthermore, under sub-immunogenic conditions T cell conversion can occur in the absence of TGF-β; IL-10 and IDO have also been shown to promote induction of T_{Regs} [9].

1.1.2.2 Novel approaches to T_{Reg} modulation

The multitude of strategies discussed in this review deliver only marginal efficacy. While some strategies have lacked potency the majority flounder on specificity. This dearth of specificity is understandable given the intersecting differentiation pathways shared by all cells of the T cell lineage. Selective approaches to T_{Reg} modulation are warranted. Simple depletion of T_{Regs} maybe naive and the benefit short-lived, while inhibiting their migration to the tumour ignores the *in situ* generation of these cells. Thus strategies focused on negating T_{Reg} function or reprogramming their functional phenotype would seem more meritorious.

A unique cell surface marker which facilitates selective targeting of T_{Regs} has yet to be uncovered. Thus targeting CD25 or CTLA-4 has been encumbered by a

concomitant effect on $T_{effectors}$. Introducing a second layer of specificity, so called dual specificity, to receptor targeting would likely be synergistic. This is a strategy under investigation in our laboratory whereby a relatively T_{Reg}-specific gene therapy approach is coupled to ligand selectivity.

A global T_{Reg} modulation is undesirable as it may increase susceptibility to autoimmunity. Tumour-T_{Regs} could be targeted via their antigen-specific T cell receptors (TCRs); antigen-specific T_{Regs} engaged melanoma-expressed CTAG2 (Cancer/testis antigen 2) and ARTC1 (Antigen recognised by T_{Reg} cells 1) [33] and in colorectal cancer patients CEA (carcinoembryonic antigen), telomerase, HER2/neu (human epidermal growth factor receptor 2) and MUC-1 (mucin 1) reactive T_{Regs} were detected in the peripheral blood [34]. On a practical level this could be achieved by harnessing tetramer technology; Saporin-coupled MHC class I tetramers specifically ablated IGRP (islet-specific glucose-6-phosphatase catalytic subunit related protein)-autoreactive T cells and delayed diabetes in NOD (non-obese diabetic) mice [35]. Identification of $CD4^+$ T_{Regs} specific for a given tumour antigen would facilitate their targeting with MHC class II tetramers by similar means.

While such agents would be specific for a given subset of T_{Regs} they would also target other CD4+ helper cells expressing the same antigen specificity – $CD8^+$ cells would be unaffected. To circumvent this issue the effector component attached to the tetramer could be modified to confer another level of specificity. It could be miR-31 as 100% of target cells internalise the tetrameric complexes [35]. Although the consequence of FOXP3 knockdown in non-T_{Regs} is unknown TCR engagement in these cells may simply lead to activation – further augmenting the immune effector response.

Alternatively one could target tumour-T_{Regs} indirectly by modulating dendritic cell activation. This could be achieved by blockade of DC p38 MAPK, COX-2 or PI3K which inhibits innate production of TGF-β and IL-10 and thereby suppresses induction of T_{Regs}. Such strategies enhance the efficacy of TLR (toll-like receptor) agonists or HSPs (heat shock proteins) as immunotherapeutics or adjuvants for DC vaccines and permit an un-restrained development of protective Th1 and Th17 cells [27].

In conclusion, T_{Reg} inhibition in the cancer environment would permit an anti-tumour immune effector competency with containment or elimination of

disease. Such responses would be tumour specific and durable and should be effective against systemic disease, particularly micrometastases. There is clinical potential for T_{Reg} inhibitory strategies as part of multimodal programmes or combined with targeted therapies or local immunogene stimulation of anti-tumour immune effector cells. The objective should be to selectively modulate T_{Regs} within the tumour microenvironment rather than their global depletion in order to minimize the risk of autoimmune manifestations. Strategies targeting T_{Reg} function or differentiation seem currently to be the best option as they are less susceptible to compensatory mechanisms. Emerging technologies such as tetramer or RNA interference approaches should improve specificity and efficacy and thus favour the preferential inhibition of T_{Regs} within the tumour environment.

Macrophages represent innate immune cells with an inherent adaptive component as evidenced by a variety of polarised responses [36,37]. Adaptive responses or reprogramming of macrophages occur following exposure to environmental signals from microbes, damaged tissues and lymphocytes. The diversity and plasticity of macrophages is perhaps most evident in solid tumours [38].

The different polarised states can be defined by their activation stimuli, their phenotype in terms of cytokines/chemokines secreted, and their function [39,40]. M1 or classically activated macrophages, derive from polarisation by bacterial moieties such as LPS and the T_H1 cytokine IFN-γ. They secrete high levels of IL-12 but low IL-10 and express the T_H1-attracting CXCL9 and CXCL10. M1 macrophages are involved in killing of intracellular pathogens and tumour destruction, but can also lead to tissue damage [38]. In contrast, M2 or alternatively activated macrophages are polarised by the T_H2 cytokine IL-4 [41] and secrete low levels of IL-12 with high IL-10. They express chemokines CCL17, CCL22 and CCL24 [42]. They are involved in parasite clearance, tumour progression and have immunoregulatory functions. Importantly, the different polarised states do not represent distinct phenotypes, as overlapping characteristics exist [43,44]. M1 and M2 macrophages are probably best looked upon as being at opposite ends of a spectrum of functional activation [45].

Within the tumour microenvironment, M2-like macrophages generally predominate where they play a part in tumour immune evasion [38,46]. Indeed, for the majority of human tumours, increasing TAM numbers negatively correlates with prognosis [47]. They release angiogenic growth factors including IL-8, VEGFA, VEGFC and EGF, which support development of a new blood and lymph system for the emerging tumour [48,49]. M2 macrophages also recruit pro-tumourigenic T_{Regs} and T_H2 cells through expression of chemokines CCL17, CCL22 and CCL24 which are chemotactic for these lymphocyte subsets [37]. They further drive the differentiation of $CD25^+GITR^+FOXP3^+$ T_{Regs} [50].

The macrophage polarisation state that predominates within the tumour is influenced by their interaction with lymphocytes, especially T_{Regs}. While T_{Regs} directly undermine anti-tumour immunity (see previous), they also have an indirect effect through their manipulation of macrophage plasticity. The interaction between T_{Regs} and macrophages is best described as bi-directional as macrophages attract T_{Regs} to the tumour (see above) where they are then influenced by the T_{Regs} themselves. Human monocytes have been observed to differentiate into M2-like macrophages when cultured in the presence of T_{Regs} [51], while addition of T_{Regs} to the peritoneal cavity of SCID mice polarized the resident macrophages to an M2-like phenotype [52]. Furthermore, T_{Regs} but not effector T cells, have been shown to induce B7-H4 expression in a variety of APCs including macrophages [7]. Significantly, in that study, normal macrophages were refractory to stimulation of B7-H4 expression while ovarian-TAMs were not. $B7\text{-}H4^+$ macrophages have been shown to inhibit T-cell mediated anti-tumour responses [53-55]. Moreover, T_{Reg}-derived IL-10 induces expression of the PD-L1 receptor on TAMs, which also inhibits T cell mediated immunity [56].

Based on the evidence presented, efforts to eradicate or re-programme TAMs would seem meritorious.

RNA interference (RNAi) is an evolutionary conserved regulatory mechanism, common to most eukaryotic cells, that uses small RNAs to orchestrate homology-dependent control of gene activity [57]. Currently, more than 1000 microRNAs (miRNAs) have been identified which are thought to regulate expression of greater than 30% of human genes [58]. Given their abundance, it is unsurprising that miRNAs play a crucial role in the maintenance of health. As a corollary, one would predict that when the RNAi pathway runs awry, through over or under expression of RNAi mediators for example, disease would result. Given the regulatory control afforded to the RNAi pathway and the potential that this control mechanism is subverted in disease, the opportunity for a novel category of RNAi therapeutics is self evident.

RNAi-based therapeutics promise many advantages over conventional treatment modalities [59]. Principal among these is the potential to reach all targets, including previously "undruggable" targets, since in theory, any transcript that encodes a protein linked to a disease can be targeted [60]. For example, in diseases which derive from a single nucleotide polymorphism (often dominant negative genetic disorders) it is very challenging to design effective small molecule and biological therapies (proteins or antibodies) as there is insufficient structural difference between the normal and disease-causing variant. RNAi mediators surmount this issue with single nucleotide selectivity. Furthermore, RNAi mediators can easily be combined to reach multiple targets simultaneously making them more suitable for treatment of polygenic diseases. The time taken from target identification to therapy development is comparatively much shorter for RNAi molecules also. Often this can result from being able to use a single RNAi drug candidate all the way through the development process where the molecule displays cross-species reactivity [61].

Endogenous RNAi is mediated by miRNAs and siRNAs which, although distinct entities, follow a converging biogenesis pathway (Table 1.1 and figure 1.2). miRNAs are embedded in the host genome and transcribed as part of a long primary transcript (pri-miRNA) from pol II promoters [62]. The pri-miRNAs are processed within the nucleus to ~70 nucleotide precursor stem-loop RNA (pre-miRNA) by the microprocessor complex consisting of Drosha and DGCR8 (DiGeorge syndrome critical region gene 8) [63,64]. Pre-miRNAs are exported to the cytoplasm by exportin-5 where the stem-loop is removed by the actions of the RNAse III Dicer. The miRNA duplexes that result are structurally similar to siRNAs [65] and are loaded into the RNA-induced silencing complex (RISC). Either strand of the duplex can carry out gene silencing, but many miRNAs show asymmetry, whereby one "guide" strand is preferred and the passenger strand is then discarded.

Within RISC, the mature miRNA associates with an Argonaute protein family member, of which there are four (AGO 1-4) [66,67]; the majority of miRNAs imperfectly match their target mRNA strand and thus engage with AGO 1. The guide strand generally guides the RISC to the 3' untranslated region (3'-UTR) of the target mRNA where imperfect complementarity leads to translational repression [68], mRNA destabilisation or both [69].

In the absence of total complementarity, perfect alignment in the seed region (nucleotides 2-8 from the 5' end of the miRNA) is seen as crucial to the specificity and function of miRNAs [70]. The guide strand stays within the RISC where it can turnover and enable repeated binding and perpetuate the silencing of the target mRNA. This leads to long term silencing of the target gene [71,72]. It is important to note that similar to siRNAs, some miRNAs are (near) perfectly complementary and bind to AGO 2 where they promote mRNA cleavage (see below) [73].

siRNAs are produced from cleavage of longer dsRNA precursors by the direct actions of Dicer. One strand is referred to as the "guide" strand and directs silencing. Cleavage of the other, "passenger" strand is necessary to facilitate assembly of the guide strand into the AGO 2-containing RISC [74,75]. Strand selection is determined by the thermodynamic properties of the siRNA duplex [76]. In contrast to miRNAs, most siRNAs share 100% complementarity with their target mRNA. This permits interaction with AGO 2, the only member of this protein family with

cleavage capability [77]. The end result is cutting of the mRNA strand at position 10-12 (from the 5' end of the guide strand) [78].

Table 1.1: Differences between endogenous miRNA and siRNA

	miRNA	siRNA
Origin	Transcribed from genome as part of a long primary transcript	Derived from long dsRNA by direct cleavage by Dicer
Level of processing	Drosha & Dicer	Dicer only
Complementarity	Generally imperfect	Total
Method of gene silencing	Translational repression & mRNA destabilisation	mRNA cleavage

The natural phenomenon that is RNAi can be exploited to answer fundamental biological questions about gene function and also for therapeutic endeavour (figure 1.2). The three principle approaches are to use siRNA (an RNA-based approach), short-hairpin RNA (shRNA) or miRNA (both DNA-based strategies). Their terminal mode of action is largely similar but they differ widely in the stage at which they hi-jack the endogenous pathway, their mode of delivery and duration of activity. In the simplest classification, recombinant inhibitory RNAs are designed to mimic primary miRNAs (in the case of artificial or exogenous miRNAs) or precursor miRNAs (in the case of shRNAs) or the products of Dicer processing (in case of chemically synthesised RNA duplexes) [79]. Each strategy has advantages and disadvantages and often the choice of mediator depends on the target gene to be silenced and the planned phenotypic alteration.

Exogenously produced siRNAs were the first approach to exploiting RNAi. Synthetic siRNAs of ~21 bp with 2-nt 3' overhangs were designed to mimic the natural Drosha/Dicer cleavage products [80]. These siRNAs were mainly designed to share perfect complementarity with their target mRNA and thus effect cleavage through an interaction with AGO 2. Early approaches focused solely on sequence alignments with the target mRNA but subsequent design strategies sought to introduce functional asymmetry to the synthesised duplexes. Backbone and terminal nucleotide modifications, such as 2'-O-Me or locked nucleic acids, destabilised the 5'-end of the siRNA duplex which favoured loading of the guide strand into the

RISC with concomitant destruction of the passenger strand [81]. Such modifications had a number of advantages; they minimised sequence-dependent off-target effects by the passenger strand, improved efficacy of the guide strand and increased the likelihood of avoiding Toll-like receptor responses [82].

siRNA as an approach to RNAi has two major drawbacks [83]; 1) delivery: Unformulated siRNA molecules do not readily permeate the cell membrane due to their negative charge and size. Furthermore these 22 bp duplexes cannot be delivered by viral vector delivery systems in their native form. As a result siRNA delivery is largely dependent on non-viral gene therapy strategies which to date have lagged behind viral vectors in terms of efficiency of delivery. Many researchers have sought to encapsulate siRNA molecules in cationic liposomes and polymers which have yielded some success in mice [84,85] but many lipid based systems are rapidly cleared by the liver. Other *in vivo* delivery strategies have included cholesterol conjugated to the siRNA [86], antibody-protamine fusions to bind the siRNA [87], cyclodextrin-based encapsulation [88] and aptamers as targeting moieties for the siRNA [89]. All these approaches brought an element of specificity to the delivery but the efficiency remained limited. Indeed the first display of siRNA silencing in humans used nanoparticles guided by transferrin-receptor ligands to specifically enhance uptake by cancer cells [90].

2) short half-life: the chemical nature of siRNA duplexes renders them susceptible to degradation by RNase A-type nucleases in serum. Some progress has been made in this area whereby RNA backbone modifications such as 2'F, 2'O-Me and 2'H substitutions have increased serum stability [82]. However even within the cell siRNAs are readily degraded and their concentration decreases with every cell division leading to a transient silencing effect. Silencing can be as short as three to five days for transiently transfected cells *in vitro* but may be several weeks in non-dividing cells [91]. However for both dividing and non-dividing cells in an *in vivo* setting this transient silencing would probably mandate repeated administrations which could prove cost-prohibitive. In summary siRNA may be more suitable for *in vitro* proof of principle to verify silencing of a target gene at a sequence level. They can readily be introduced to growing cell cultures with various commercial transfection reagents where transient silencing is generally sufficient for validation. Translation into an *in vivo* setting seems challenging thus far.

shRNAs are DNA-based RNAi triggers that when introduced into cells are transcribed as sense and antisense sequences connected by a loop of unpaired nucleotides. They are designed to mimic pre-miRNAs. However shRNA transcripts often do not reflect the Drosha cleavage products they were designed to mimic [92]. In many instances they lack the 3' dinucleotide overhang which impairs their transport by exportin 5. The subsequent nuclear accumulation of hairpins can be toxic to cells. However a bigger issue with shRNAs has been the RNA polymerase III-based promoter systems into which they are incorporated. The U6 promoter has been a common choice given its natural function in the generation of small cellular transcripts [93]. These strong Pol III promoters drive massive over-expression and saturate the endogenous pathway leading to severe toxicity [94-96]. The toxicity has been shown to correlate with both shRNA expression levels and an accumulation of unprocessed shRNAs. Many solutions have been postulated to overcome the saturation problem and these are discussed below (Section 1.2.4.2). Of note artificial miRNAs do not appear to saturate the endogenous miRNA pathway [92,95] and as such represent an advancement on shRNAs.

Artificial microRNAs are also DNA-based triggers of RNAi and are designed to mimic pri-miRNAs. In this approach a perfectly complementary siRNA is embedded within a miRNA-scaffold derived from an endogenous miRNA. To date the best characterised pri-miRNA backbones are based on miR-30 and miR-155 [97]. The miRNA mimics that result, are thought to enhance RNAi via more efficient interactions with the RNAi processing machinery [64]. One study demonstrated artificial miRNAs to be superior to shRNAs both *in vitro* and *in vivo* when knocking down the same target gene [98]. Artificial miRNAs are usually transcribed using a Pol II promoter in keeping with the natural promoter for the majority of miRNA genes [99]. Compatibility with Pol II promoters offers the researcher several well characterised inducible systems and tissue specific promoters allowing for greater temporal and spatial control of expression.

Crucially artificial miRNAs appear devoid of the saturating toxicity associated with shRNAs. Incorporation of a saturating shRNA into an artificial miRNA-30 scaffold attenuated its toxicity and knockdown efficiency was maintained [95]. This can be attributed to the lower steady-state levels of the mature antisense RNAs from artificial miRNAs and hence failure to overload the machinery.

This theory is supported by competition studies showing that two co-transfected shRNAs compete with each other and that shRNAs compete with both artificial and endogenous miRNAs [92,100]. In the same studies no competition was seen between two co-transfected artificial miRNAs or between artificial miRNAs and the endogenous miRNA pathway. Taken en masse the evidence would suggest that the artificial miRNA approach is more suitable as a therapeutic strategy for inducing RNAi.

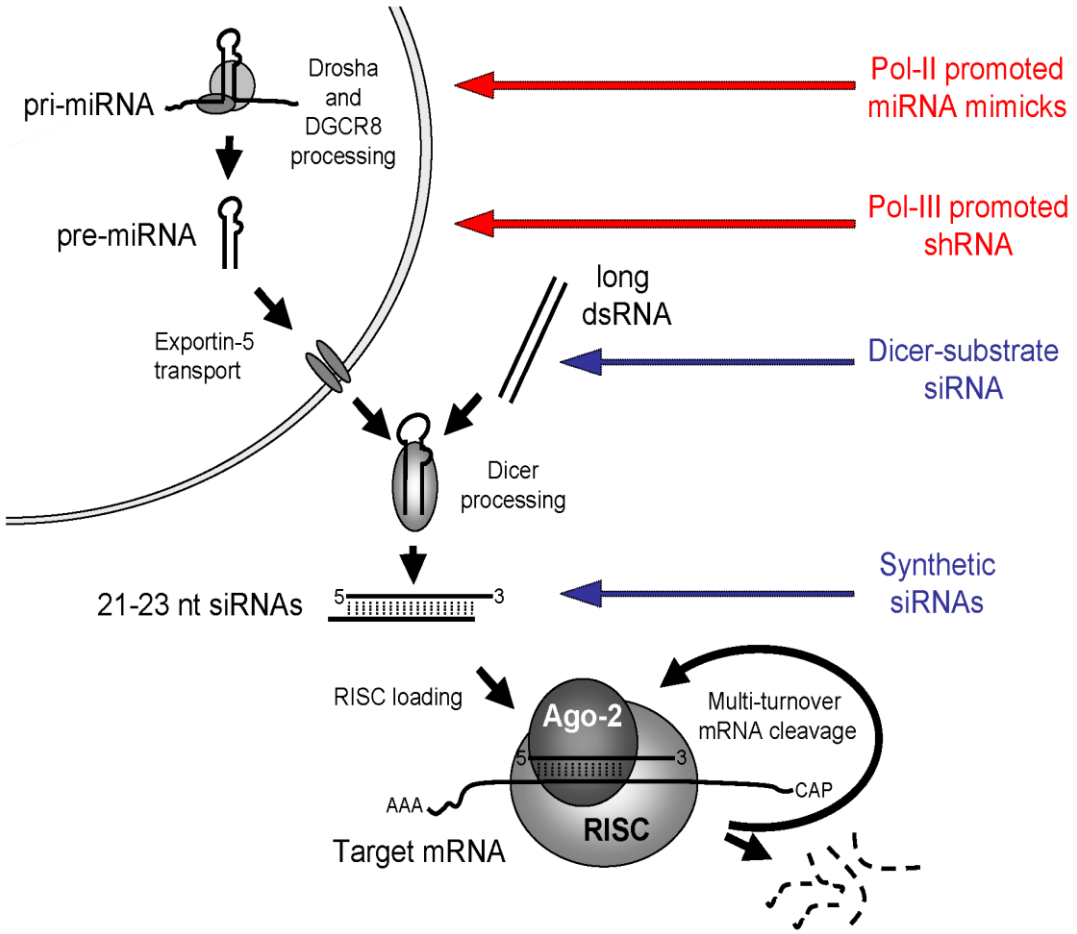

Figure 1.2: The endogenous RNAi pathway and opportunities for exploitation. The left hand side shows the endogenous origin of mature RNAi mediators from either miRNAs embedded in the host genome or siRNAs produced from cleavage of long dsRNA precursors. The right hand side shows options for harnessing the endogenous pathway for therapeutic endeavour using DNA-based (red) or RNA-based (blue) approaches (From [71]).

1.2.4.1 Delivery

At its simplest interpretation exploiting RNAi for therapeutic endeavour is another form of gene therapy where the goal is to deliver nucleic acids to cells specifically and efficiently. Thus it is unsurprising that development of RNAi as a therapy has been hampered by a difficulty common to the entire gene therapy field – delivery. A wide variety of gene/RNAi delivery strategies are available including non-microbial (physical and chemical strategies) and microbial systems such as viral and bacterial vectors (reviewed in section 1.3.2).

RNAi mediators by their nature are difficult to deliver; they are highly negatively charged which repels them from the cell surface – this makes the use of some type of encapsulation or targeting moiety almost essential. They are also large molecular weight molecules – a typical siRNA is greater than 13 kDa for example. Given their potency within the cell targeted delivery is paramount. A myriad of strategies have been trialled in an effort to enhance efficiency and specificity of siRNA delivery (reviewed in [101]). Proof of principle has been demonstrated for many in animal studies but the efficiency is often poor. Furthermore many involved focal delivery such as direct injection to the eye or tumour which some may consider clinically unworkable.

That said two studies using siRNA are noteworthy. One group used an aptamer targeting the prostate specific membrane antigen receptor to carry an siRNA capable of inducing cell death in a xenograft tumour model. They succeeded in impeding tumour growth [89]. A project that has progressed further is now in clinical trials for patients with refractory solid tumours, involves cyclodextrin nanoparticles coated with transferrin carrying an siRNA selectively to tumour cells (www.clinicaltrials.gov). Although proof of principle has been demonstrated for siRNA approaches their effect is transient with repeat administrations likely for a sustained alteration of disease phenotype. Such dosage schedules, given that oral formulations are unlikely in the near future, may be the undoing of the siRNA apporoach.

shRNAs and artificial miRNAs on the other hand have more potential given that they are plasmid-based and hence poised to take advantage of the advances in

viral vector technology. They hold the promise of bettering the delivery and short duration of action of siRNAs. With the appropriate virus the RNAi mediator can potentially be stably integrated into the target cell and thus mediate sustained gene silencing with a single administration. Viral vectors have a tremendous propensity for specificity when combining transductional and transcriptional targeting; Transductional targeting can be conferred through capsid or envelope protein engineering and pseudotyping whereby foreign proteins from a different virus are used to alter the tropism of the core virus carrying the therapeutic gene (transductional targeting of lentivirus vectors is reviewed in section 1.3.3). Transcriptional targeting involves the use of inducible or tissue-specific promoters whereby expression of the therapeutic gene is controlled by exogenously introduced agents (e.g. tetracycline antibiotic) or agents unique to the specific target cell/tissue respectively. It must be noted however that some concerns remain around the use of viruses, particularly surrounding insertional mutagenesis.

1.2.4.2 Saturation of endogenous pathway

Excessive delivery and/or over-expression of an RNAi mediator can overload the processing machinery with potentially fatal consequences [94]. Toxicity was shown to correlate with vector dose. Such saturation is possible with siRNA and shRNA based systems but artificial miRNAs avoid this complication as previously outlined (section 1.2.3). An obvious solution to the problem is to transpose the mature RNAi sequence from siRNA and shRNA molecules into artificial miRNA scaffolds, which has been shown to be effective [95].

However other potential solutions, particularly for shRNA-mediated saturation have been explored (reviewed in [65]). One could simply lower the dose of vector administered – depending on the target disease this may [94] or may not [95] be tolerated as this will also reduce the percentage of cells transduced. Alternatively for shRNAs, one could substitute a weaker Pol III promoter. The U6 promoter has been frequently associated with saturation but changing to the weaker H1 (or 7SK) can be acceptable in certain scenarios [102]. A further option is to drive expression of the shRNA with a Pol II promoter but this may not always be successful. Pol II promoters often have poorly defined transcriptional start sites. This can be problematic downstream as the RNAi machinery needs to engage with the first base of the shRNA for correct processing [103]. A more elaborate method of dealing with

the saturation is to concomitantly overexpress the processing proteins with the shRNA. Extra copies of Exportin-5 and argonaute proteins have been delivered to animals [104] but this approach may not be clinically acceptable in the absence of a robust cell-specific delivery platform.

1.2.4.3 Off-target effects

Off-targeting can be defined as the silencing of unintended mRNA sequences. Despite the early promise of exquisite specificity associated with RNAi this has not been realised at a practical level. Off-targeting was first reported *in vitro* from microarray analysis following siRNA-transfection of HeLa cells [105]. Indeed a more recent *in vitro* study showed that one third of randomly selected siRNA had an unintended negative effect on cell viability [106]. This highlighted the potential of off-targeting to invoke cellular toxicity. Off-targeting has also been verified *in vivo* in a mouse model of Huntington's disease [107]. The consequences of off-target effects are potentially very serious as the silencing of any gene by RNAi will undoubtedly have knock-on effects on other genes and perturb a complex gene network [108]. Given that many gene networks have yet to be elucidated the cellular phenotype that may manifest is largely unpredictable.

Off-target effects manifest predominantly from three scenarios; 1) Sequences in the mature RNAi mediator are identical to seed regions of an endogenous miRNA (nucleotides 2-8 from the 5'end of the guide strand) [109]. The siRNA then partly pairs with a weakly complementary sequence in the 3'UTR region of an unintended mRNA. When this happens the siRNA can mimic the actions of the endogenous miRNA leading to silencing. Screening out sequences that match human or cross-species specific miRNA seed sequences using BLAST will minimise this problem. Where the RNAi mediator is a chemically-synthesised siRNA addition of an O-methyl group to the second nucleotide of the guide and passenger strands further helps reduce indiscriminate silencing effects [105]. This option is however not available to plasmid-based RNAi induction approaches. 2) Incorrect processing of the RNAi mediator such that an altered sequence is loaded into RISC. This represents a less common cause of off-targeting but sequencing of the processed product is essential to identify the correct mature silencing RNA and spurious RNAs that result from cleavage sites moving one or more nucleotides.

3) The incorrect strand of the mature duplex is incorporated into RISC. Careful design of the RNAi mediator will improve strand selectively and disfavour loading of the passenger strand [71]. For example introduction of a thermodynamic differential between the 5' ends of the guide and passenger strands favours loading of the strand with the lower pairing energy [76]. Also deliberate mismatches at appropriate sites on the passenger strand will limit its involvement and greatly enhance the overall efficiency of gene silencing. When developing an RNAi mediator it is important to ascertain which strand is loaded into RISC. A number of methods are suitable for this including northern blots, small RNA PCRs and luciferase-based reporter plasmids where targets for either the guide or passenger strand are placed in the 3'UTR of the luciferase gene [79].

1.2.4.4 Stimulation of immune responses

An immune reaction to double-stranded RNA represents an innate mechanism of defence against invading viral pathogens. However in the context of siRNA delivery for therapeutic gain such immune responses compromise the benefits bestowed through harnessing the endogenous RNAi pathway. siRNA molecules stimulate an interferon response through interaction with toll-like receptor 3 (TLR 3) on the cell surface. This response can be rather easily abrogated by shielding the siRNA with a carrier molecule such as a lipid bilayer or cholesterol [86,110]

A bigger issue which may extend to all RNAi mediators including shRNAs and artificial miRNAs is the activation of TLR 7 and 8. DNA-based approaches to RNAi may not directly engage these receptors as they subtly enter the endogenous pathway and mimic naturally occurring miRNAs [111]. However it is possible that following expression and export from the nucleus such mediators may be recognised by cytoplasmic pattern recognition receptors which may also trigger an interferon response [112]. Engagement of TLR 7 and 8 has been shown to be sequence-specific [113,114]. GU rich motifs such as 5'-UGUGU-3' or 5'-GUCCUUCAA-3' have been the main culprits. An obvious means of preventing interferon responses is to screen out mediators bearing such "danger" sequences. Given that for many target mRNAs several candidate RNAi sequences are available such exclusion should not offer a significant impediment to the development of RNAi therapeutics. Alternatively

certain chemical modifications such as inclusion of at least one 2'-OMe in either strand of the siRNA duplex can abrogate the interferon response [115].

In spite of the aforementioned barriers to RNAi therapy development RNAi molecules have reached clinical trial stage (reviewed in [116]). However as of yet there remains no RNAi mediator on the market, perhaps reflecting the complexity of such medicines. As for other therapeutic categories the route from bench to bedside is long and arduous. A schematic representation of the RNAi drug design workflow is presented below (figure 1.3).

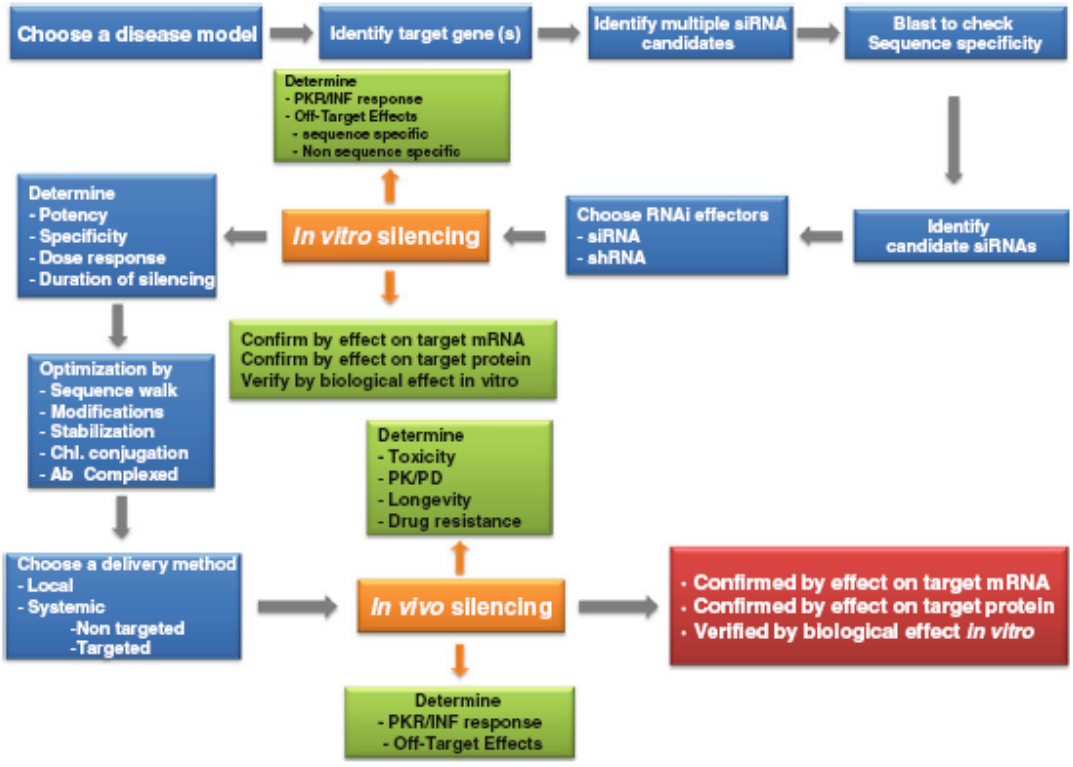

Figure 1.3: The steps involved in the rational design of an RNAi therapeutic (From [59]).

As of August 2013 a database search of clinical trials under "RNA interference" returns just 5 studies (www.clinicaltrials.gov). "siRNA" as a search term yielded 31 results, "shRNA" had just 7 results and "miRNA" had 157. Based on this analysis several conclusions can be drawn; the high number of "miRNA" trials is misleading in this context as the majority of such studies involved miRNA expression profiling and/or biomarker discovery. Most did not involve evaluation of a therapeutic (artificial) miRNA. Most therapeutic evaluations of RNAi mediators involved synthetic siRNA molecules. This can be attributed to their relative ease of design and lower cost of production – Indeed one siRNA entity, bevasiranib made it to Phase 3 trials but was withdrawn due to insufficient efficacy. It is worth noting that most trials to date have involved non-viral delivery, often to readily accessible tissues such as the eye and solid tumours which can be reached by direct injection and hence circumvent the problems attached to systemic delivery. The scarcity of studies involving therapeutic use of artificial miRNAs perhaps reflects their more recent discovery. Given their enhanced safety features and equal if not superior knockdown efficiency over shRNAs (see above) it is likely that future interest may focus more on artificial miRNAs. Furthermore recent advances in viral vector technology involving specific cellular targeting and improved safety should also propel the field of DNA-based RNAi delivery.

Some optimism for the future of RNA-based medicines comes from Pegaptanib (Macugen®) which was licensed for use in the USA in 2004 and Europe in 2006. Although its mode of action does not involve RNAi it represents an RNA molecule that is successfully and safely delivered to patients. Pegaptanib, an aptamer, is a pegylated modified RNA oligonucleotide that binds with high specificity and affinity to extracellular Vascular Endothelial Growth Factor ($VEGF_{165}$) inhibiting its activity (www.medicines.ie). Its physicochemical characteristics are such that Pegaptanib must be delivered directly to the eye by intra-vitreal injection, generally at six week intervals. Pegaptanib is licensed for the treatment of age-related macular degeneration – the greatest cause of vision loss in elderly patients in the Western world. By selectively inhibiting the "165" isoform of VEGF Pegaptanib prevents pathological ocular neovascularisation while sparing normal vasculature (www.ema.europa.eu/).

Despite the advances in modern medicine, even in the developed world there remains many diseases for which there is an unmet therapeutic need – diseases for which cure is unheard of and palliation is the best on offer as the inevitable succumbent to disease approaches. Still for many other diseases, treatment is available which prolongs life and may even be curative but few treatments are devoid of side effects which impinge upon quality of life. Furthermore, the "one size fits all" approach that shrouds the majority of medicines in regular use today, offers little regard to the individual intricacies that constitute a person's genetic makeup. In many instances, this predisposes recipients to potentially fatal idiosyncratic drug reactions. The holy grail of disease management is a therapeutic entity which is both curative and tailored, but also tolerable to the patient. Existing small molecule entities and protein-based therapies (e.g. monoclonal antibodies) deliver huge benefits to patients, but many sufferers continue to die prematurely as a result of their disease. Thus, novel therapeutic approaches are mandated. Gene therapy represents one approach and carries tremendous potential to revolutionise modern therapeutics with enormous benefits for patients.

At its broadest, "gene therapy" could be defined as the exploitation of genetic material for therapeutic endeavour. The term would encompass *in vivo* and *ex vivo* manipulations of DNA and RNA and the introduction, modification or removal of genetic material. Gene therapy represents an umbrella term for a range of different strategies. The simplest and most commonly attempted involves gene addition whereby a missing or functionally inept protein is supplied. Gene knockdown is also routinely attempted in the form of RNA interference whereby DNA encoding siRNAs or miRNAs or the RNA molecules themselves are delivered to cells to facilitate post-transcriptional gene silencing [79]. A more novel approach involves direct correction of the mutated gene using zinc finger nucleases in conjunction with DNA recombination technologies [117]. Paradoxically, the same approach can be employed to create mutations in certain beneficial scenarios. Emerging gene therapy strategies include the use of non-coding RNA molecules to alter protein function by interfering with splicing – through exon skipping for example [118] or to upregulate

gene expression [119] or to function as aptamers where they function independently or guide other therapeutics to enable selective delivery [120].

Despite the promise of gene therapy and the enormous amount of research on this topic, few gene-based therapeutics are in routine clinical use today. Indeed last year (2012) yielded the first licensing of a gene-based therapy in the western world - EU EMA licensing of Glybera® - an AAV vector engineered to express lipoprotein lipase in the muscle [121]. Previously two gene-based therapies have been licensed for use in China; Gendicine® - a recombinant adenovirus carrying the tumour suppressor gene p53 was granted approval in 2003 for the treatment of head and neck squamous cell carcinoma [122] while in 2005 Oncorine® - a type 5 adenovirus defective of the E1B-55 kDa molecule was licensed, also for head and neck cancer treatment [123].

The field has suffered some noteworthy setbacks however; in 1999 a clinical trial participant died following an adenoviral vector-induced fatal immune response [124]; the following year apprehension surrounding this novel field was compounded with reports that a γ-retroviral vector successfully restored X-SCID patients' immune systems but also caused leukaemia in several of these patients [125]. Despite these reports gene therapy clinical trials have a good safety record – indeed the above mentioned fatal outcome in response to adenovirus represented the first death in nearly 400 gene therapy trials involving over 4000 patients [126].

The above notwithstanding, many barriers to successful gene therapy have emerged over the years. In the first instance making sufficient quantities of the chosen vector (in particular viral vectors) at a realistic cost remains challenging. Furthermore, the nature of the diseases being targeted by gene therapy (often rare, "orphan" diseases) hampers recruitment of sufficient subjects for clinical trials.

This is before one even considers the *in vivo* concerns of which four predominate [127] (figure 1.4); 1) Delivery – efficient delivery of the nucleic acid therapeutic (although still an issue for many non-viral vectors) is not on its own sufficient, as specific delivery is also mandated to avoid off-target effects; 2) Vector persistence – depending on the vector used, the transgene will remain episomal or be integrated into the host chromosome. Either outcome can be useful depending on the turnover kinetics of the target cells and the disease being treated. However chromosomal integration at the wrong location carries the added risk of malignant transformation while episomal existence may warrant repeat administration which

may be precluded by immune responses (see below); 3) Duration of transgene expression – depending on the target disease, a continued therapeutic response may be required. Often this continuity can be extinguished by epigenetic interference with the vector genome; 4) The host immune response – this unwanted reaction can be to the vector (although less problematic with non-viral vectors) or to the transgene itself. If severe enough, such an immune response can be fatal (see above) or in milder cases therapeutic efficiency is lost and/or repeat administration is prohibited.

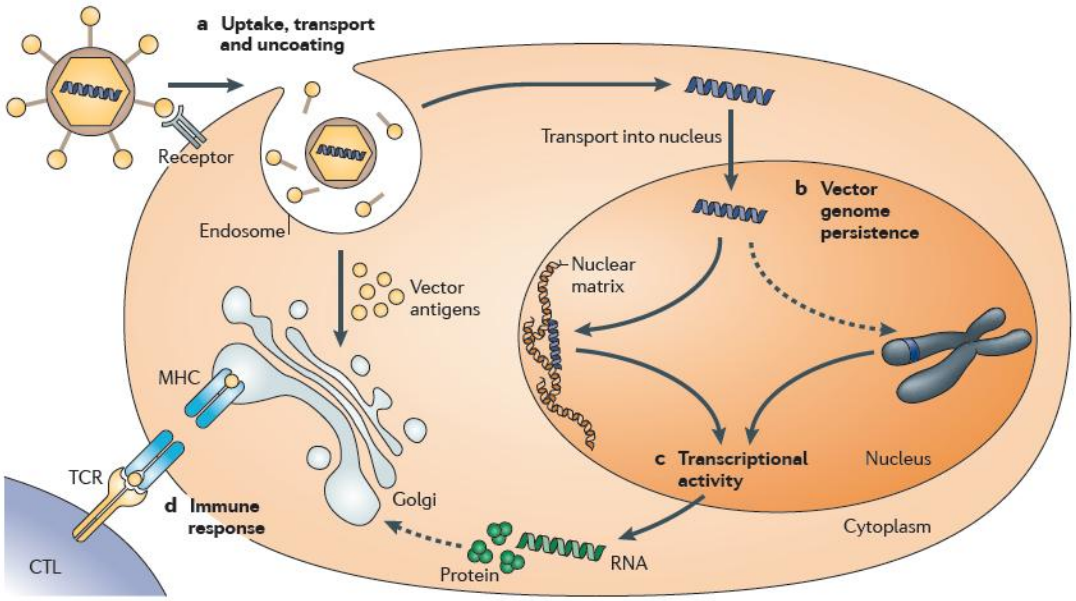

Figure 1.4 Issues to consider for successful gene therapy. Depicted are 4 crucial steps faced by a gene therapy vector (either microbial or non-microbial) as it attempts to mediate successful delivery and expression of its transgene within the target cell population. Further details are provided in the text. CTL, cytotoxic T lymphocyte; MHC, major histocompatibility complex; TCR, T cell receptor (From [127]).

A major hurdle in the advancement of gene therapy has proven to be the development of a delivery vector that is efficient, non-toxic and has ease of application. There are a number of properties that the ideal vector for cancer gene therapy should possess; i) it should be amenable to commercial production and processing; ii) on delivery, the vector should be capable of sustained expression of the genetic material, ideally in a regulatable fashion; iii) the vector should also be immunologically inert; iv) a vector that specifically targets certain cells or tissues is highly desirable, particularly where the target cells are dispersed throughout the body or where the cells are part of a heterogeneous population; v) there should be no constraint on the size of the transgene; vi) the vector should be capable of transfecting both dividing and non dividing cells [128,129]. While some of these properties exist in various classes of vectors, to date, all of these properties have not been found in any one vector. It is feasible that the optimal delivery modality for different diseases and anatomical locations and/or tissue types will vary. The delivery systems currently being used for gene therapy can be divided into two distinct groups- microbial and non- microbial gene delivery systems (Table 1.2). Each of these groups has its own advantages and disadvantages, while the key element for any vector strategy involves the balance between efficacy and safety.

Table 1.2 Gene delivery methods

Modality	Benefits	Drawbacks	Reference
Viral	High efficiency Nuclear entry Self delivery Systemic administration suitability	Safety Concerns Anti-vector immune response	[130,131]
Bacterial	Self delivery Systemic administration suitability-Targeting to tumours Cell or gene therapy Potential for oral delivery	Immune responses Low-medium transfection efficiency	[132,133]
Physical Techniques Electroporation Sonoporation Microinjection Particle bombardment Laser Irradiation Magnetofection	Site specific Safety of plasmid-based approach	Limited tissue accessibility Tissue damage Low transfection efficiency	[134,135]
Chemical Techniques Cationic polymers, peptides, lipids (liposomes) aka Nanoparticles	Self delivery May have nuclear entry Systemic Safety of plasmid-based approach	Low transfection efficiency	[136,137]

1.3.2.1 Non-microbial gene delivery

Non-microbial gene delivery systems normally involve the transfer of genes carried on plasmid DNA. Plasmids do not generally replicate in mammalian cells. Plasmid DNA is a relatively safe alternative to viral vectors. The toxicity is generally very low, and large-scale production is relatively easy. Plasmid delivery systems involve the use of chemical or physical means to mediate cellular entry of the plasmid molecules. The use of chemical means to carry DNA into cells involves cationic polymers, cationic peptides and cationic lipids (liposomes) [137]. Mechanical or physical techniques include the application of energy waves to cells to create transient pores in the cell membrane, thereby permitting entry of plasmid without killing the cell. Cell 'poration' systems include electroporation [134,138] and sonoporation [135]. Overall, while the safety profile of non-microbial vectors is attractive, the efficiency of current non- microbial approaches is considerably below that observed with viral vectors [139].

1.3.2.2 Viral gene delivery

By virtue of their natural life cycle, pathogenic viruses possess an innate ability to effectively invade human cells and express their genes within the cell. Gene therapists have harnessed the capacity of viruses to package DNA, transfer it to a cell, and produce proteins within it. Engineered viral gene delivery systems are typically rendered replication deficient by replacing those regions of the virus that are essential for viral propagation with the genetic sequence of a therapeutic gene. In this way, infectious progeny viruses are not produced from these viral vector particles, and hence are no longer pathogenic. Viral vectors have the advantage that their efficiency as delivery vehicles has evolved naturally [131]. The most commonly used viral gene transfer systems are derived from adenovirus (Ad), adeno-associated virus (AAV), lentivirus, retrovirus, herpes simplex virus (HSV) and semliki forest virus (SFV). These can be categorized into integrating and non-integrating vectors. In the normal virus life cycle AAV, retrovirus and lentivirus are able to integrate their viral genome in to the chromosomal DNA of the host cell. Ad and HSV however deliver their genomes to the nucleus of the host cell and remain episomal. Vectors derived from adenovirus represent the most widely used class of viral vector

for prostate and other cancers, and have shown great promise at clinical trial level [130,140].

However, several problems exist with current viral gene therapies. In terms of practicality of usage, there are associated difficulties in production, size restrictions on transgenes in some viral vectors, anti-vector immunological responses limit their usage to a single application, while several human cancers are devoid of viral receptors and are not transducable by viral vectors [141-145]. Many viruses are toxic and elicit systemic inflammatory reactions – one such immune response was fatal following use of an adenoviral vector [124]. Although confined to retroviral vectors random vector integration (which has resulted in cases of leukaemia[125]) has raised safety concerns. It should be noted however that newer, non-integrating lentiviral vectors (NILV) do not integrate and are hence devoid of this risk (see below) [143]. While vector promiscuity is also a concern perhaps the greatest limitations are the immunogenicity of the vector and the potential for insertional mutagenesis. Strategies are under development to overcome these limitations.

Vector immunogenicity Inactivation of the delivery vector by the same immune responses that eliminate wt viruses poses a significant problem. A number of approaches have been adopted in order to overcome this limitation.

Ad vectors have been used extensively in cancer immunotherapy; they are easy to propagate enabling high titre viral stocks to be generated; they have a broad host range and are capable of infecting both dividing and non-dividing cells [146,147]; they can be manipulated relatively easily to accommodate large DNA cassettes. However Ad vectors are the most immunogenic of all the viral vector groups, inducing strong cellular and humoural immune responses [148-150] and this limitation resulted in the first fatality in clinical trials [124,151]. The humoural response involves the secretion of antibodies against the Ad vectors resulting in its elimination whilst the cellular immune response involves the activation of cytotoxic T cells, macrophages and natural killer cells that result in the destruction of the virally infected cells. For this reason, a gutless Ad vector was developed. This vector is deprived of nearly all viral genes, retaining only the viral ITRs and packaging signal. These vectors are helper dependent, demonstrate less immunogenicity and persist longer in animals [152-154]. The vector exists episomally and does not integrate into the host genome, therefore the expression of the transgene has been found to be at best

transient [155], which depending on the therapeutic strategy, presents an increased safety profile, but possibly reduced efficacy. Induction of humoural responses has been demonstrated to vary depending on the antigen, the processing and presentation of the antigen and the route of administration.

Wild-type (wt) viruses can be recognised by the innate immune system resulting in antiviral immune responses. Receptors of the innate immune system recognize specific molecular patterns that are conserved in viruses but absent in the host. In a bid to overcome the innate immune response, 'cloaking' of the viral vector by encapsulating the vector or conjugating a protective substance to the viral capsid is under investigation. These approaches have focused mainly on Ad vectors, being the most immunogenic of the viral vector systems, but have also been studied for AAV vectors [156]. Strategies for adenoviral vectors include encapsulating the vector with cationic liposomes [157] or conjugating polyethylene glycol (PEG) onto the viral capsid [158-161]. Croyle *et al* [158-160] have shown that pegylation of both E1-deleted Ad and helper dependent Ad resulted in prolonged transgene expression following a reduction in cellular immune responses against transduced cells. However re-administration of these vectors results in a decrease in transgene expression, which may be due to an immune response against viral gene products.

Integration The initial promise of an integrating viral vector for gene therapy strategies meant that repeated administration of the vector would no longer be required in order to sustain the therapeutic effect. However, the first clinical trial using an integrating retroviral vector for the treatment of severe combined immune deficiency (SCID) took a tragic turn for the worse when 3 of the patients developed leukaemia following the activation of the LMO-2 proto-oncogene following integration of the vector [162-164]. Despite the potential that RV offers for gene therapy the problems associated with integration need to be resolved before these vectors can again be considered for the treatment of most diseases. Vectors derived from LV offer the same efficiency for gene transfer and also integrate randomly, but NILVs have been identified which overcome this issue. NILVs were identified as by-products of integration during wt HIV infection and following transduction with other retroviruses [165-167]. On binding of the wt virus to the cell, the LV genome enters the cell where the viral RNA undergoes reverse transcription in the cytoplasm prior to nuclear entry. Three forms of lentiviral DNA exist: double stranded linear, circular

with a single long terminal repeat (1-LTR) and circular with two LTRs (2-LTR) [168]. The linear form integrates into the host genome, whilst the 1-LTR and 2-LTR exist episomally, yet transgenes can be actively transcribed from all three [169]. Vector development has shown that LV vector integration can be blocked by mutating the viral integrase while all other functions can be maintained [170-173]. Integration can also be blocked by pharmacological agents, such as diketo acids [174,175].

1.3.2.3 Bacterial gene delivery

Interest in bacterial gene therapy vectors increased following safety concerns over viral vectors. While being potentially safer than viral delivery platforms, bacterial vectors retain many attributes of a biological agent. They are versatile in that any therapeutic encoded by nucleic acid can be delivered. This paves the way for a variety of strategies including direct cell killing (e.g. by toxin delivery), anti-angiogenic therapy and immunotherapy [176]. Many successful applications of bacteria as tumour-specific delivery vectors have emerged, e.g. *Salmonella Typhimurium* delivered mouse GM-CSF and IL-12 to tumours which induced regression in mice bearing lewis lung carcinomas [177]. Like other gene delivery modalities, bacteria can also be employed in vaccination strategies, e.g. an attenuated *Listeria monocytogenes* was used to deliver the HPV16 E7 antigen as part of a Phase I clinical trial for metastatic cervical cancer. Tumour reduction and prolonged survival were achieved [178].

Bacteria are not without their limitations as gene therapy vectors however. Many strains are pathogenic and carry toxins and thus need to be attenuated before use as a vector to avoid complications associated with systemic infection. Moreover, as vectors for cancer, full penetration of the primary tumour mass and reaching distant metastases is not always achievable due to their variable constitution [179]. The transfection process faces additional obstacles in terms of plasmid release from the phagolysosome following cellular internalisation of bacteria. The efficiency of this release is poor for most species with the exception of *Listeria monocytogenes* which produces listeriolysin O, an enzyme that disrupts the phagolysosomal membrane [180]. Fortunately the *hlyA* gene which codes for listeriolysin O can be incorporated into other bacteria for therapeutic improvement [181]. Even after release of the plasmid into the cytosol, it must still enter the nucleus in order to facilitate transcription of its

therapeutic entity. Like other 'non-viral' or plasmid-based modalities, this step may be boosted by incorporation of nuclear localisation sequences on the plasmid itself.

These limitations notwithstanding, bacterial mediated gene delivery offers many unique advantages which may be highly applicable in appropriate strategies.

HIV-based lentiviral vectors represent a promising candidate for gene delivery as they are relatively non-immunogenic, capable of transducing both dividing and non-dividing cells and they maintain long-term transgene expression [182-184]. Current state-of-the-art vectors are pseudotyped with the glycoprotein of the vesicular stomatitis virus (VSV-G) in an effort to achieve maximal production yield. However such pseudotyping mediates non-selective cell entry into virtually any cell type of mouse, rat or human origin. Further refinement of such vectors is clearly desirable to improve the efficacy and safety of transgene delivery. Ideally, transgene expression would be restricted to only the cell type relevant for a particular therapeutic application. Strategies to achieve this selectivity include the use of tissue-specific promoters and switching off gene expression in irrelevant cells by incorporation of target sequences for tissue-specific miRNAs [185]. However, the preferred approach to selectivity would be to limit transgene expression at the step of cell entry using cell-specific delivery vectors. In light of this several strategies have emerged for engineering targeted lentiviral vectors including novel pseudotyping viruses, use of adaptors or bridging molecules and the genetic incorporation of cell-specific ligands or combination approaches (reviewed in [186]). Here we review advances in targeted lentiviral gene therapy.

An early approach by the Chen group involved pseudotyping HIV-1 lentivirus with the envelope of the Sindbis virus [187]. By inserting the Fc binding domain of protein A (ZZ) into the E2 region of the Sindbis virus, it was possible to couple any targeting antibody of choice. By coupling antibodies specific for HLA and CD4 a significant enhancement in delivery specificity was achieved *in vitro*. However two limitations exist with this approach; 1) the non-covalent coupling of the antibody means that in an *in vivo* setting the targeting antibody may become dislodged by endogenous antibodies in the circulation – this could lead to unpredictable and dangerous off-target effects; 2) the requirement for the target

cellular receptor to be endocytosed following vector engagement – this is necessary in order to activate the membrane fusion function of the Sindbis glycoprotein by low pH. Furthermore a residual non-specific tropism for the liver and spleen attributed to the ZZ Sindbis glycoprotein was subsequently detected *in vivo* [188]. The same research team improved upon this promiscuity by identifying a modified ZZ Sindbis envelope (designated m168) which was used in conjunction with an anti p-glycoprotein antibody to successfully retarget lentivirus to metastatic melanoma cells following systemic administration [189]. Alternative approaches that do not involve antibodies have also been explored in the Chen lab including insertion of integrin-targeting peptides into the envelope [190] and modification of N-linked glycans in the envelope proteins for lectin-mediated targeting [191].

Wang and Baltimore took a different approach to engineering targeted lentiviral particles and developed a system that involved separating the cell recognition and fusion functions of the Sindbis glycoprotein. They used the same binding-deficient, fusion competent Sindbis glycoprotein as the Chen group (except the ZZ domain was replaced with a 10-residue tag sequence) but the targeting antibody was incorporated as a distinct molecule on the lentiviral surface. Their first report provided proof of concept by displaying receptor-specific delivery via CD20 to B cells [192]. They further directed lentivirus specifically towards dendritic cells for *in vivo* immunisation by manipulating the natural tropism of the Sindbis virus– this natural tropism relies on the widely distributed heparan sulphate receptor and the more restricted expression of DC-SIGN (CD209) which is only found on subsets of dendritic cells. By mutating the heparan sulphate binding domain on the Sindbis virus glycoprotein transduction was exclusively confined to DC-SIGN-expressing cells. This immunisation strategy successfully protected against the emergence of nascent tumours and induced regression of established tumours in antigenically-defined OVA tumour models [193].

While Wang and colleagues initially relied upon the natural fusogenic capability of the Sindbis virus, they later sought to improve this crucial fusion step - introduction of mutations in the loop region of the fusogen molecule enhanced delivery efficiency [194]. In a further improvement of their original conceptual paper [192] they introduced single chain antibodies (as opposed to their full-sized counterparts) as the targeting entities on the lentiviral surface [195]. The Wang lab has

continued to pioneer targeted lentiviral-based platforms culminating in particles pseudotyped with a CD4 receptor and fusogenic protein (derived from Sindbis) capable of specific delivery to HIV-1 envelope-expressing cells in culture [196].

The Buchholz lab sought to use a similar pseudotyping strategy to target lentiviral particles to cells of choice but employed Measles virus glycoproteins, namely haemaglutinin (H) which is responsible for receptor recognition and the fusion protein (F). They built upon earlier work which endeavoured to redirect Measles virus itself [197] – the natural tropism of Measles had been ablated by mutations in the H protein [198] and a single chain antibody had been fused to its ectodomain [199]. Buchholz and colleagues identified cytoplasmic tail variants of H and F with these features which could efficiently pseudotype HIV-1 vector particles [200]. Proof of concept was demonstrated by incorporation of an anti-CD20 single chain antibody – the resultant particles had high target versus non-target cell discrimination when added to a mixed cell population.

Using Measles over Sindbis glycoproteins should be advantageous in that H and F mediate cell entry directly at the cell membrane in a pH-independent manner without the requirement for the target receptor to be endocytosed [201]. The Buchholz group advanced Measles-pseudotyped lentiviral delivery into animals where they achieved greater than 94% specificity for gene delivery to neurons in the adult mouse brain [202]. This strategy was also successfully adopted for specific gene delivery via MHC II to antigen presenting cells with the generation of robust immunity [203].

A preferential growth of bacteria within tumour tissue as distinct from healthy tissue has long been recognised [204]. However, the basis for this selectivity remains to be determined with many theories being furthered; the original suggestion that the hypoxic nature of solid tumours provides a niche for bacteria [205] over-simplifies matters. It now appears this phenomenon may be independent of the tumour type and the bacterial type (in terms of oxygen requirements). Other factors common to most tumours, such as the provision of cancer-derived purine nutrients to promote bacterial growth [206] and secretion of chemo-attractant molecules (e.g. aspartate,

ribose or galactose) [207] are now thought to play an important role. It is prudent to also consider the contribution of the chaotic and leaky vasculature which predominates in the tumour. Indeed the leaky blood vessel theory is supported by parallel evidence from wound-healing studies [208]. The inertia of the immune system within the tumour microenvironment has been well espoused previously and this clearly fosters a bacteria-friendly sanctuary [209]. Given their inherent tumour tropism it seems a logical extension to seek to use bacteria as selective gene delivery vectors.

While capable of delivering any nucleic-acid based therapeutic to tumours (section 1.3.2.3), the use of bacteria to deliver prodrug-converting enzymes, so-called "BDEPT", represents a particularly interesting strategy. The selective localisation of the bacteria within the tumour succeeds in converting a systemically-applied prodrug into a toxic agent while negating harmful effects to non-tumour healthy tissue. Several enzyme/prodrug combinations have been successfully trialled using a variety of different strains including cytosine deaminase (CD) with 5-fluorcytosine, nitroreductase with CB1954 and HSV-thymidine kinase with ganciclovir [179].

To date the majority of bacterial strains chosen as delivery vectors for cancer have been invasive with the goal of invading tumour cells and subsequent production of tumouricidal toxins or immuno-stimulatory cytokines. The target is the tumour cells themselves with cellular entry hinging on the natural properties of the bacterium. A novel slant on bacterial gene delivery involves using non-invasive strains that are captured by phagocytic cells such as dendritic cells and macrophages. This "passive" delivery mechanism recapitulates the normal functioning of the immune system as might occur in the context of a bacterial infection for example. The concept of directly targeting immune cells represents a paradigm shift in our approach to cancer therapy driven largely by advances in our understanding of the dynamic interplay that exists between the tumour and the immune system.

Overall, bacteria show great, but as yet unfulfilled promise as a gene delivery vector for cancer.

The rationale for the development of novel therapeutics in the form of gene and cell-based therapies has already been espoused in this review. Such treatment modalities are not in routine clinical use, but rather on the cusp of clinical translation. A significant impediment to their advancement to the clinic is a paucity of knowledge surrounding their *in vivo* characteristics and an inability to convert promising preclinical data into positive patient outcomes. Methodologies to track therapeutics and their efficacy/effect *in vivo* have not kept pace with the design and experimental testing of novel therapeutics *in vitro*. This underdevelopment is acknowledged by the call from the NIH Recombinant DNA Advisory Committee (RAC) for improved assays to measure transgene expression in cells and tissues [210]. Existing clinical approaches to monitoring of biological therapeutics are unfit for this purpose. These involve biopsies and serial specimen sampling, supported by various nucleic acid and protein assays. Such approaches are retrospective rather than real-time, as well as being invasive and time-consuming, impinging on patients' quality of life. Putting the impracticality of repeated biopsies to one side, sampling at multiple sites cannot accurately track transgene expression kinetics and levels or recapitulate the disease phenotype within an entire organ or tissue. Issues arise as to the stability of samples and delays between sampling and testing. The nature of gene and cell-based therapies is such that real-time and continuous monitoring is necessary as transgene expression, and hence therapeutic response, can fluctuate according to design (e.g. with regulatable promoters) and physiological conditions. Furthermore, traditional approaches generally require a terminal assay to macroscopically assess an organ of interest – an option which is rarely clinically appropriate. Thus, novel, innovative monitoring strategies are mandated.

The benefits promised by superior monitoring technologies are far reaching. In many instances, gene and cell-based therapies are experimentally tested in a small cohort of patients, whereby appropriate monitoring can lead to i) optimisation of route and timing of administration, ii) determine whether repeat administration is

warranted or safe and iii) provoke manipulation of pharmacokinetic and pharmacodynamic properties of the therapeutic. The more powerful the monitoring technology, the more information can be gleaned from a small number of subjects. Appropriate monitoring is paramount to facilitate a continuum in the drug discovery pathway as minor tweaks in formulation and utilisation take place iteratively from bench to bedside and back to bench again. Data generated from improved monitoring shortens time-to-market for these medicines which can be life-prolonging or even curative [211].

Optical imaging (OI) has been at the forefront of preclinical testing of therapeutics in this field, but has struggled somewhat in terms of clinical utility. It does, however, promise many benefits over other imaging modalities. Firstly, in the pre-clinical setting, utilisation of OI is facile and inexpensive while being amenable to high-throughput work, whereby multiple subjects can be imaged simultaneously [212]. In terms of safety and costs for clinical translation, no radiation is required and single cell sensitivity can be achieved at a low cost level [213]. That said, OI is not without its limitations; as a result of light scattering and absorption, OI is difficult to directly quantify, the resolution for whole body imaging is inferior to Computed Tomography (CT) and Magnetic Resonance Imaging (MRI), but with a higher resolution at depths of 0-1.0 cm and the penetration depth of imaging is still somewhat limited to max 1.5 cm compared with CT, MRI and Positron Emission Tomography (PET), although novel developments like optoacoustics might outperform current reflectance based optical imaging modalities [214]. These barriers to clinical translation are slowly being overcome and many impressive examples of OI-driven advancement of novel therapies exist (see below). Novel combination approaches involving OI such as photoacoustic imaging partially overcome the depth limitations associated with more traditional approaches (bioluminescent and fluorescent imaging) facilitating imaging up to several centimeters of tissue in patients [215]. The attributes of rival and often complementary technologies such as PET, CT and MRI-based imaging are reviewed elsewhere [216,217]. Section 1.4 highlights the use of OI strategies in the clinical arena. A detailed review of how OI has advanced early stage and pre-clinical drug discovery is beyond the scope of this thesis – the interested reader is referred to [218].

As a functional imaging modality, OI serves a similar role to PET imaging in its ability to track and monitor biological activity *in vivo*. OI involves detecting visible wavelength light emitted from biomarkers; Bioluminescence imaging (BLI) hinges on the liberation of light energy by a reporter luciferase gene which oxidises a substrate in an energy-dependent (ATP or $FMNH_2$) manner [219]. Fluorescence imaging (FLI) is based on excitation of a fluorophore (generally a protein or chemical dye) using an external light source. However, unlike PET scans in which the high energy gamma-ray photons emanating from the site of the radio-labelled probe traverse tissue essentially unencumbered before reaching the imaging detectors, the visible wavelength photons of OI are at much lower energies and are subject to scatter and absorption in the tissue.

While photon scatter by tissue structures such as mitochondria and cell nuclei can be of large angle, the scattering is primarily in the forward direction. Eventually the multiple scattering events cause the photon direction to become randomized. For weakly anisotropic media such as tissue, the distance at which the directional distribution becomes approximately isotropic is $1/\mu_s'$ for visible wavelengths, where μ_s' is the reduced scattering coefficient. Absorption of photons by endogenous chromophores in tissue, such as oxy- and deoxy-hemoglobin, water, melanin and fat can also be problematic. Fortunately, the discovery of the near infra-red window (600-900 nm) negates this problem as absorption by these physiologically abundant molecules is reduced to the minimum at such wavelengths [220,221]. The photon absorption length, $1/\mu_{a,}$ refers to the distance at which the number of photons has dropped to ~1/*e* due to absorption, where *e* refers to the mathematical constant. The fraction of the photons which can eventually reach the imaging subject surface is dependent on these tissue optical properties, μ_s' and $\mu_{a,}$ and the distance to the surface [222].

The light intensity that reaches the surface is usually below the ambient light necessary to visualize the imaging subject. This is particularly true for *in vivo* bioluminescence imaging. In order to detect the light which originates from the luminescent biomarker, the *in vivo* OI instrument for small animals typically consists of a light-tight dark box mounted with a charge coupled device (CCD) camera, cooled to prevent thermal electronic noise from dominating the signal [223]. CCDs with

high quantum efficiency of photon conversion to electronic signal are especially advantageous for optical imaging of these types of reporters in vivo. The dark box is also useful for fluorescence imaging of weak or deep fluorophores. However, fluorophore brightness is also dependent on the excitation source power density, and therefore for superficially located fluorophores that have a sufficiently high quantum yield, and use of proper filtering methods, fluorophore detection can be achieved in the presence of ambient light.

Two-dimensional optical imaging involves collection of the light emission from the animal surface onto the pixel array of the CCD chip, allowing for immediate interpretation of the image data for gross biomarker localization and concentration. Although a greater issue when imaging deeper tissues multiple scattering and absorption of the photons can lead to a diffuse pattern of emission. This makes it difficult to determine the origination location of the emitted light as the emission pattern at the surface appears diffuse and unfocused. This explains why optical images, typically rendered in pseudocolour, will appear in broad patterns for deep sources and narrow peaks for shallow sources. When imaged longitudinally, efficacy of therapeutics or disease progression can be inferred from temporal decrease or increase in detected signal intensity.

However, the signal intensity at the animal surface is dependent on the underlying thickness of tissue through which the photons must travel, and therefore is dependent on the luminescent biomarker source depth. Conclusions drawn from two-dimensional OI longitudinal studies rest on the assumption that luminescent biomarker depths in tissue are invariable throughout the time frame of the study. The attenuation of the light signal which tissue mass imposes can be excluded from the measurement of source strength by modelling the light propagation through the tissue. Photon propagation in tissue can be modelled by stochastic methods which consider the probability of photon scatter, scattering angle, and absorption for each incremental step of the photon path [224,225]. Other methods include solving the radiative transport equation for a finite element mesh representation of the tissue volume [226,227]. Finally, the photon fluence rate can be approximated by the diffusion equation for tissue in which $\mu_s' >> \mu_a$, and given specific boundary conditions; expressions which relate the source strength to surface signal can be analytically derived [228].

With the ability to model the photon propagation in the animal body, the unaltered source strength and location can be established in three-dimensions with numerical techniques which aim to minimize the difference between the simulated data and the measured signal at the animal surface [229]. In order to accomplish this, the animal surface should be defined for appropriate treatment of the boundary between tissue and air. Animal surfaces have been approximated as slabs, where the animal is placed into a chamber giving it a bulk slab shape. Animal surfaces have been more accurately measured with structured light methods [230], silhouette back-projection methods [231], or segmentation of CT images [232].

Resolution in 3D optical imaging is largely limited by the tissue optic properties and the wavelength band used for detection [233]. Prudent selection of data is important to minimise the effect of unknown parameters on the overall imaging success. In bioluminescent 3D imaging, acquiring image data at discrete spectral bands over a wider bandpass which encompasses strong changes in optical properties is advantageous for resolution [230,234]. In fluorescence 3D imaging, in addition to relevant wavelengths, the selection of excitation light irradiance pattern on the animal surface can be crucial for resolution [235] (see below).

Targeted OI has only very recently had its first clinical application (see below). Thus, most arguments endorsing OI are based on pre-clinical evaluations with novel therapeutics. The improvements in technology and labelling required to make OI a routine companion for novel therapeutic translation and utilisation are also predominantly pre-clinically based. The vast majority of OI encompasses exploitation of visible light from two different phenomena; bioluminescence and fluorescence.

1.4.3.1 Bioluminescent Imaging (BLI)

Bioluminescence hinges on the liberation of light energy by a reporter luciferase gene which oxidises a substrate in an energy-dependent (ATP or $FMNH_2$) manner [219]. Importantly, no external light source is required for the reaction. Various luciferase genes have been trialled, including firefly (*Fluc*), Click Beetle (*CBluc*),

Renilla (*Rluc*), *Gaussia* (*Gluc*) and the bacterial luciferase gene cassette/operon (*lux*) [236-238]. Of these, *Fluc* is the most widely used. The oxidation of D-Luciferin by *Fluc* or *CBluc* is exemplified below;

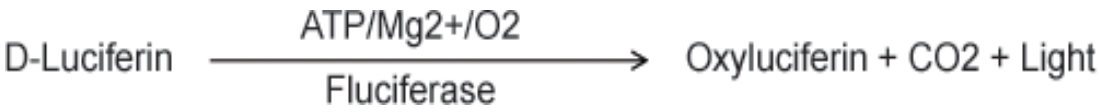

Although not yet licensed for human use, D-luciferin has not exhibited toxicity in pre-clinical animal studies. Its small molecular size makes it an ideal *in vivo* reporter substrate with the capability to penetrate many anatomical barriers, including the placenta and blood-brain-barrier [239].

BLI has been explored as an imaging modality for many types of gene and cell therapies in a variety of disease settings (reviewed in [212]) – a testament to its broad appeal. BLI is routinely used pre-clinically as an initial screening methodology to assess the delivery capacity and *in vivo* dissemination of novel gene therapy vectors, including cellular therapies [240,241]. It represents an efficient and affordable technology for most laboratories, as the required instrumentation and consumables are relatively inexpensive, the imaging methodology is easy to learn, and interpretation of the data requires little technical expertise BLI generally reflects the product of both delivery and expression of the transgene. In this context, BLI is well suited to optimising both the transduction/transfection [242] and transcription/translation [243] steps involved in therapeutic development. By improving the efficiency of these steps, BLI is enabling novel therapeutics to reach patients and improve outcomes.

1.4.3.2 Fluorescence Imaging (FLI)

Fluorescence imaging (FLI) is based on excitation of a fluorophore (generally a protein or chemical dye) using an external light source. As the excited electron in the fluorophore transitions to a lower state, light of a different wavelength (fluorescence) is emitted and can be detected. When deciding on a fluorophore, many characteristics must be considered such as the suitability of the excitation and emission wavelengths, photostability, brightness, and maturation speed [244,245].

Fluorescent proteins The original and perhaps the most commonly utilised fluorescent probe to date is the green fluorescent protein (GFP) derived from the jellyfish *Aequorea Victoria.* Technical issues quickly emerged with GFP use, however, as spectral wavelengths in the green range have limited penetration *in vivo* (1–5 mm in mammalian tissues for example) [246]. This issue inspired the development of a range of optimised and stabilised mutants of this gene emitting blue, cyan or yellow light. Moreover, novel sources of fluorescent proteins emitting light at the other end of the spectrum (orange, red and far-red) emerged [247]. With such a diverse collection of fluorescent proteins (each with unique emission wavelengths) available, the modern researcher is capable of simultaneously monitoring multiple targets.

A further issue with GFP is autofluorescence whereby molecules such as flavins, lipofuscin, NAPDH, collagens and elastins of connective tissues and the animal's food also fluoresce following application of an external light source. This confuses the output data. Autofluorescence undermines the signal-to-noise ratio with resultant poor quality imaging[248]. Moving to the far-red and near-infrared spectrum promises to ameliorate both the tissue penetration and autofluorescence limitations. Proteins that emit at longer wavelengths such as the DsRed derivative, mCherry and tdTomato, derived from Discosomastriata, are desirable as red light penetrates tissues more efficiently than green [249]. Further refinements geared towards *in vivo* imaging include the brighter mKate2 [247] and further red-shifted iRFP [250]. Indeed, the use of iterated somatic hyper-mutation to optimise monomeric red fluorescent proteins may advance FLI to the clinic [251].

Fluorescent dyes and Quantum dots Alternative options to fluorescent proteins include fluorescent dyes and quantum dots. Fluorescent dyes can be categorised as non-targeted or targeted probes [213]. Non-targeted probes are generally more amenable to tracking cellular therapies as they bind indiscriminately to the cellular membrane (phospholipid bilayer) when added to cells in suspension – efficacy has been demonstrated both *in vitro* and *in vivo* in conjunction with OI [252]. Targeted probes can be subdivided into simple targeting probes, cross-linking probes and enzyme-activatable, so-called “smart” probes. Targeted probes are more selective with fluorescence emanating only from defined cell populations that carry a specific functionality. Consequentially many targeted probes have derived from diagnostic endeavours [253].

Various inorganic and organic fluorophores for have been developed. Wavelength, quantum yield, photo- bleaching resistance, aggregation, stability, cell penetration, biocompatibility and toxicity are important criteria to consider. Quantum dots (QD) are robust, exhibit a large stokes shift and can emit at tuneable wavelengths. They are composed of fluorescent semiconductor cores (Au, Cd, Zn) embedded within an outer coating that defines their surface chemistry [254]. QDs offer many advantages over fluorescent proteins and dyes; autofluorescence is less of a concern and they permit greater sensitivity enabling single molecule detection. Due to their continuous broad absorption spectrum, multiplexing is possible whereby a single light source can be used to track multiple QDs [255,256]. Photobleaching is less problematic which gives rise to enhanced stability – QDs can remain fluorescent *in vivo* for months[257]. QDs are not without concerns however, particularly in terms of: 1) cytotoxicity as their heavy metal cores can oxidize and 2) tissue absorption of the excitation light which reduces the detectable fluorescence. An elegant solution to this latter issue has recently emerged however. It involves the use of "self-illuminating" QDs whereby the light source to excite the QD is *in situ* in the form of Renilla luciferase [258]. To offset toxicity, Li *et al* have recently produced photostable fluorescent organic dots with aggregation induced emission [259]. These dots contain a propeller shaped dye, non-emissive in solution, but highly fluorescent upon aggregation. When conjugated to the TAT cell penetration peptide, C6 tumour cells could be traced for 21 days *in vivo*.

While QDs may well be superior to fluorescent proteins and dyes, the poor signal-to-noise ratio remains the Achilles tendon of FLI, particularly in deeper tissue as the emergent signal fades. However plans are apace to overcome this limitation; the advent of "spectral unmixing" enables detection of separate wavelengths from different sources and thus minimisesautofluorescence [260]. Moreover newer imaging approaches such as fluorescence-mediated tomography make deep tissue imaging more plausible [261]. This uses fluorophores to create a volumetric model of an organ through reconstruction of multiple images formed from light transmitted through and scattered from the organ. While still in its infancy this approach shows promise in many contexts [262].

While the use of OI to advance novel therapies to the clinic has largely focused on pre-clinical work, robust examples of the use of OI in the clinical setting have emerged (figure 1.5). A multitude of studies have reported on the use of fluorescence-guided surgery with 5-aminolevulinic acid (5-ALA) for resection of malignant gliomas (reviewed in [263]). 5-ALA is a non-fluorescent prodrug that facilitates the accumulation of fluorescent porphyrins within malignant glioma cells. While 5-ALA had been granted orphan drug status as far back as 2002 it was not until 2007, when the positive results of a Phase III clinical trial emerged, that it was granted full authorisation under the tradename Gliolan®. This pivotal trial showed that complete resection of tumour was much more readily achievable with 5-ALA versus white light [264]. Furthermore 6-month progression free survival was significantly enhanced in the 5-ALA cohort (41% versus 21%).

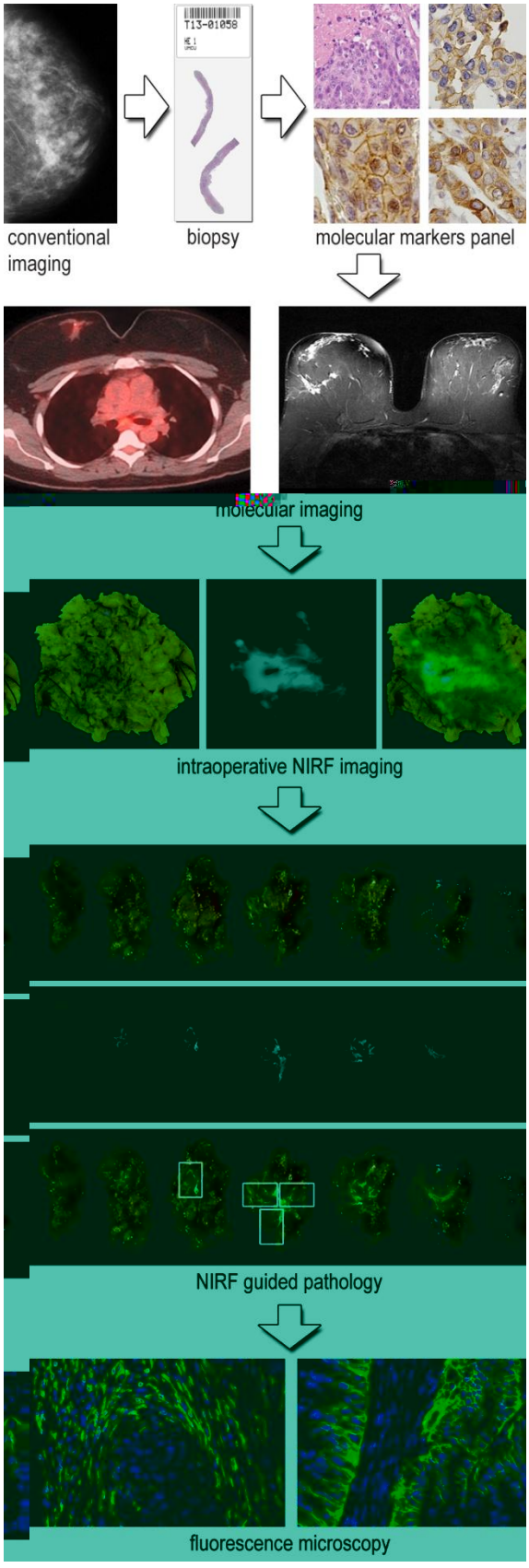
conventional imaging
biopsy
molecular markers panel
molecular imaging
intraoperative NIRF imaging
NIRF guided pathology
fluorescence microscopy

Figure 1.5: Fluorescence imaging from patient to surgeon to pathologist. After detection of a tumour with conventional imaging a biopsy of the tumour is taken. Expression of tumour-specific targets for molecular imaging can be determined by immunohistochemistry on the biopsy. Since targeted fluorescence tracers can have a long tissue stability without bleaching (simulated in this figure), the same tracer can be used for preoperative, intraoperative as well as postoperative localization of tumour cells, ranging from macro- to microscopic investigation of the tumour process. After formaldehyde tissue fixation the targeted fluorescent tracer is still visible for the pathologist for validation of pre- and intra-operative fluorescence imaging.

Troyan *et al*. undertook a first-in-human clinical trial using the FLARE intraoperative near-infrared (NIR) fluorescence imaging system [265]. This represented a significant advancement on previous studies which had used the same NIR fluorophore (indocyanine green) [266-271] as it permitted simultaneous visualisation of the surgical anatomy and used an improved fluorophore formulation. In the context of the underlying goal, to map sentinel lymph nodes in breast cancer patients, NIR fluorescence imaging was comparable to the current standard of care, ^{99m}Tc-lymphoscintigraphy. Following intra-tumoural injection of indocyanine green dissolved in human serum albumin no adverse effects were observed. This OI approach paves the way for greater clarity surrounding sentinel lymph node detection while avoiding use of ionising radiation.

Van Dam *et al*. employed intra-operative tumour-specific fluorescence imaging whereby a folate-FITC conjugate molecule was used to target folate-receptor-α which is over-expressed in epithelial ovarian cancer [272]. OI produced superior outcomes in terms of detection of tumour deposits with surgeons identifying a median of 34 deposits using fluorescence in contrast to a median of just 7 deposits by standard visual observation. In this context OI paves the way for enhanced surgical debulking and more accurate staging of disease with subsequent better patient outcomes. The intra-operative fluorescence imaging was consistent with *ex vivo* analysis of tissue sections. This study provides an important proof of principle regarding the monitoring of therapeutic interventions in humans. Not alone can surgical interventions be monitored, this identical approach lends itself to assessing efficacy of other therapeutic modalities such as chemotherapy and molecular based therapies. Furthermore by targeting different cellular receptors with a similarly designed ligand-fluorophore combination OI could be used to follow interventions in other cancer types and indeed other disease settings. Moreover the versatile and non-invasive nature of this approach could permit labelling of therapeutic entities such as monoclonal antibodies directly with FITC or similar molecules. This would provide invaluable data surrounding *in vivo* pharmacokinetics and pharmacodynamics and pave the way for iterative optimisation of such novel therapeutics.

In summary, OI has made a significant contribution to the advancement of novel therapeutics to the clinic. While both FLI and BLI are forms of optical imaging, the potential to translate these techniques (and the therapies they support)

to the clinic differs. FLI certainly has a place in advancing novel therapies to the clinic, but perhaps more in the pre-clinical stage as high background levels and poor tissue penetration of both input and output light sources restrict efficacy *in vivo*. In contrast, autoluminescence is almost nonexistent for BLI approaches leading to superior sensitivity. As few as 1-100 *FLuc2*–expressing cells can be detected *in vivo* whereas a minimum of 10,000 fluorescent cells are required [273]. Nevertheless, the need to genetically encode the bioluminescent source certainly hinders translation into the clinic. On the other hand FLI is substrate independent, a major advantage in the context of potential for clinical translation. Limitations aside, given the pace of advancements in the field, FLI could yet overtake BLI en route to the clinic.

The use of OI as an aid to surgical intervention continues to grow with the promise of greater acceptance and embracement of this non-invasive monitoring modality in clinical circles. Perpetual improvements in optical contrast agents paralleled with innovations in imaging technologies pave the way for the widespread utilisation of OI in the clinical drug discovery process. Indeed the possibility of harnessing OI to titrate the dose of novel gene and cell therapies safely and in real time in patients is no longer an intangible goal.

This thesis review explores the interaction between the immune system and cancer. A focus is placed primarily on two suppressive immune cell types - T_{Regs} and TAMs that undermine anti-tumour immunity and the rationale for targeting these cells in cancer is outlined. The merits of a novel, emerging therapeutic modality (RNAi) are discussed and the potential use of viral and bacterial gene therapy vectors in cancer is highlighted. Finally the potential role of optical imaging in advancing revolutionary novel therapies to the clinic is explored. Throughout the review future developments are hypothesised upon and clinical translatability is emphasised.

1. Beral V, Newton R. Overview of the epidemiology of immunodeficiency-associated cancers. *J Natl Cancer Inst Monogr* 1998**:** 1-6.

2. Rakhra K, Bachireddy P, Zabuawala T, Zeiser R, Xu L, Kopelman A *et al*. CD4(+) T cells contribute to the remodeling of the microenvironment required for sustained tumor regression upon oncogene inactivation. *Cancer Cell* 2010; **18:** 485-498.

3. Hanahan D, Weinberg RA. Hallmarks of cancer: the next generation. *Cell* 2011; **144:** 646-674.

4. Zou W. Immunosuppressive networks in the tumour environment and their therapeutic relevance. *Nat Rev Cancer* 2005; **5:** 263-274.

5. Vesely MD, Kershaw MH, Schreiber RD, Smyth MJ. Natural innate and adaptive immunity to cancer. *Annu Rev Immunol* 2010; **29:** 235-271.

6. Steer HJ, Lake RA, Nowak AK, Robinson BW. Harnessing the immune response to treat cancer. *Oncogene* 2010; **29:** 6301-6313.

7. Kryczek I, Zou L, Rodriguez P, Zhu G, Wei S, Mottram P *et al*. B7-H4 expression identifies a novel suppressive macrophage population in human ovarian carcinoma. *J Exp Med* 2006; **203:** 871-881.

8. Turk MJ, Guevara-Patino JA, Rizzuto GA, Engelhorn ME, Sakaguchi S, Houghton AN. Concomitant tumor immunity to a poorly immunogenic melanoma is prevented by regulatory T cells. *J Exp Med* 2004; **200:** 771-782.

9. Mougiakakos D, Choudhury A, Lladser A, Kiessling R, Johansson CC. Regulatory T cells in cancer. *Adv Cancer Res* 2010; **107:** 57-117.

10. Rasku MA, Clem AL, Telang S, Taft B, Gettings K, Gragg H *et al*. Transient T cell depletion causes regression of melanoma metastases. *J Transl Med* 2008; **6:** 12.

11. Whelan MC, Casey G, MacConmara M, Lederer JA, Soden D, Collins JK *et al*. Effective immunotherapy of weakly immunogenic solid tumours using a combined immunogene therapy and regulatory T-cell inactivation. *Cancer Gene Ther* 2010; **17:** 501-511.

12. Rech AJ, Vonderheide RH. Clinical use of anti-CD25 antibody daclizumab to enhance immune responses to tumor antigen vaccination by targeting regulatory T cells. *Ann N Y Acad Sci* 2009; **1174:** 99-106.

13. Ghiringhelli F, Menard C, Puig PE, Ladoire S, Roux S, Martin F *et al*. Metronomic cyclophosphamide regimen selectively depletes CD4+CD25+ regulatory T cells and restores T and NK effector functions in end stage cancer patients. *Cancer Immunol Immunother* 2007; **56:** 641-648.

14. Colombo MP, Piconese S. Regulatory-T-cell inhibition versus depletion: the right choice in cancer immunotherapy. *Nat Rev Cancer* 2007; **7:** 880-887.

15. Byrne WL, Mills KH, Lederer JA, O'Sullivan GC. Targeting regulatory T cells in cancer. *Cancer Res*; **71:** 6915-6920.

16. Fallarino F, Grohmann U, You S, McGrath BC, Cavener DR, Vacca C *et al*. The combined effects of tryptophan starvation and tryptophan catabolites down-regulate T cell receptor zeta-chain and induce a regulatory phenotype in naive T cells. *J Immunol* 2006; **176:** 6752-6761.

17. Hodi FS, O'Day SJ, McDermott DF, Weber RW, Sosman JA, Haanen JB *et al*. Improved survival with ipilimumab in patients with metastatic melanoma. *N Engl J Med* 2010; **363:** 711-723.

18. Khan S, Burt DJ, Ralph C, Thistlethwaite FC, Hawkins RE, Elkord E. Tremelimumab (anti-CTLA4) mediates immune responses mainly by direct activation of T effector cells rather than by affecting T regulatory cells. *Clin Immunol* 2010; **138:** 85-96.

19. Ko K, Yamazaki S, Nakamura K, Nishioka T, Hirota K, Yamaguchi T *et al*. Treatment of advanced tumors with agonistic anti-GITR mAb and its effects on tumor-infiltrating Foxp3+CD25+CD4+ regulatory T cells. *J Exp Med* 2005; **202:** 885-891.

20. Coe D, Begom S, Addey C, White M, Dyson J, Chai JG. Depletion of regulatory T cells by anti-GITR mAb as a novel mechanism for cancer immunotherapy. *Cancer Immunol Immunother* 2010; **59:** 1367-1377.

21. Cote AL, Zhang P, O'Sullivan JA, Jacobs VL, Clemis CR, Sakaguchi S *et al*. Stimulation of the glucocorticoid-induced TNF receptor family-related receptor on CD8 T cells induces protective and high-avidity T cell responses to tumor-specific antigens. *J Immunol* 2010; **186:** 275-283.

22. Tan W, Zhang W, Strasner A, Grivennikov S, Cheng JQ, Hoffman RM *et al*. Tumour-infiltrating regulatory T cells stimulate mammary cancer metastasis through RANKL-RANK signalling. *Nature* 2011; **470:** 548-553.

23. Amendola M, Passerini L, Pucci F, Gentner B, Bacchetta R, Naldini L. Regulated and multiple miRNA and siRNA delivery into primary cells by a lentiviral platform. *Mol Ther* 2009; **17:** 1039-1052.

24. Karanikas V, Speletas M, Zamanakou M, Kalala F, Loules G, Kerenidi T *et al*. Foxp3 expression in human cancer cells. *J Transl Med* 2008; **6:** 19.

25. Peng G, Guo Z, Kiniwa Y, Voo KS, Peng W, Fu T *et al*. Toll-like receptor 8-mediated reversal of CD4+ regulatory T cell function. *Science* 2005; **309:** 1380-1384.

26. Zhang Y, Luo F, Cai Y, Liu N, Wang L, Xu D *et al*. TLR1/TLR2 agonist induces tumor regression by reciprocal modulation of effector and regulatory T cells. *J Immunol* 2011; **186:** 1963-1969.

27. Conroy H, Marshall NA, Mills KH. TLR ligand suppression or enhancement of Treg cells? A double-edged sword in immunity to tumours. *Oncogene* 2008; **27:** 168-180.

28. Mandapathil M, Hilldorfer B, Szczepanski MJ, Czystowska M, Szajnik M, Ren J *et al*. Generation and accumulation of immunosuppressive adenosine by human CD4+CD25highFOXP3+ regulatory T cells. *J Biol Chem* 2010; **285:** 7176-7186.

29. Curiel TJ, Coukos G, Zou L, Alvarez X, Cheng P, Mottram P *et al*. Specific recruitment of regulatory T cells in ovarian carcinoma fosters immune privilege and predicts reduced survival. *Nat Med* 2004; **10:** 942-949.

30. Tan MC, Goedegebuure PS, Belt BA, Flaherty B, Sankpal N, Gillanders WE *et al*. Disruption of CCR5-dependent homing of regulatory T cells inhibits tumor growth in a murine model of pancreatic cancer. *J Immunol* 2009; **182:** 1746-1755.

31. Lee H, Kwon Y, Lee JH, Kim J, Shin MK, Kim SH *et al*. Methyl gallate exhibits potent antitumor activities by inhibiting tumor infiltration of CD4+CD25+ regulatory T cells. *J Immunol* 2010; **185:** 6698-6705.

32. Zhou L, Chong MM, Littman DR. Plasticity of CD4+ T cell lineage differentiation. *Immunity* 2009; **30:** 646-655.

33. Wang HY, Peng G, Guo Z, Shevach EM, Wang RF. Recognition of a new ARTC1 peptide ligand uniquely expressed in tumor cells by antigen-specific CD4+ regulatory T cells. *J Immunol* 2005; **174:** 2661-2670.

34. Bonertz A, Weitz J, Pietsch DH, Rahbari NN, Schlude C, Ge Y *et al*. Antigen-specific Tregs control T cell responses against a limited repertoire of tumor antigens in patients with colorectal carcinoma. *J Clin Invest* 2009; **119:** 3311-3321.

35. Vincent BG, Young EF, Buntzman AS, Stevens R, Kepler TB, Tisch RM *et al*. Toxin-coupled MHC class I tetramers can specifically ablate autoreactive CD8+ T cells and delay diabetes in nonobese diabetic mice. *J Immunol* 2010; **184:** 4196-4204.

36. Bowdish DM, Loffredo MS, Mukhopadhyay S, Mantovani A, Gordon S. Macrophage receptors implicated in the "adaptive" form of innate immunity. *Microbes Infect* 2007; **9:** 1680-1687.

37. Mantovani A. From phagocyte diversity and activation to probiotics: back to Metchnikoff. *Eur J Immunol* 2008; **38:** 3269-3273.

38. Biswas SK, Mantovani A. Macrophage plasticity and interaction with lymphocyte subsets: cancer as a paradigm. *Nat Immunol*; **11:** 889-896.

39. Gordon S, Taylor PR. Monocyte and macrophage heterogeneity. *Nat Rev Immunol* 2005; **5:** 953-964.

40. Mantovani A, Sozzani S, Locati M, Allavena P, Sica A. Macrophage polarization: tumor-associated macrophages as a paradigm for polarized M2 mononuclear phagocytes. *Trends Immunol* 2002; **23:** 549-555.

41. Stein M, Keshav S, Harris N, Gordon S. Interleukin 4 potently enhances murine macrophage mannose receptor activity: a marker of alternative immunologic macrophage activation. *J Exp Med* 1992; **176:** 287-292.

42. Martinez FO, Gordon S, Locati M, Mantovani A. Transcriptional profiling of the human monocyte-to-macrophage differentiation and polarization: new molecules and patterns of gene expression. *J Immunol* 2006; **177:** 7303-7311.

43. Chan G, Bivins-Smith ER, Smith MS, Smith PM, Yurochko AD. Transcriptome analysis reveals human cytomegalovirus reprograms monocyte differentiation toward an M1 macrophage. *J Immunol* 2008; **181:** 698-711.

44. Shaul ME, Bennett G, Strissel KJ, Greenberg AS, Obin MS. Dynamic, M2-like remodeling phenotypes of CD11c+ adipose tissue macrophages during high-fat diet--induced obesity in mice. *Diabetes*; **59:** 1171-1181.

45. Mosser DM, Edwards JP. Exploring the full spectrum of macrophage activation. *Nat Rev Immunol* 2008; **8:** 958-969.

46. Sica A, Bronte V. Altered macrophage differentiation and immune dysfunction in tumor development. *J Clin Invest* 2007; **117:** 1155-1166.

47. Lewis CE, Pollard JW. Distinct role of macrophages in different tumor microenvironments. *Cancer Res* 2006; **66:** 605-612.

48. Lin EY, Li JF, Gnatovskiy L, Deng Y, Zhu L, Grzesik DA *et al*. Macrophages regulate the angiogenic switch in a mouse model of breast cancer. *Cancer Res* 2006; **66:** 11238-11246.

49. Murdoch C, Muthana M, Coffelt SB, Lewis CE. The role of myeloid cells in the promotion of tumour angiogenesis. *Nat Rev Cancer* 2008; **8:** 618-631.

50. Savage ND, de Boer T, Walburg KV, Joosten SA, van Meijgaarden K, Geluk A *et al*. Human anti-inflammatory macrophages induce Foxp3+ GITR+ CD25+ regulatory T cells, which suppress via membrane-bound TGFbeta-1. *J Immunol* 2008; **181:** 2220-2226.

51. Tiemessen MM, Jagger AL, Evans HG, van Herwijnen MJ, John S, Taams LS. CD4+CD25+Foxp3+ regulatory T cells induce alternative activation of human monocytes/macrophages. *Proc Natl Acad Sci U S A* 2007; **104:** 19446-19451.

52. Liu G, Ma H, Qiu L, Li L, Cao Y, Ma J *et al*. Phenotypic and functional switch of macrophages induced by regulatory CD4+CD25+ T cells in mice. *Immunol Cell Biol*; **89:** 130-142.

53. Prasad DV, Richards S, Mai XM, Dong C. B7S1, a novel B7 family member that negatively regulates T cell activation. *Immunity* 2003; **18:** 863-873.

54. Sica GL, Choi IH, Zhu G, Tamada K, Wang SD, Tamura H *et al*. B7-H4, a molecule of the B7 family, negatively regulates T cell immunity. *Immunity* 2003; **18:** 849-861.

55. Zang X, Loke P, Kim J, Murphy K, Waitz R, Allison JP. B7x: a widely expressed B7 family member that inhibits T cell activation. *Proc Natl Acad Sci U S A* 2003; **100:** 10388-10392.

56. Kuang DM, Zhao Q, Peng C, Xu J, Zhang JP, Wu C *et al*. Activated monocytes in peritumoral stroma of hepatocellular carcinoma foster immune privilege and disease progression through PD-L1. *J Exp Med* 2009; **206:** 1327-1337.

57. Almeida R, Allshire RC. RNA silencing and genome regulation. *Trends Cell Biol* 2005; **15:** 251-258.

58. Krek A, Grun D, Poy MN, Wolf R, Rosenberg L, Epstein EJ *et al*. Combinatorial microRNA target predictions. *Nat Genet* 2005; **37:** 495-500.

59. Seyhan AA. RNAi: a potential new class of therapeutic for human genetic disease. *Hum Genet*; **130:** 583-605.

60. Perrimon N, Ni JQ, Perkins L. In vivo RNAi: today and tomorrow. *Cold Spring Harb Perspect Biol*; **2:** a003640.

61. de Fougerolles A, Vornlocher HP, Maraganore J, Lieberman J. Interfering with disease: a progress report on siRNA-based therapeutics. *Nat Rev Drug Discov* 2007; **6:** 443-453.

62. Kim YK, Kim VN. Processing of intronic microRNAs. *EMBO J* 2007; **26:** 775-783.

63. Lee Y, Ahn C, Han J, Choi H, Kim J, Yim J *et al*. The nuclear RNase III Drosha initiates microRNA processing. *Nature* 2003; **425:** 415-419.

64. Han J, Lee Y, Yeom KH, Kim YK, Jin H, Kim VN. The Drosha-DGCR8 complex in primary microRNA processing. *Genes Dev* 2004; **18:** 3016-3027.

65. Couto LB, High KA. Viral vector-mediated RNA interference. *Curr Opin Pharmacol*; **10:** 534-542.

66. Hock J, Meister G. The Argonaute protein family. *Genome Biol* 2008; **9:** 210.

67. Hutvagner G, Simard MJ. Argonaute proteins: key players in RNA silencing. *Nat Rev Mol Cell Biol* 2008; **9:** 22-32.

68. Hammond SM, Bernstein E, Beach D, Hannon GJ. An RNA-directed nuclease mediates post-transcriptional gene silencing in Drosophila cells. *Nature* 2000; **404:** 293-296.

69. Hutvagner G, McLachlan J, Pasquinelli AE, Balint E, Tuschl T, Zamore PD. A cellular function for the RNA-interference enzyme Dicer in the maturation of the let-7 small temporal RNA. *Science* 2001; **293:** 834-838.

70. Lewis BP, Shih IH, Jones-Rhoades MW, Bartel DP, Burge CB. Prediction of mammalian microRNA targets. *Cell* 2003; **115:** 787-798.

71. Aagaard L, Rossi JJ. RNAi therapeutics: principles, prospects and challenges. *Adv Drug Deliv Rev* 2007; **59:** 75-86.

72. DeVincenzo JP. Harnessing RNA interference to develop neonatal therapies: from Nobel Prize winning discovery to proof of concept clinical trials. *Early Hum Dev* 2009; **85:** S31-35.

73. Yekta S, Shih IH, Bartel DP. MicroRNA-directed cleavage of HOXB8 mRNA. *Science* 2004; **304:** 594-596.

74. Matranga C, Tomari Y, Shin C, Bartel DP, Zamore PD. Passenger-strand cleavage facilitates assembly of siRNA into Ago2-containing RNAi enzyme complexes. *Cell* 2005; **123:** 607-620.

75. Rand TA, Petersen S, Du F, Wang X. Argonaute2 cleaves the anti-guide strand of siRNA during RISC activation. *Cell* 2005; **123:** 621-629.

76. Schwarz DS, Hutvagner G, Du T, Xu Z, Aronin N, Zamore PD. Asymmetry in the assembly of the RNAi enzyme complex. *Cell* 2003; **115:** 199-208.

77. Song JJ, Smith SK, Hannon GJ, Joshua-Tor L. Crystal structure of Argonaute and its implications for RISC slicer activity. *Science* 2004; **305:** 1434-1437.

78. Zamore PD. Somatic piRNA biogenesis. *EMBO J*; **29:** 3219-3221.

79. Davidson BL, McCray PB, Jr. Current prospects for RNA interference-based therapies. *Nat Rev Genet*; **12:** 329-340.

80. Elbashir SM, Harborth J, Lendeckel W, Yalcin A, Weber K, Tuschl T. Duplexes of 21-nucleotide RNAs mediate RNA interference in cultured mammalian cells. *Nature* 2001; **411:** 494-498.

81. Khvorova A, Reynolds A, Jayasena SD. Functional siRNAs and miRNAs exhibit strand bias. *Cell* 2003; **115:** 209-216.

82. Behlke MA. Chemical modification of siRNAs for in vivo use. *Oligonucleotides* 2008; **18:** 305-319.

83. Whitehead KA, Langer R, Anderson DG. Knocking down barriers: advances in siRNA delivery. *Nat Rev Drug Discov* 2009; **8:** 129-138.

84. Sorensen DR, Leirdal M, Sioud M. Gene silencing by systemic delivery of synthetic siRNAs in adult mice. *J Mol Biol* 2003; **327:** 761-766.

85. Sioud M, Sorensen DR. Cationic liposome-mediated delivery of siRNAs in adult mice. *Biochem Biophys Res Commun* 2003; **312:** 1220-1225.

86. Soutschek J, Akinc A, Bramlage B, Charisse K, Constien R, Donoghue M *et al*. Therapeutic silencing of an endogenous gene by systemic administration of modified siRNAs. *Nature* 2004; **432:** 173-178.

87. Song E, Zhu P, Lee SK, Chowdhury D, Kussman S, Dykxhoorn DM *et al*. Antibody mediated in vivo delivery of small interfering RNAs via cell-surface receptors. *Nat Biotechnol* 2005; **23:** 709-717.

88. Hu-Lieskovan S, Heidel JD, Bartlett DW, Davis ME, Triche TJ. Sequence-specific knockdown of EWS-FLI1 by targeted, nonviral delivery of small interfering RNA inhibits tumor growth in a murine model of metastatic Ewing's sarcoma. *Cancer Res* 2005; **65:** 8984-8992.

89. McNamara JO, 2nd, Andrechek ER, Wang Y, Viles KD, Rempel RE, Gilboa E *et al*. Cell type-specific delivery of siRNAs with aptamer-siRNA chimeras. *Nat Biotechnol* 2006; **24:** 1005-1015.

90. Davis ME, Zuckerman JE, Choi CH, Seligson D, Tolcher A, Alabi CA *et al*. Evidence of RNAi in humans from systemically administered siRNA via targeted nanoparticles. *Nature*; **464:** 1067-1070.

91. Bartlett DW, Davis ME. Insights into the kinetics of siRNA-mediated gene silencing from live-cell and live-animal bioluminescent imaging. *Nucleic Acids Res* 2006; **34:** 322-333.

92. Boudreau RL, McBride JL, Martins I, Shen S, Xing Y, Carter BJ *et al*. Nonallele-specific silencing of mutant and wild-type huntingtin demonstrates

therapeutic efficacy in Huntington's disease mice. *Mol Ther* 2009; **17:** 1053-1063.

93. Brummelkamp TR, Bernards R, Agami R. A system for stable expression of short interfering RNAs in mammalian cells. *Science* 2002; **296:** 550-553.

94. Grimm D, Streetz KL, Jopling CL, Storm TA, Pandey K, Davis CR *et al*. Fatality in mice due to oversaturation of cellular microRNA/short hairpin RNA pathways. *Nature* 2006; **441:** 537-541.

95. McBride JL, Boudreau RL, Harper SQ, Staber PD, Monteys AM, Martins I *et al*. Artificial miRNAs mitigate shRNA-mediated toxicity in the brain: implications for the therapeutic development of RNAi. *Proc Natl Acad Sci U S A* 2008; **105:** 5868-5873.

96. An DS, Qin FX, Auyeung VC, Mao SH, Kung SK, Baltimore D *et al*. Optimization and functional effects of stable short hairpin RNA expression in primary human lymphocytes via lentiviral vectors. *Mol Ther* 2006; **14:** 494-504.

97. Liu YP, Berkhout B. miRNA cassettes in viral vectors: problems and solutions. *Biochim Biophys Acta*; **1809:** 732-745.

98. Georgiadis A, Tschernutter M, Bainbridge JW, Robbie SJ, McIntosh J, Nathwani AC *et al*. AAV-mediated knockdown of peripherin-2 in vivo using miRNA-based hairpins. *Gene Ther*; **17:** 486-493.

99. Lee Y, Kim M, Han J, Yeom KH, Lee S, Baek SH *et al*. MicroRNA genes are transcribed by RNA polymerase II. *EMBO J* 2004; **23:** 4051-4060.

100. Castanotto D, Sakurai K, Lingeman R, Li H, Shively L, Aagaard L *et al*. Combinatorial delivery of small interfering RNAs reduces RNAi efficacy by selective incorporation into RISC. *Nucleic Acids Res* 2007; **35:** 5154-5164.

101. Tiemann K, Rossi JJ. RNAi-based therapeutics-current status, challenges and prospects. *EMBO Mol Med* 2009; **1:** 142-151.

102. Chen CC, Ko TM, Ma HI, Wu HL, Xiao X, Li J *et al*. Long-term inhibition of hepatitis B virus in transgenic mice by double-stranded adeno-associated virus 8-delivered short hairpin RNA. *Gene Ther* 2007; **14:** 11-19.

103. Xia H, Mao Q, Paulson HL, Davidson BL. siRNA-mediated gene silencing in vitro and in vivo. *Nat Biotechnol* 2002; **20:** 1006-1010.

104. Grimm D, Wang L, Lee JS, Schurmann N, Gu S, Borner K *et al*. Argonaute proteins are key determinants of RNAi efficacy, toxicity, and persistence in the adult mouse liver. *J Clin Invest*; **120:** 3106-3119.

105. Jackson AL, Bartz SR, Schelter J, Kobayashi SV, Burchard J, Mao M *et al*. Expression profiling reveals off-target gene regulation by RNAi. *Nat Biotechnol* 2003; **21:** 635-637.

106. Fedorov Y, Anderson EM, Birmingham A, Reynolds A, Karpilow J, Robinson K *et al*. Off-target effects by siRNA can induce toxic phenotype. *RNA* 2006; **12:** 1188-1196.

107. Denovan-Wright EM, Rodriguez-Lebron E, Lewin AS, Mandel RJ. Unexpected off-targeting effects of anti-huntingtin ribozymes and siRNA in vivo. *Neurobiol Dis* 2008; **29:** 446-455.

108. Zhao HF, L'Abbe D, Jolicoeur N, Wu M, Li Z, Yu Z *et al*. High-throughput screening of effective siRNAs from RNAi libraries delivered via bacterial invasion. *Nat Methods* 2005; **2:** 967-973.

109. Birmingham A, Anderson EM, Reynolds A, Ilsley-Tyree D, Leake D, Fedorov Y *et al*. 3' UTR seed matches, but not overall identity, are associated with RNAi off-targets. *Nat Methods* 2006; **3:** 199-204.

110. Zimmermann TS, Lee AC, Akinc A, Bramlage B, Bumcrot D, Fedoruk MN *et al*. RNAi-mediated gene silencing in non-human primates. *Nature* 2006; **441:** 111-114.

111. Cullen BR. Is RNA interference involved in intrinsic antiviral immunity in mammals? *Nat Immunol* 2006; **7:** 563-567.

112. Liu YP, Haasnoot J, ter Brake O, Berkhout B, Konstantinova P. Inhibition of HIV-1 by multiple siRNAs expressed from a single microRNA polycistron. *Nucleic Acids Res* 2008; **36:** 2811-2824.

113. Judge AD, Sood V, Shaw JR, Fang D, McClintock K, MacLachlan I. Sequence-dependent stimulation of the mammalian innate immune response by synthetic siRNA. *Nat Biotechnol* 2005; **23:** 457-462.

114. Hornung V, Guenthner-Biller M, Bourquin C, Ablasser A, Schlee M, Uematsu S *et al*. Sequence-specific potent induction of IFN-alpha by short interfering RNA in plasmacytoid dendritic cells through TLR7. *Nat Med* 2005; **11:** 263-270.

115. Robbins M, Judge A, Liang L, McClintock K, Yaworski E, MacLachlan I. 2'-O-methyl-modified RNAs act as TLR7 antagonists. *Mol Ther* 2007; **15:** 1663-1669.

116. Chen J, Xie J. Progress on RNAi-based molecular medicines. *Int J Nanomedicine*; **7:** 3971-3980.

117. Urnov FD, Rebar EJ, Holmes MC, Zhang HS, Gregory PD. Genome editing with engineered zinc finger nucleases. *Nat Rev Genet*; **11:** 636-646.

118. Lu QL, Yokota T, Takeda S, Garcia L, Muntoni F, Partridge T. The status of exon skipping as a therapeutic approach to duchenne muscular dystrophy. *Mol Ther*; **19:** 9-15.

119. Janowski BA, Corey DR. Minireview: Switching on progesterone receptor expression with duplex RNA. *Mol Endocrinol*; **24:** 2243-2252.

120. Zhou J, Rossi JJ. Aptamer-targeted cell-specific RNA interference. *Silence*; **1:** 4.

121. Yla-Herttuala S. Endgame: glybera finally recommended for approval as the first gene therapy drug in the European union. *Mol Ther*; **20:** 1831-1832.

122. Chinese firm develops gene therapy injection. *The People's Daily*.

123. Ma GS, H. Hiroshima, K. Tada, Y. Suzuki, N. Tagawa, M. Gene medicine for cancer treatment: Commercially available medicine and accumulated clinical data in China. *Drug Design, Development and Therapy* 2008 115-122.

124. Raper SE, Chirmule N, Lee FS, Wivel NA, Bagg A, Gao GP *et al*. Fatal systemic inflammatory response syndrome in a ornithine transcarbamylase deficient patient following adenoviral gene transfer. *Mol Genet Metab* 2003; **80:** 148-158.

125. Cavazzana-Calvo M, Hacein-Bey S, de Saint Basile G, Gross F, Yvon E, Nusbaum P *et al*. Gene therapy of human severe combined immunodeficiency (SCID)-X1 disease. *Science* 2000; **288:** 669-672.

126. Verma IM. A tumultuous year for gene therapy. *Mol Ther* 2000; **2:** 415-416.

127. Kay MA. State-of-the-art gene-based therapies: the road ahead. *Nat Rev Genet*; **12:** 316-328.

128. Friedmann T. *The Development of Human Gene Therapy*. Cold Spring Harbor Laboratory Press: New York, 1999.

129. Templeton NSL, D. D. (2000) (eds) Gene Therapy: Therapeutic Mechanisms and Strategies (Marcel Dekker, Inc., New York). *Gene Therapy: Therapeutic Mechanisms and Strategies* Marcel Dekker: New York, 2000.

130. de Vrij J, Willemsen RA, Lindholm L, Hoeben RC. Adenovirus-Derived Vectors for Prostate Cancer Gene Therapy. *Hum Gene Ther* 2009.

131. Collins SA, Guinn BA, Harrison PT, Scallan MF, O'Sullivan GC, Tangney M. Viral vectors in cancer immunotherapy: which vector for which strategy? *Curr Gene Ther* 2008; **8:** 66-78.

132. Morrissey D, O'Sullivan, GC, Tangney, M. Tumour targeting with systemically administered bacteria. *Curr Gene Ther* 2010; **10**.

133. Tangney M, Gahan CG. Listeria Monocytogenes as a Vector for Anti-Cancer Therapies. *Curr Gene Ther* 2009.

134. Tangney M, Casey G, Larkin JO, Collins CG, Soden D, Cashman J *et al*. Non-viral in vivo immune gene therapy of cancer: combined strategies for treatment of systemic disease. *Cancer Immunol Immunother* 2006; **55:** 1443-1450.

135. Casey G, Cashman JP, Morrissey D, Whelan MC, Larkin JO, Soden DM *et al*. Sonoporation mediated immunogene therapy of solid tumours. *Ultrasound Med Biol* 2010.

136. Wen Y, Giri D, Yan DH, Spohn B, Zinner RG, Xia W *et al*. Prostate-specific antitumor activity by probasin promoter-directed p202 expression. *Mol Carcinog* 2003; **37:** 130-137.

137. Walsh M, Tangney M, O'Neill MJ, Larkin JO, Soden DM, McKenna SL *et al*. Evaluation of cellular uptake and gene transfer efficiency of pegylated poly-L-lysine compacted DNA: implications for cancer gene therapy. *Mol Pharm* 2006; **3:** 644-653.

138. Ahmad S, Casey G, Sweeney P, Tangney M, O'Sullivan GC. Optimised electroporation mediated DNA vaccination for treatment of prostate cancer *Genet Vaccines Ther* 2010; **8**.

139. Alton EW, Middleton PG, Caplen NJ, Smith SN, Steel DM, Munkonge FM *et al*. Non-invasive liposome-mediated gene delivery can correct the ion transport defect in cystic fibrosis mutant mice. *Nat Genet* 1993; **5:** 135-142.

140. Schenk E, Essand M, Bangma C. Clinical adenoviral gene therapy for prostate cancer. *Hum Gene Ther* 2009.

141. Cusack JC, Jr., Tanabe KK. Introduction to cancer gene therapy. *Surg Oncol Clin N Am* 2002; **11:** 497-519, v.

142. Lundstrom K. Latest development in viral vectors for gene therapy. *Trends Biotechnol* 2003; **21:** 117-122.

143. Thomas CE, Ehrhardt A, Kay MA. Progress and problems with the use of viral vectors for gene therapy. *Nat Rev Genet* 2003; **4:** 346-358.

144. Emtage PC, Wan Y, Hitt M, Graham FL, Muller WJ, Zlotnik A *et al*. Adenoviral vectors expressing lymphotactin and interleukin 2 or lymphotactin and interleukin 12 synergize to facilitate tumor regression in murine breast cancer models. *Hum Gene Ther* 1999; **10:** 697-709.

145. Nasu Y, Bangma CH, Hull GW, Lee HM, Hu J, Wang J *et al*. Adenovirus-mediated interleukin-12 gene therapy for prostate cancer: suppression of

orthotopic tumor growth and pre-established lung metastases in an orthotopic model. *Gene Ther* 1999; **6:** 338-349.

146. Li Q, Kay MA, Finegold M, Stratford-Perricaudet LD, Woo SL. Assessment of recombinant adenoviral vectors for hepatic gene therapy. *Hum Gene Ther* 1993; **4:** 403-409.

147. Quantin B, Perricaudet LD, Tajbakhsh S, Mandel JL. Adenovirus as an expression vector in muscle cells in vivo. *Proc Natl Acad Sci U S A* 1992; **89:** 2581-2584.

148. Kafri T, Morgan D, Krahl T, Sarvetnick N, Sherman L, Verma I. Cellular immune response to adenoviral vector infected cells does not require de novo viral gene expression: implications for gene therapy. *Proc Natl Acad Sci U S A* 1998; **95:** 11377-11382.

149. Mack CA, Song WR, Carpenter H, Wickham TJ, Kovesdi I, Harvey BG *et al*. Circumvention of anti-adenovirus neutralizing immunity by administration of an adenoviral vector of an alternate serotype. *Hum Gene Ther* 1997; **8:** 99-109.

150. Yang Y, Nunes FA, Berencsi K, Furth EE, Gonczol E, Wilson JM. Cellular immunity to viral antigens limits E1-deleted adenoviruses for gene therapy. *Proc Natl Acad Sci U S A* 1994; **91:** 4407-4411.

151. Raper SE, Yudkoff M, Chirmule N, Gao GP, Nunes F, Haskal ZJ *et al*. A pilot study of in vivo liver-directed gene transfer with an adenoviral vector in partial ornithine transcarbamylase deficiency. *Hum Gene Ther* 2002; **13:** 163-175.

152. Kochanek S, Clemens PR, Mitani K, Chen HH, Chan S, Caskey CT. A new adenoviral vector: Replacement of all viral coding sequences with 28 kb of DNA independently expressing both full-length dystrophin and beta-galactosidase. *Proc Natl Acad Sci U S A* 1996; **93:** 5731-5736.

153. Kochanek S, Schiedner G, Volpers C. High-capacity 'gutless' adenoviral vectors. *Curr Opin Mol Ther* 2001; **3:** 454-463.

154. Parks RJ, Chen L, Anton M, Sankar U, Rudnicki MA, Graham FL. A helper-dependent adenovirus vector system: removal of helper virus by Cre-mediated excision of the viral packaging signal. *Proc Natl Acad Sci U S A* 1996; **93:** 13565-13570.

155. Kelly Jnr. TJ. *Adenovirus DNA replication*. Plenum: New York, 1984, 271-308pp.

156. Le HT, Yu QC, Wilson JM, Croyle MA. Utility of PEGylated recombinant adeno-associated viruses for gene transfer. *J Control Release* 2005; **108:** 161-177.

157. Yotnda P, Chen DH, Chiu W, Piedra PA, Davis A, Templeton NS *et al*. Bilamellar cationic liposomes protect adenovectors from preexisting humoral immune responses. *Mol Ther* 2002; **5:** 233-241.

158. Croyle MA, Chirmule N, Zhang Y, Wilson JM. "Stealth" adenoviruses blunt cell-mediated and humoral immune responses against the virus and allow for significant gene expression upon readministration in the lung. *J Virol* 2001; **75:** 4792-4801.

159. Croyle MA, Chirmule N, Zhang Y, Wilson JM. PEGylation of E1-deleted adenovirus vectors allows significant gene expression on readministration to liver. *Hum Gene Ther* 2002; **13:** 1887-1900.

160. Croyle MA, Le HT, Linse KD, Cerullo V, Toietta G, Beaudet A *et al*. PEGylated helper-dependent adenoviral vectors: highly efficient vectors with an enhanced safety profile. *Gene Ther* 2005; **12:** 579-587.

161. Mok H, Palmer DJ, Ng P, Barry MA. Evaluation of polyethylene glycol modification of first-generation and helper-dependent adenoviral vectors to reduce innate immune responses. *Mol Ther* 2005; **11:** 66-79.

162. Cavazzana-Calvo M, Lagresle C, Hacein-Bey-Abina S, Fischer A. Gene therapy for severe combined immunodeficiency. *Annu Rev Med* 2005; **56:** 585-602.

163. Cavazzana-Calvo M, Fischer A. Efficacy of gene therapy for SCID is being confirmed. *Lancet* 2004; **364:** 2155-2156.

164. Check E. A tragic setback. *Nature* 2002; **420:** 116-118.

165. Pang S, Koyanagi Y, Miles S, Wiley C, Vinters HV, Chen IS. High levels of unintegrated HIV-1 DNA in brain tissue of AIDS dementia patients. *Nature* 1990; **343:** 85-89.

166. Pauza CD, Galindo JE, Richman DD. Reinfection results in accumulation of unintegrated viral DNA in cytopathic and persistent human immunodeficiency virus type 1 infection of CEM cells. *J Exp Med* 1990; **172:** 1035-1042.

167. Robinson HL, Zinkus DM. Accumulation of human immunodeficiency virus type 1 DNA in T cells: results of multiple infection events. *J Virol* 1990; **64:** 4836-4841.

168. Cara A, Reitz MS, Jr. New insight on the role of extrachromosomal retroviral DNA. *Leukemia* 1997; **11:** 1395-1399.

169. Terskikh AV, Ershler MA, Drize NJ, Nifontova IN, Chertkov JL. Long-term persistence of a nonintegrated lentiviral vector in mouse hematopoietic stem cells. *Exp Hematol* 2005; **33:** 873-882.

170. Brown HE, Chen H, Engelman A. Structure-based mutagenesis of the human immunodeficiency virus type 1 DNA attachment site: effects on integration and cDNA synthesis. *J Virol* 1999; **73:** 9011-9020.

171. Cereseto A, Manganaro L, Gutierrez MI, Terreni M, Fittipaldi A, Lusic M *et al*. Acetylation of HIV-1 integrase by p300 regulates viral integration. *Embo J* 2005; **24:** 3070-3081.

172. Johnson AA, Santos W, Pais GC, Marchand C, Amin R, Burke TR, Jr. *et al*. Integration requires a specific interaction of the donor DNA terminal 5'-cytosine with glutamine 148 of the HIV-1 integrase flexible loop. *J Biol Chem* 2006; **281:** 461-467.

173. Nightingale SJ, Hollis RP, Pepper KA, Petersen D, Yu XJ, Yang C *et al*. Transient gene expression by nonintegrating lentiviral vectors. *Mol Ther* 2006; **13:** 1121-1132.

174. Hazuda DJ, Young SD, Guare JP, Anthony NJ, Gomez RP, Wai JS *et al*. Integrase inhibitors and cellular immunity suppress retroviral replication in rhesus macaques. *Science* 2004; **305:** 528-532.

175. Hazuda DJ, Felock P, Witmer M, Wolfe A, Stillmock K, Grobler JA *et al*. Inhibitors of strand transfer that prevent integration and inhibit HIV-1 replication in cells. *Science* 2000; **287:** 646-650.

176. Baban CK, Cronin M, O'Hanlon D, O'Sullivan GC, Tangney M. Bacteria as vectors for gene therapy of cancer. *Bioeng Bugs*; **1:** 385-394.

177. Yuhua L, Kunyuan G, Hui C, Yongmei X, Chaoyang S, Xun T *et al*. Oral cytokine gene therapy against murine tumor using attenuated Salmonella typhimurium. *Int J Cancer* 2001; **94:** 438-443.

178. Maciag PC, Radulovic S, Rothman J. The first clinical use of a live-attenuated Listeria monocytogenes vaccine: a Phase I safety study of Lm-LLO-E7 in patients with advanced carcinoma of the cervix. *Vaccine* 2009; **27:** 3975-3983.

179. Patyar S, Joshi R, Byrav DS, Prakash A, Medhi B, Das BK. Bacteria in cancer therapy: a novel experimental strategy. *J Biomed Sci*; **17:** 21.

180. Bielecki J, Youngman P, Connelly P, Portnoy DA. Bacillus subtilis expressing a haemolysin gene from Listeria monocytogenes can grow in mammalian cells. *Nature* 1990; **345:** 175-176.

181. Grillot-Courvalin C, Goussard S, Huetz F, Ojcius DM, Courvalin P. Functional gene transfer from intracellular bacteria to mammalian cells. *Nat Biotechnol* 1998; **16:** 862-866.

182. Naldini L, Blomer U, Gage FH, Trono D, Verma IM. Efficient transfer, integration, and sustained long-term expression of the transgene in adult rat

brains injected with a lentiviral vector. *Proc Natl Acad Sci U S A* 1996; **93:** 11382-11388.

183. Naldini L, Blomer U, Gallay P, Ory D, Mulligan R, Gage FH *et al*. In vivo gene delivery and stable transduction of nondividing cells by a lentiviral vector. *Science* 1996; **272:** 263-267.

184. Kohn DB. Lentiviral vectors ready for prime-time. *Nat Biotechnol* 2007; **25:** 65-66.

185. Brown BD, Venneri MA, Zingale A, Sergi Sergi L, Naldini L. Endogenous microRNA regulation suppresses transgene expression in hematopoietic lineages and enables stable gene transfer. *Nat Med* 2006; **12:** 585-591.

186. Waehler R, Russell SJ, Curiel DT. Engineering targeted viral vectors for gene therapy. *Nat Rev Genet* 2007; **8:** 573-587.

187. Morizono K, Bristol G, Xie YM, Kung SK, Chen IS. Antibody-directed targeting of retroviral vectors via cell surface antigens. *J Virol* 2001; **75:** 8016-8020.

188. Morizono K, Chen IS. Targeted gene delivery by intravenous injection of retroviral vectors. *Cell Cycle* 2005; **4:** 854-856.

189. Morizono K, Xie Y, Ringpis GE, Johnson M, Nassanian H, Lee B *et al*. Lentiviral vector retargeting to P-glycoprotein on metastatic melanoma through intravenous injection. *Nat Med* 2005; **11:** 346-352.

190. Morizono K, Pariente N, Xie Y, Chen IS. Redirecting lentiviral vectors by insertion of integrin-tageting peptides into envelope proteins. *J Gene Med* 2009; **11:** 549-558.

191. Morizono K, Ku A, Xie Y, Harui A, Kung SK, Roth MD *et al*. Redirecting lentiviral vectors pseudotyped with Sindbis virus-derived envelope proteins to DC-SIGN by modification of N-linked glycans of envelope proteins. *J Virol*; **84:** 6923-6934.

192. Yang L, Bailey L, Baltimore D, Wang P. Targeting lentiviral vectors to specific cell types in vivo. *Proc Natl Acad Sci U S A* 2006; **103:** 11479-11484.

193. Yang L, Yang H, Rideout K, Cho T, Joo KI, Ziegler L *et al*. Engineered lentivector targeting of dendritic cells for in vivo immunization. *Nat Biotechnol* 2008; **26:** 326-334.

194. Yang H, Joo KI, Ziegler L, Wang P. Cell type-specific targeting with surface-engineered lentiviral vectors co-displaying OKT3 antibody and fusogenic molecule. *Pharm Res* 2009; **26:** 1432-1445.

195. Lei Y, Joo KI, Zarzar J, Wong C, Wang P. Targeting lentiviral vector to specific cell types through surface displayed single chain antibody and fusogenic molecule. *Virol J*; **7:** 35.

196. Lee CL, Dang J, Joo KI, Wang P. Engineered lentiviral vectors pseudotyped with a CD4 receptor and a fusogenic protein can target cells expressing HIV-1 envelope proteins. *Virus Res*; **160:** 340-350.

197. Moll M, Klenk HD, Maisner A. Importance of the cytoplasmic tails of the measles virus glycoproteins for fusogenic activity and the generation of recombinant measles viruses. *J Virol* 2002; **76:** 7174-7186.

198. Vongpunsawad S, Oezgun N, Braun W, Cattaneo R. Selectively receptor-blind measles viruses: Identification of residues necessary for SLAM- or CD46-induced fusion and their localization on a new hemagglutinin structural model. *J Virol* 2004; **78:** 302-313.

199. Nakamura T, Peng KW, Harvey M, Greiner S, Lorimer IA, James CD *et al*. Rescue and propagation of fully retargeted oncolytic measles viruses. *Nat Biotechnol* 2005; **23:** 209-214.

200. Funke S, Maisner A, Muhlebach MD, Koehl U, Grez M, Cattaneo R *et al*. Targeted cell entry of lentiviral vectors. *Mol Ther* 2008; **16:** 1427-1436.

201. Yanagi Y, Takeda M, Ohno S, Seki F. Measles virus receptors and tropism. *Jpn J Infect Dis* 2006; **59:** 1-5.

202. Anliker B, Abel T, Kneissl S, Hlavaty J, Caputi A, Brynza J *et al*. Specific gene transfer to neurons, endothelial cells and hematopoietic progenitors with lentiviral vectors. *Nat Methods*; **7:** 929-935.

203. Ageichik A, Buchholz CJ, Collins MK. Lentiviral vectors targeted to MHC II are effective in immunization. *Hum Gene Ther*; **22:** 1249-1254.

204. Nauts HC, Fowler GA, Bogatko FH. A review of the influence of bacterial infection and of bacterial products (Coley's toxins) on malignant tumors in man; a critical analysis of 30 inoperable cases treated by Coley's mixed toxins, in which diagnosis was confirmed by microscopic examination selected for special study. *Acta Med Scand Suppl* 1953; **276:** 1-103.

205. Wei MQ, Mengesha A, Good D, Anne J. Bacterial targeted tumour therapy-dawn of a new era. *Cancer Lett* 2008; **259:** 16-27.

206. Al-Mariri A, Tibor A, Lestrate P, Mertens P, De Bolle X, Letesson JJ. Yersinia enterocolitica as a vehicle for a naked DNA vaccine encoding Brucella abortus bacterioferritin or P39 antigen. *Infect Immun* 2002; **70:** 1915-1923.

207. Kasinskas RW, Forbes NS. Salmonella typhimurium lacking ribose chemoreceptors localize in tumor quiescence and induce apoptosis. *Cancer Res* 2007; **67:** 3201-3209.

208. Yu YA, Shabahang S, Timiryasova TM, Zhang Q, Beltz R, Gentschev I *et al*. Visualization of tumors and metastases in live animals with bacteria and vaccinia virus encoding light-emitting proteins. *Nat Biotechnol* 2004; **22:** 313-320.

209. Sznol M, Lin SL, Bermudes D, Zheng LM, King I. Use of preferentially replicating bacteria for the treatment of cancer. *J Clin Invest* 2000; **105:** 1027-1030.

210. Hollon T. Researchers and regulators reflect on first gene therapy death. *Nat Med* 2000; **6:** 6.

211. Amir-Aslani A, & Mangematin, V. The future of drug discovery and development: shifting emphasis towards personalized medicine. . *Technological Forecasting and Social Change,* 2010; **77:** 203-217.

212. Tangney M, Francis KP. In vivo optical imaging in gene & cell therapy. *Curr Gene Ther*; **12:** 2-11.

213. Sutton EJ, Henning TD, Pichler BJ, Bremer C, Daldrup-Link HE. Cell tracking with optical imaging. *Eur Radiol* 2008; **18:** 2021-2032.

214. Taruttis A, Ntziachristos V. Translational optical imaging. *AJR Am J Roentgenol*; **199:** 263-271.

215. Yang Y, Li X, Wang T, Kumavor PD, Aguirre A, Shung KK *et al*. Integrated optical coherence tomography, ultrasound and photoacoustic imaging for ovarian tissue characterization. *Biomed Opt Express*; **2:** 2551-2561.

216. Collins SA, Hiraoka K, Inagaki A, Kasahara N, Tangney M. PET imaging for gene & cell therapy. *Curr Gene Ther*; **12:** 20-32.

217. Bulte JW. In vivo MRI cell tracking: clinical studies. *AJR Am J Roentgenol* 2009; **193:** 314-325.

218. Byrne WL, Delille A, Kuo C, de Jong JS, van Dam GM, Francis KP *et al*. Use of optical imaging to progress novel therapeutics to the clinic. *J Control Release*.

219. Chuang K. Noninvasive Imaging of Reporter Gene Expression and Distribution In Vivo. *Fooyin J Health Sci* 2010; **2:** 1-11.

220. Jo Bsis-Vandervliet FF. Discovery of the near-infrared window into the body and the early development of near-infrared spectroscopy. *J Biomed Opt* 1999; **4:** 392-396.

221. Smith AM, Mancini MC, Nie S. Bioimaging: second window for in vivo imaging. *Nat Nanotechnol* 2009; **4:** 710-711.

222. Tuchin V. Tissue Optics: Light Scattering Methods and Instruments for Medical Diagnosis *The International Society for Optical Engineering, 2000*; Bellingham, WA.

223. Rice BW, Cable MD, Nelson MB. In vivo imaging of light-emitting probes. *J Biomed Opt* 2001; **6:** 432-440.

224. Boas D, Culver J, Stott J, Dunn A. Three dimensional Monte Carlo code for photon migration through complex heterogeneous media including the adult human head. *Opt Express* 2002; **10:** 159-170.

225. Fang Q. Mesh-based Monte Carlo method using fast ray-tracing in Plucker coordinates. *Biomed Opt Express*; **1:** 165-175.

226. Arridge SR, Schweiger M, Hiraoka M, Delpy DT. A finite element approach for modeling photon transport in tissue. *Med Phys* 1993; **20:** 299-309.

227. Dehghani H, Srinivasan S, Pogue BW, Gibson A. Numerical modelling and image reconstruction in diffuse optical tomography. *Philos Transact A Math Phys Eng Sci* 2009; **367:** 3073-3093.

228. Pogue BW, Geimer S, McBride TO, Jiang S, Osterberg UL, Paulsen KD. Three-dimensional simulation of near-infrared diffusion in tissue: boundary condition and geometry analysis for finite-element image reconstruction. *Appl Opt* 2001; **40:** 588-600.

229. Ahn S, Chaudhari AJ, Darvas F, Bouman CA, Leahy RM. Fast iterative image reconstruction methods for fully 3D multispectral bioluminescence tomography. *Phys Med Biol* 2008; **53:** 3921-3942.

230. Kuo C, Coquoz O, Troy TL, Xu H, Rice BW. Three-dimensional reconstruction of in vivo bioluminescent sources based on multispectral imaging. *J Biomed Opt* 2007; **12:** 024007.

231. Meyer H, Garofalakis A, Zacharakis G, Psycharakis S, Mamalaki C, Kioussis D *et al*. Noncontact optical imaging in mice with full angular coverage and automatic surface extraction. *Appl Opt* 2007; **46:** 3617-3627.

232. Klose AD, Beattie BJ, Dehghani H, Vider L, Le C, Ponomarev V *et al*. In vivo bioluminescence tomography with a blocking-off finite-difference SP3 method and MRI/CT coregistration. *Med Phys*; **37:** 329-338.

233. Wang G, Li Y, Jiang M. Uniqueness theorems in bioluminescence tomography. *Med Phys* 2004; **31:** 2289-2299.

234. Dehghani H, Davis SC, Jiang S, Pogue BW, Paulsen KD, Patterson MS. Spectrally resolved bioluminescence optical tomography. *Opt Lett* 2006; **31:** 365-367.

235. Dutta J, Ahn S, Joshi AA, Leahy RM. Illumination pattern optimization for fluorescence tomography: theory and simulation studies. *Phys Med Biol*; **55:** 2961-2982.

236. Morrissey D, O'Sullivan GC, Tangney M. Tumour targeting with systemically administered bacteria. *Curr Gene Ther*; **10:** 3-14.

237. Tangney M, Gahan CG. Editorial [Hot Topic: Bacterial Vectors for Gene & Cell Therapy]. *Curr Gene Ther*; **10:** 1-2.

238. Cronin M, Morrissey D, Rajendran S, El Mashad SM, van Sinderen D, O'Sullivan GC *et al*. Orally administered bifidobacteria as vehicles for delivery of agents to systemic tumors. *Mol Ther*; **18:** 1397-1407.

239. Conn PM. Methods in Enzymology. Preface. *Methods Enzymol*; **506:** xxi.

240. Waerzeggers Y, Monfared P, Viel T, Winkeler A, Voges J, Jacobs AH. Methods to monitor gene therapy with molecular imaging. *Methods* 2009; **48:** 146-160.

241. Wu JC, Inubushi M, Sundaresan G, Schelbert HR, Gambhir SS. Optical imaging of cardiac reporter gene expression in living rats. *Circulation* 2002; **105:** 1631-1634.

242. Li HJ, Everts M, Yamamoto M, Curiel DT, Herschman HR. Combined transductional untargeting/retargeting and transcriptional restriction enhances adenovirus gene targeting and therapy for hepatic colorectal cancer tumors. *Cancer Res* 2009; **69:** 554-564.

243. Sato M, Johnson M, Zhang L, Zhang B, Le K, Gambhir SS *et al*. Optimization of adenoviral vectors to direct highly amplified prostate-specific expression for imaging and gene therapy. *Mol Ther* 2003; **8:** 726-737.

244. Mehta SR, Huang R, Yang M, Zhang XQ, Kolli B, Chang KP *et al*. Real-time in vivo green fluorescent protein imaging of a murine leishmaniasis model as a new tool for Leishmania vaccine and drug discovery. *Clin Vaccine Immunol* 2008; **15:** 1764-1770.

245. Kong Y, Subbian S, Cirillo SL, Cirillo JD. Application of optical imaging to study of extrapulmonary spread by tuberculosis. *Tuberculosis (Edinb)* 2009; **89 Suppl 1:** S15-17.

246. Min J. Molecular Imaging of Biological Gene Delivery Vehicles for Targeted Cancer Therapy: Beyond Viral Vectors. *Nuclear Medicine and Molecular Imaging* 2010; **44:** 15-24.

247. Kremers GJ, Gilbert SG, Cranfill PJ, Davidson MW, Piston DW. Fluorescent proteins at a glance. *J Cell Sci*; **124:** 157-160.

248. Ntziachristos V, Ripoll J, Wang LV, Weissleder R. Looking and listening to light: the evolution of whole-body photonic imaging. *Nat Biotechnol* 2005; **23:** 313-320.

249. Shaner NC, Campbell RE, Steinbach PA, Giepmans BN, Palmer AE, Tsien RY. Improved monomeric red, orange and yellow fluorescent proteins derived from Discosoma sp. red fluorescent protein. *Nat Biotechnol* 2004; **22:** 1567-1572.

250. Filonov GS, Piatkevich KD, Ting LM, Zhang J, Kim K, Verkhusha VV. Bright and stable near-infrared fluorescent protein for in vivo imaging. *Nat Biotechnol*; **29:** 757-761.

251. Wang L, Jackson WC, Steinbach PA, Tsien RY. Evolution of new nonantibody proteins via iterative somatic hypermutation. *Proc Natl Acad Sci U S A* 2004; **101:** 16745-16749.

252. Giepmans BN, Adams SR, Ellisman MH, Tsien RY. The fluorescent toolbox for assessing protein location and function. *Science* 2006; **312:** 217-224.

253. Tung CH. Fluorescent peptide probes for in vivo diagnostic imaging. *Biopolymers* 2004; **76:** 391-403.

254. Kirchner C, Liedl T, Kudera S, Pellegrino T, Munoz Javier A, Gaub HE *et al*. Cytotoxicity of colloidal CdSe and CdSe/ZnS nanoparticles. *Nano Lett* 2005; **5:** 331-338.

255. Jaiswal JK, Mattoussi H, Mauro JM, Simon SM. Long-term multiple color imaging of live cells using quantum dot bioconjugates. *Nat Biotechnol* 2003; **21:** 47-51.

256. Smith AM, Dave S, Nie S, True L, Gao X. Multicolor quantum dots for molecular diagnostics of cancer. *Expert Rev Mol Diagn* 2006; **6:** 231-244.

257. Michalet X, Pinaud FF, Bentolila LA, Tsay JM, Doose S, Li JJ *et al*. Quantum dots for live cells, in vivo imaging, and diagnostics. *Science* 2005; **307:** 538-544.

258. Loening AM, Fenn TD, Wu AM, Gambhir SS. Consensus guided mutagenesis of Renilla luciferase yields enhanced stability and light output. *Protein Eng Des Sel* 2006; **19:** 391-400.

259. Li K, Qin W, Ding D, Tomczak N, Geng J, Liu R *et al*. Photostable fluorescent organic dots with aggregation-induced emission (AIE dots) for noninvasive long-term cell tracing. *Sci Rep*; **3:** 1150.

260. Levenson RM, Lynch DT, Kobayashi H, Backer JM, Backer MV. Multiplexing with multispectral imaging: from mice to microscopy. *ILAR J* 2008; **49:** 78-88.

261. Ntziachristos V, Tung CH, Bremer C, Weissleder R. Fluorescence molecular tomography resolves protease activity in vivo. *Nat Med* 2002; **8:** 757-760.

262. Shah K. Current advances in molecular imaging of gene and cell therapy for cancer. *Cancer Biol Ther* 2005; **4:** 518-523.

263. Hefti M. Fluorescence-guided surgery for malignant glioma: a review on aminolevulinic acid induced protoporphyrin IX photodynamic diagnostic in brain tumors. *Curr Med Imaging Rev* 2010**:** 1-5.

264. Stummer W, Pichlmeier U, Meinel T, Wiestler OD, Zanella F, Reulen HJ. Fluorescence-guided surgery with 5-aminolevulinic acid for resection of malignant glioma: a randomised controlled multicentre phase III trial. *Lancet Oncol* 2006; **7:** 392-401.

265. Troyan SL, Kianzad V, Gibbs-Strauss SL, Gioux S, Matsui A, Oketokoun R *et al*. The FLARE intraoperative near-infrared fluorescence imaging system: a first-in-human clinical trial in breast cancer sentinel lymph node mapping. *Ann Surg Oncol* 2009; **16:** 2943-2952.

266. Fujiwara M, Mizukami T, Suzuki A, Fukamizu H. Sentinel lymph node detection in skin cancer patients using real-time fluorescence navigation with indocyanine green: preliminary experience. *J Plast Reconstr Aesthet Surg* 2009; **62:** e373-378.

267. Kitai T, Inomoto T, Miwa M, Shikayama T. Fluorescence navigation with indocyanine green for detecting sentinel lymph nodes in breast cancer. *Breast Cancer* 2005; **12:** 211-215.

268. Kusano M, Tajima Y, Yamazaki K, Kato M, Watanabe M, Miwa M. Sentinel node mapping guided by indocyanine green fluorescence imaging: a new method for sentinel node navigation surgery in gastrointestinal cancer. *Dig Surg* 2008; **25:** 103-108.

269. Miyashiro I, Miyoshi N, Hiratsuka M, Kishi K, Yamada T, Ohue M *et al*. Detection of sentinel node in gastric cancer surgery by indocyanine green fluorescence imaging: comparison with infrared imaging. *Ann Surg Oncol* 2008; **15:** 1640-1643.

270. Ogasawara Y, Ikeda H, Takahashi M, Kawasaki K, Doihara H. Evaluation of breast lymphatic pathways with indocyanine green fluorescence imaging in patients with breast cancer. *World J Surg* 2008; **32:** 1924-1929.

271. Sevick-Muraca EM, Sharma R, Rasmussen JC, Marshall MV, Wendt JA, Pham HQ *et al*. Imaging of lymph flow in breast cancer patients after

microdose administration of a near-infrared fluorophore: feasibility study. *Radiology* 2008; **246:** 734-741.

272. van Dam GM, Themelis G, Crane LM, Harlaar NJ, Pleijhuis RG, Kelder W *et al*. Intraoperative tumor-specific fluorescence imaging in ovarian cancer by folate receptor-alpha targeting: first in-human results. *Nat Med*; **17:** 1315-1319.

273. Kim JB, Urban K, Cochran E, Lee S, Ang A, Rice B *et al*. Non-invasive detection of a small number of bioluminescent cancer cells in vivo. *PLoS One*; **5:** e9364.

RNAi is a useful experimental tool on the cusp of clinical translation into a new therapeutic modality. RNAi-based therapeutics have the potential to improve on existing small molecule and antibody/protein-based therapeutics, for various strategies, including tumour immunotherapy. T_{Regs} are recognised as the predominant cell mediating suppression of anti-tumour immunity, and mouse FOXP3 (mFOXP3) has been identified as a central target for their manipulation in the mouse. In this chapter, mFOXP3 was targeted by RNAi with the long term goal of abrogating the suppressive contribution of T_{Regs} within the tumour microenvironment and enhancing anti-tumour immunity.

An *in vitro* mFOXP3 expression assay was developed and optimised. Examination of an endogenous miRNA (miR-31), which was previously shown to knockdown expression of the human version of this gene, failed to knockdown mFOXP3 expression. Attention was then focused on the design and validation of a novel RNAi mediator against mFOXP3. Various candidate RNAi mediators were designed and tested, and two candidates confirmed to significantly silence mFOXP3.

T_{Regs} are considered the most powerful inhibitors of anti-tumour immunity and the greatest barrier to successful immunotherapy [1].The primary goal of this project was to abrogate the suppression of anti-tumour immunity mediated by $T_{Regs.}$ Various strategies exist for T_{Reg} modulation [2]. Simple T_{Reg} ablation strategies have been shown to be ineffective as T_{Reg} numbers are quickly replenished by conversion of effector $CD4^+$ cells [3]. Thus a therapeutic modality which does not destroy this subset but rather induces a functional dormancy while leaving the cells *in situ* is desirable. RNA interference fulfils these criteria.

RNAi has been previously explored as a method to manipulate T_{Regs} (both mouse and human) via a variety of targets. Silencing of tumour necrosis factor-α induced protein 8 like-2 (TNFAIP8L2, TIPE2) in naturally occurring T_{Regs} isolated from murine spleens led to downregulation of FOXP3 and CTLA-4 as well as a reduction in secreted cytokines (TGF-β and IL-10)[4]. Subsequently, T-cell proliferation and differentiation were boosted. Elsewhere, silencing of Eos in T_{Regs} abrogated their ability to suppress immune responses and endowed them with partial effector function [5]. Eos, a zinc-finger transcription factor, was found to interact directly with FOXP3, inducing chromatin modifications that result in gene silencing in T_{Regs} and leading to their suppressive phenotype.

FOXP3 has been previously referred to as a master regulator of T_{Regs}[6,7]. Indeed, high level overexpression of FOXP3 has been shown to confer suppressive capacity to human T cells [8]. Furthermore, numerous reports have attested that inhibition of FOXP3 abolishes the suppressor phenotype of both mouse and human T_{Regs}. Lentiviral vector delivery of an artificial miRNA construct against FOXP3 to primary human T_{Regs} in culture reversed their anergic/suppressive phenotype as measured by mixed leukocyte reaction [9]. More recently, human T_{Reg} inhibition using a morpholino oligomer targeting FOXP3 was shown to enhance generation of antigen-specific T cells in response to peptide stimulation [10]. Similar evidence exists for mouse T_{Regs}, where lentiviral-mediated FOXP3 RNAi was shown to hinder growth of a regulatory T cell-like leukaemia cell line [11]. This suppression of growth was shown to be an indirect effect as the RNAi-treated leukaemia developed at the same pace in an immuno-deficient animal. It is suggested that silencing of FOXP3 reduces secretion of suppressive cytokines which facilitates an enhanced immune

response. This evidence supported the selection of FOXP3 as a target gene for RNAi-mediated T_{Reg} inhibition.

In the human setting, an endogenous miRNA has previously been shown to silence hFOXP3. miRNAs are indispensable for the correct development and function of T_{Regs} [12]. Abolition of Dicer, the RNAse III enzyme that generates functional miRNAs abrogates their suppressive capability and leads to autoimmune pathology [13,14]. Ideally, the chosen miRNA would function specifically in T_{Regs} without modulating other cell populations. A previous miRNA signature for human T_{Regs} identified miR-31 to be expressed at much lower levels in T_{Regs} relative to other $CD4^+$ T cells [15]. Moreover, a functional target site for miR-31 was identified in the 3'UTR of human FOXP3 mRNA and miR-31 was confirmed to silence human FOXP3 expression.

The aim of this study was to identify and validate an RNAi mediator capable of specific silencing of mFOXP3.

Two independent bioinformatic databases were explored to verify an interaction between miR-31 and mFOXP3. They included the recently developed miRanda-mirSVR algorithm (www.microRNA.org) [16-19] and DIANA-microT [20].

The original strategy for this thesis work involved adeno-associated virus (AAV) as the delivery vector. Thus, to facilitate production of AAV particles carrying miR-31 the sequence was cloned into the pAAV-MCS plasmid (Stratagene – Agilent Technologies). pAAV-miR-31 was generated as follows; the miR-31 fragment was amplified from the parent plasmid, pCDH-CMV-MIR31-EF1-copGFP (Systems Biosciences) using two primers: miR-For (5'-AGCAGCATCGATGAATTC-3') and miR-Rev (5'- AGCAGCGGATCCAGCGA-3'). The miR-31 fragment was gel extracted using the QIAquick Gel Extraction Kit (Qiagen) and purified using the QIAquick PCR Purification Kit (Qiagen). The 518 bp miR-31 fragment was digested with *ClaI* and *BamHI* and subcloned into the pAAV-MCS plasmid which had been digested with the same enzymes.

HeLa cells were maintained in RPMI 1640 medium (Sigma-Aldrich) supplemented with 10% v/v fetal bovine serum and 2mM L-glutamine in a 37^0C incubator with 5% CO_2.

pCDH-CMV-MIR31-EF1-copGFP carrying pre-microRNA-31 (pmiR-31) and its backbone equivalent (pCDH-CMV-EF1-copGFP) (pmiR-BB**)** were both purchased from Systems Biosciences. Novel RNAi mediators targeting mFOXP3 mRNA transcript variant 2 (Accession # NM_054039.2) were designed using the Block-iT^{TM} miR RNAi Select Tool (Invitrogen). The mature miR sequence for each candidate RNAi mediator was discerned and a 3' "G" (derived from native miR-155)

was added (see section 3.4.2). The mature miR sequence and its complementary strand were synthesised as a 22 bp duplex siRNA (Qiagen). The two candidates were designated mimic #2 and mimic #4 to acknowledge their derivation from the longer pre-microRNA oligos. The mimics had the following sequences;
mimic #2: 5’ AATTCATCTACGGTCCACACTG 3’
mimic #4: 5’ AAACTCTTCTGGCTCCTCGAAG 3’

No suitable cell line that stably expressed mFOXP3 was available. Thus, to facilitate development of an expression assay, both the target FOXP3 gene and miR-31 were artificially introduced by transfection. HeLa cells were co-transfected with a miRNA 3' UTR target clone for FOXP3 (either mouse or human) in a Firefly luciferase reporter vector (Genecopoeia) and either pmiR-31 or pmiR-BB. $2.5x10^6$ cells in 10 ml media were seeded in a 58 cm^2 tissue culture plate 24 h prior to transfection. 10 µg each plasmid was diluted in serum-free media and incubated with 20 µl Turbofect™ (Fermentas) for 15 min. 1 ml of transfection mixture was then added to the cells. After 24 h of culture, cells were lysed using 2 ml reporter lysis buffer (Promega). 100 µl cell lysate was mixed with 100 µl luciferin substrate (Promega) and luminescence read using a luminometer. Knockdown of FOXP3 could be detected as a reduction in luminescence.

To verify that the pmiR-31 plasmid was functional and that the pre-microRNA was correctly processed intra-cellularly, mature miR-31 was detected by RT-PCR. Total cellular RNA was extracted using the miRNeasy Mini Kit (Qiagen) and subjected to on-column DNase treatment with the RNase-Free DNase Set (Qiagen). cDNA synthesis was performed with 1µg of total RNA using the miScript Reverse Transcription Kit and PCR detection carried out using the miScript SYBR Green PCR Kit combined with miScript Primer Assays (all Qiagen). cDNA synthesis was assumed to be 100% efficient such that 1µg of RNA yielded 1µg of cDNA. 15 ng of cDNA template in a 20 µl volume was used per PCR reaction under the following

conditions; 15 min pre-incubation at 95^0C, followed by 50 cycles of 15 s at 94^0C, 30 s at 55^0C, 30 s at 70^0C. 15 ng of RNA template was also subjected to PCR amplification as a control for amplification of genomic DNA. Water template served as a negative control while a miScript miRNA Mimic of miR-31 (Qiagen) served as a positive control for the PCR reaction. All samples were normalised against the widely used endogenous house-keeping miRNA RNU6B [21].

Quantitative PCR was carried out using the "Delta-Delta" mathematical technique as previously described [22]. This technique involves normalising the amount of transcript of interest (miR-31 in this case) against an internal control transcript (RNU6B in this case) for each sample. This controls for variations in the amount of template between different samples. Following this internal normalisation each treatment sample ("backbone plasmid" or "miR-31 plasmid" in this experiment) was normalised against a control sample ("untransfected") to indicate the fold change in expression as a consequence of the different interventions. To carry out these calculations the crossing point (Cp) was determined for each transcript using a Lightcycler machine (Roche). Cp represents the point at which fluorescence increases above background noise – the Cp value is inversely proportional to the amount of a specific mRNA/miRNA species in the sample from which the cDNA was derived. The following formula was employed to determine the fold change in miR-31 expression between the "miR-31 plasmid" and "untransfected" samples and represents an example;

Expression ratio = $2^{-[\Delta Cp \text{ "miR-31 plasmid" (Cp miR-31-Cp RNU6B)} - \Delta Cp \text{ "untransfected" (Cp miR-31-Cp RNU6B)]}}$

where 2 = the efficiency of the PCR reaction.

To confirm transfection of various siRNAs and miRNA mimics an siGLO® transfection indicator (Thermo Scientific) was used. $1x10^5$ HeLa cells were seeded per well of a 24-well plate 24 h in advance of transfection. 1 µl Lipofectamine (Invitrogen) was diluted in 50 µl serum-free media and an appropriate volume of siRNA was diluted to 50 µl with serum-free media in a separate tube. The tubes were incubated at room temperature for 5 min, combined and incubated for a further 20 min. The 100 µl mixture was then added to the well to be transfected. The final

concentration of siRNA per well was 50 nM. After 24 h transfected cells were viewed under an inverted fluorescent microscope as a qualitative indicator of siGLO® delivery. Fluorescence-activated cell sorting (FACS) was performed using a BD LSR II instrument (BD Biosciences) to determine quantitatively the transfection efficiency. The siGLO® transfection indicator could be detected in the green 488-2 channel.

EGFP

As a positive control for the *in vitro* system the gene encoding the enhanced green fluorescent protein (EGFP) was silenced using a commercially available siRNA. pIRES2-EGFP-mFOXP3 (pFOXP3) (generated by Dr Garret Casey, Cork Cancer Research Centre) was transfected using Turbofect™ (Fermentas) as outlined above and provided the target *EGFP* gene. GFP-22 siRNA was purchased from Qiagen along with a negative control siRNA (Allstars Negative Control siRNA). Both siRNAs were delivered using Lipofectamine (Invitrogen) as previously outlined. Cells were prepared for FACS where EGFP expression was detected at 509 nm (488-2 channel). Data was presented as the total number of cells expressing the relevant protein. To allow for the fact that gene silencing is not an absolute phenomenon (i.e. cells are not just positive or negative for protein expression) knockdown data was also presented as a tiered level of expression; high, medium and negative.

Mimic #2 and mimic #4 were introduced into HeLa cells using Lipofectamine as previously described. To maintain consistency and to harness the benefits of an optimised transfection protocol, the same plasmid (pFOXP3) used as the source of EGFP (section 2.4.8) was used as the source of mFOXP3. The IRES sequence within pFOXP3 afforded the opportunity to observe gene knockdown by detection of either mFOXP3 (with a conjugated antibody) or EGFP (directly). As the long term goal was to investigate endogenous mFOXP3 *in vivo* it was deemed prudent to develop a direct mFOXP3 protein detection assay from the outset and to use in this *in vitro* assay. pFOXP3 was transfected using Turbofect™. Knockdown efficiency was determined by FACS at 578 nm (PE channel) using a PE-conjugated anti-mouse/rat

FOXP3 antibody (clone FJK-16a) (0.5 µg/test) and a PE-conjugated Rat IgG2a isotype control (clone eBR2a) (both eBioscience).

To show that the two RNAi candidate molecules were target specific they were assessed on their ability to silence expression of an irrelevant target gene – the EGFP reporter. pIRES2-EGFP was used to supply the EGFP target, GFP-22 siRNA as a positive control and Allstars Negative Control siRNA. All nucleic acids were delivered as previously outlined and EGFP expression was determined by FACS as before.

For FACS analysis all cells were trypsinised, washed once and resuspended in PBS. All cells were then fixed in a 2% para-formaldehyde solution for a minimum of 1 h on ice. For detection of EGFP, cells were recovered and resuspended in 200 µl of PBS. For detection of non-fluorescent intracellular proteins (e.g. FOXP3) cells were washed once in permeabilisation buffer (0.1% Triton, 0.1% sodium azide, 10 mM HEPES, 4% FCS, 150 mM NaCl). They were then incubated with the relevant antibody made up in permeabilisation buffer for 1 h on ice. Following recovery cells were resuspended in 200 µl of PBS and FACS analysis carried out.

In vitro experiments in this chapter were performed with a minimum of 3 replicates per group. Results were tested for statistical significance using an unpaired Student's *t* test with GraphPad Prism Version 5.0 software.

Human miR-31 (hsa-miR-31) is known to silence human FOXP3[15]. Furthermore hsa-miR-31 and its mouse equivalent, mmu-miR-31, share the same sequence except that mmu-miR-31 has an extra "G" nucleotide at the 3' end. The location of this extra nucleotide was not expected to influence knockdown efficiency. Thus, the hypothesis was that mmu-miR-31 would function similarly in the mouse and silence mFOXP3.

Before testing the hypothesis experimentally, the putative interaction between mmu-miR-31 and mFOXP3 was confirmed bioinformatically. The microRNA.org resource enabled searching under a given target mRNA, "FOXP3" in this case, filtered by species for mouse only. This returned a list of all putative miRNAs which may align to and silence mFOXP3. From here, individual miRNAs of interest were viewed in more detail, including sequence alignments and mirSVR score (figure 2.1). The perfect complemantarity within the seed region (nucleotides 2-8 on the miRNA) coupled with the mirSVR score of -0.68 predicted a meaningful knockdown. These data were corroborated by the DIANA-microT algorithm which predicted alignment between mmu-miR-31 and mFOXP3 at the same site with a miTG score of 2. To put in context, the miTG score for hsa-miR-31 and human FOXP3 was 3.

Therefore, bioinformatically at least, miR-31 was predicted to silence mFOXP3.

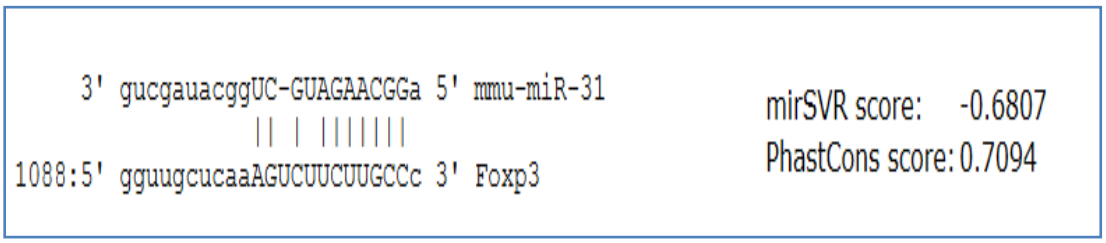

Figure 2.1 Database analysis of microRNAs which target mFOXP3. Mouse miR-31 (mmu-miR-31) was predicted as a putative RNAi mediator against mFOXP3. Shown is the proposed alignment of miR-31 within the 3'UTR of the target mFOXP3 mRNA. Note the perfect complementarity within the seed region (nucleotide 2-8 on the microRNA).

Efficacy of miR-31 in this assay mandated its over-expression in an *in vitro* system. Before examining the functionality of miR-31, successful delivery of the plasmid carrying miR-31 and appropriate intracellular processing were confirmed. This was achieved by detection of the mature miRNA by real time RT-PCR (figure 2.2). This experiment confirmed that miR-31 was over-expressed 54–fold compared with the empty backbone plasmid.

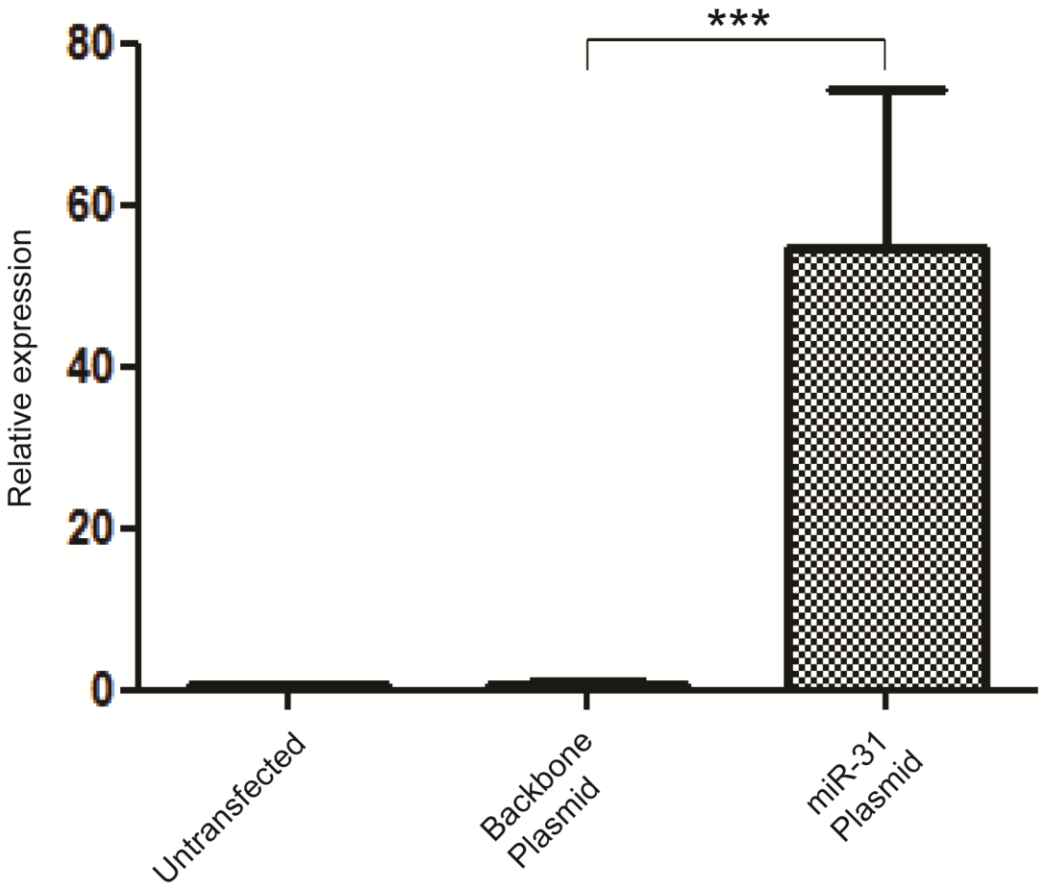

Figure 2.2 Detection of mature miR-31. Data extracted from RT-PCR using the ΔΔCT method showing the levels of mature miR-31 relative to an untransfected and a plasmid backbone sample. Levels were normalised against the RNU6B housekeeping gene, and the scale of over-expression represents the average of two independent experiments.

From figure 2.2 it was clear that a large number of mature miR-31 duplexes were were produced and available within the cell. The next step was to determine if miR-31 could silence mFOXP3. Parallel assessment of miR-31 against hFOXP3 acted as a positive control for the experiment as miR-31 has been previously published to silence hFOXP3 [15]. The same backbone plasmid without pre-microRNA-31 sequence acted as a negative control. A commercially available miR reporter assay was employed. Commercially available luc-UTR constructs served as the source of the untranslated regions (UTRs) for the hFOXP3 and the mFOXP3 genes. These constructs express the 3'UTR of the chosen target gene fused to the coding region of the Firefly *luciferase* gene. Successful silencing of the target mRNA (FOXP3) manifests as reduced luciferase protein expression with subsequent reduced luminescence. As seen in figure 2.3, miR-31 significantly silenced hFOXP3 compared with pmiR-BB ($p = 0.015$). However, it had no effect on mFOXP3 ($p = 0.261$).

This experiment demonstrated that miR-31 does not silence mFOXP3 and thus could not be expected to alter the T_{Reg} phenotype.

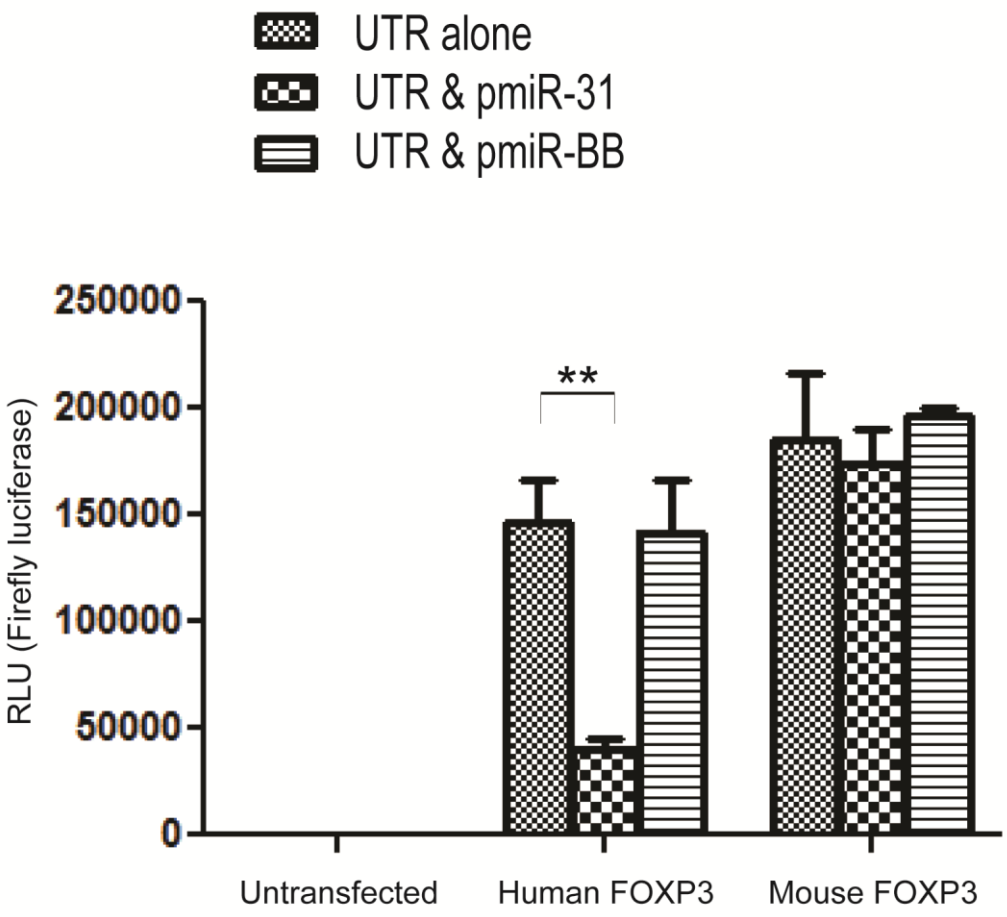

Figure 2.3 miR-31 does not silence mFOXP3. Luc-UTR constructs bearing the 3' UTR of human and mouse FOXP3 fused to the firefly *luciferase* gene were co-transfected with plasmids carrying pre-miR-31 or its backbone equivalent (pmiR-BB**)**. 48 h later, HeLa cells were lysed and luminescence read using a luminometer. Human luc-UTR (FOXP3) is included as a positive control for the experiment. Data are represented as mean +/- SEM of *n* = 3 (** p = 0.015).

It was concluded from these results, that no endogenous miR effective against mFOXP3 was available or apparent. Therefore, it was necessary to design and test an alternative miR strategy. In order to test suitable inhibitory sequences, siRNAs were initially examined, with the ultimate aim of utilising the data generated to construct a DNA-based miR.

Prior to testing siRNA molecules, *in vitro* delivery of chemically synthesised siRNAs was first validated. siGLO® was used to determine delivery efficiency by FACS analysis. Figure 2.4 shows that 74% (+/- 1%) of cells were fluorescent following siGLO® transfection, which was significantly greater than the background level from untransfected samples (4% +/- 0.05%) ($p < 0.001$).

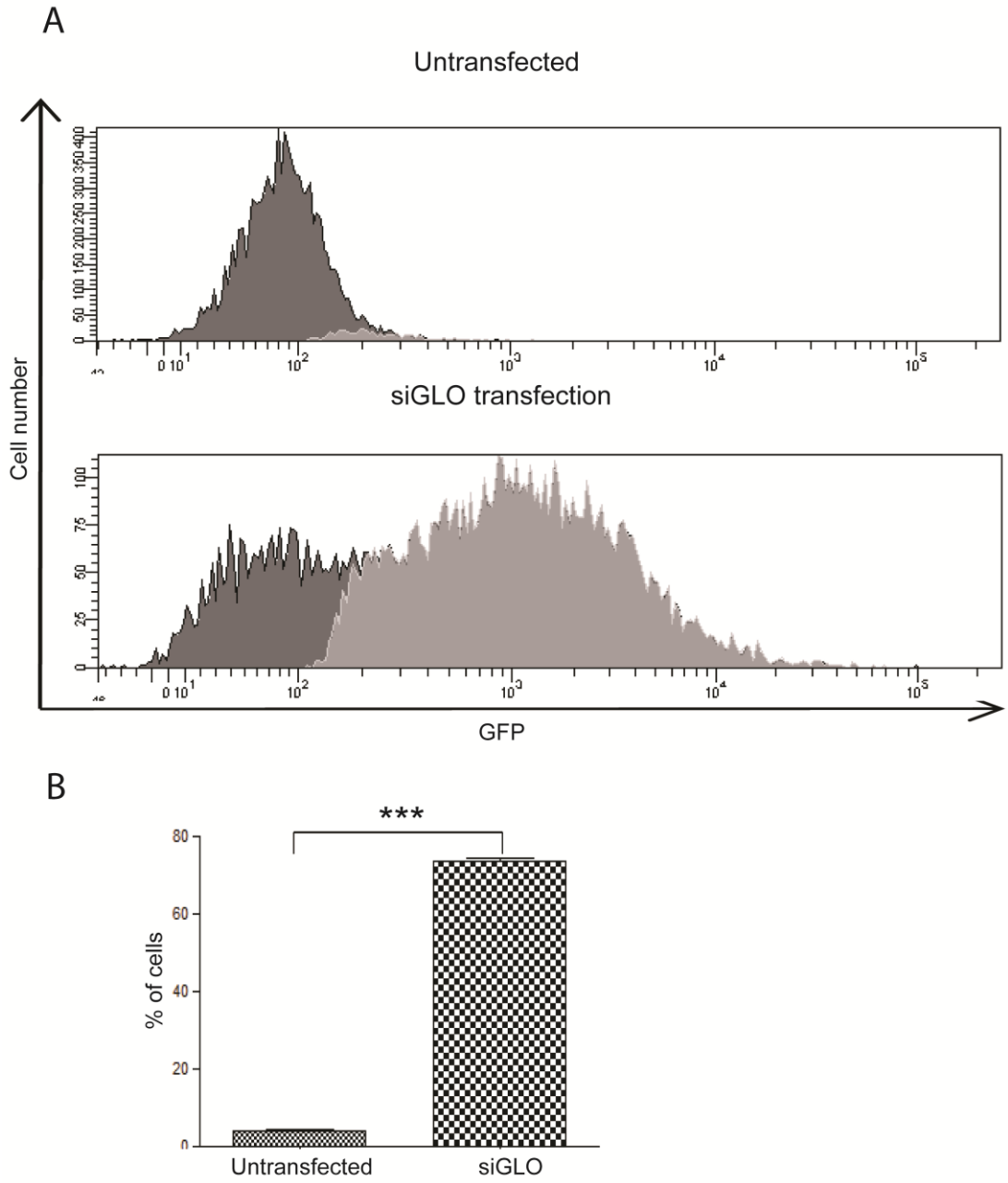

Figure 2.4 siRNA delivery to HeLa cells *in vitro*. A) Histograms from FACS analysis showing the number of cells positive (light grey) and negative (dark grey) for the fluorophore for an untransfected population and a population transfected with siGLO®. The histograms shown are representative of three independent replicates. **B)** Quantitative output for the number of transfected cells. Data are represented as mean +/- SEM of $n = 3$ (*** $p < 0.001$).

Validation of the assay for *in vitro* assessment of RNAi was established by examining silencing of expression of the fluorescent reporter protein EGFP. This assay involved co-transfection of HeLa cells with a plasmid (pFOXP3) providing co-expression of both EGFP and mFOXP3 (as a single mRNA transcript through an IRES sequence) and an siRNA targeting EGFP mRNA. For this experiment, the plasmid provides the EGFP target gene.

A global picture of the silencing efficiency was obtained by looking at the percentage of cells that were $EGFP^+$ in the various samples (figure 2.5 A and B). Transfection of the target plasmid alone yielded 57% (+/- 0.7%) $EGFP^+$ cells. Co-transfection of an siRNA against EGFP resulted in a knockdown efficiency of 58% as evidenced by a reduction in the number of $EGFP^+$ cells to 24% (+/- 1.2%). This was statistically significant ($p < 0.001$). A scrambled, negative control siRNA did not reduce the number of $EGFP^+$ cells significantly ($p = 0.124$).

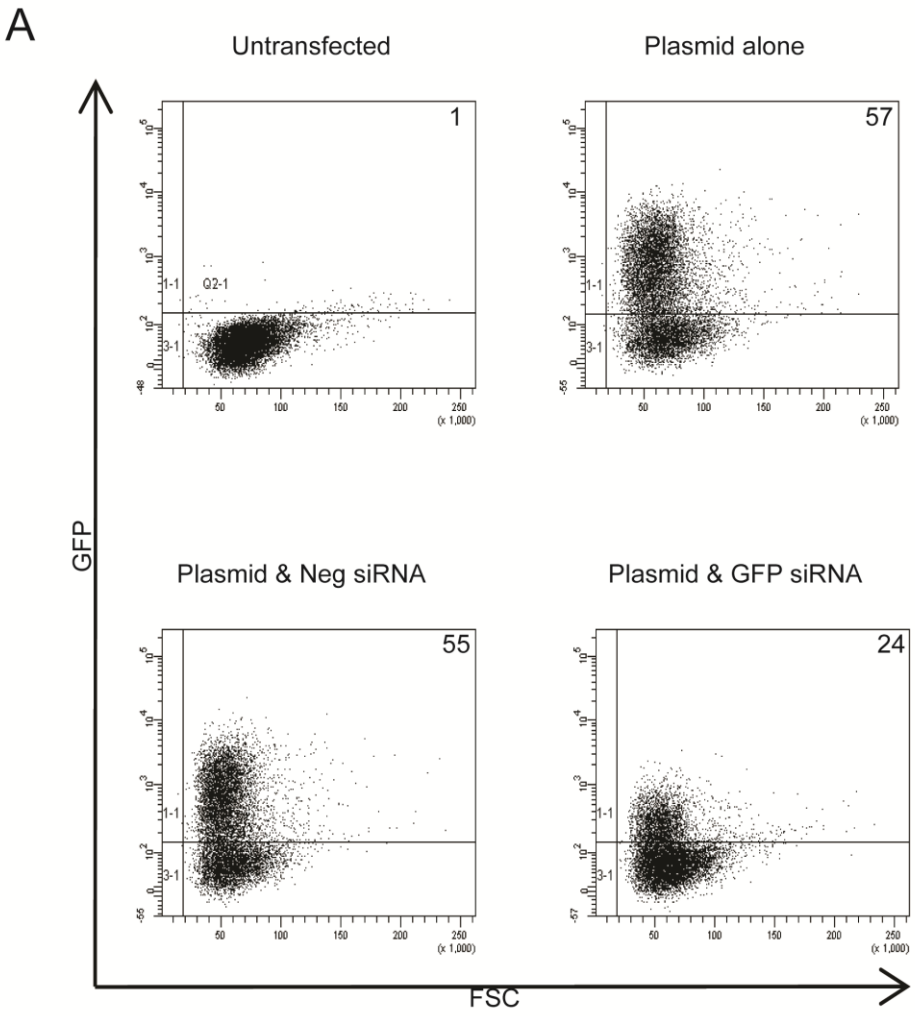
A
Untransfected
Plasmid alone
Plasmid & Neg siRNA
Plasmid & GFP siRNA
1
57
55
24
Q2-1
1-1
3-1
GFP
FSC
(x 1,000)

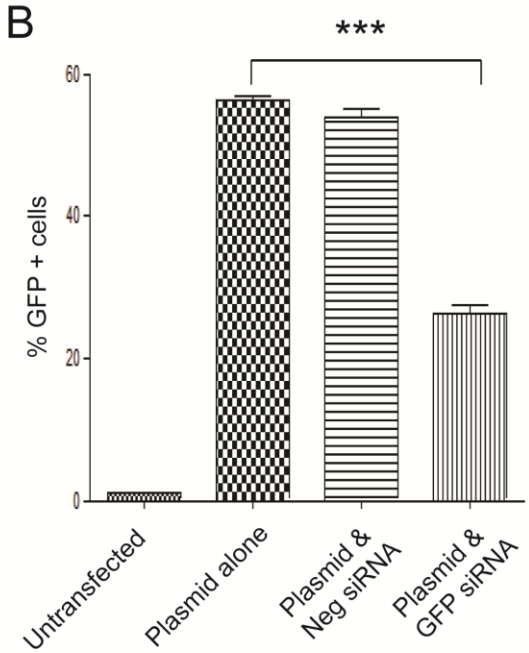
B
***
% GFP + cells
60
40
20
0
Untransfected
Plasmid alone
Plasmid & Neg siRNA
Plasmid & GFP siRNA

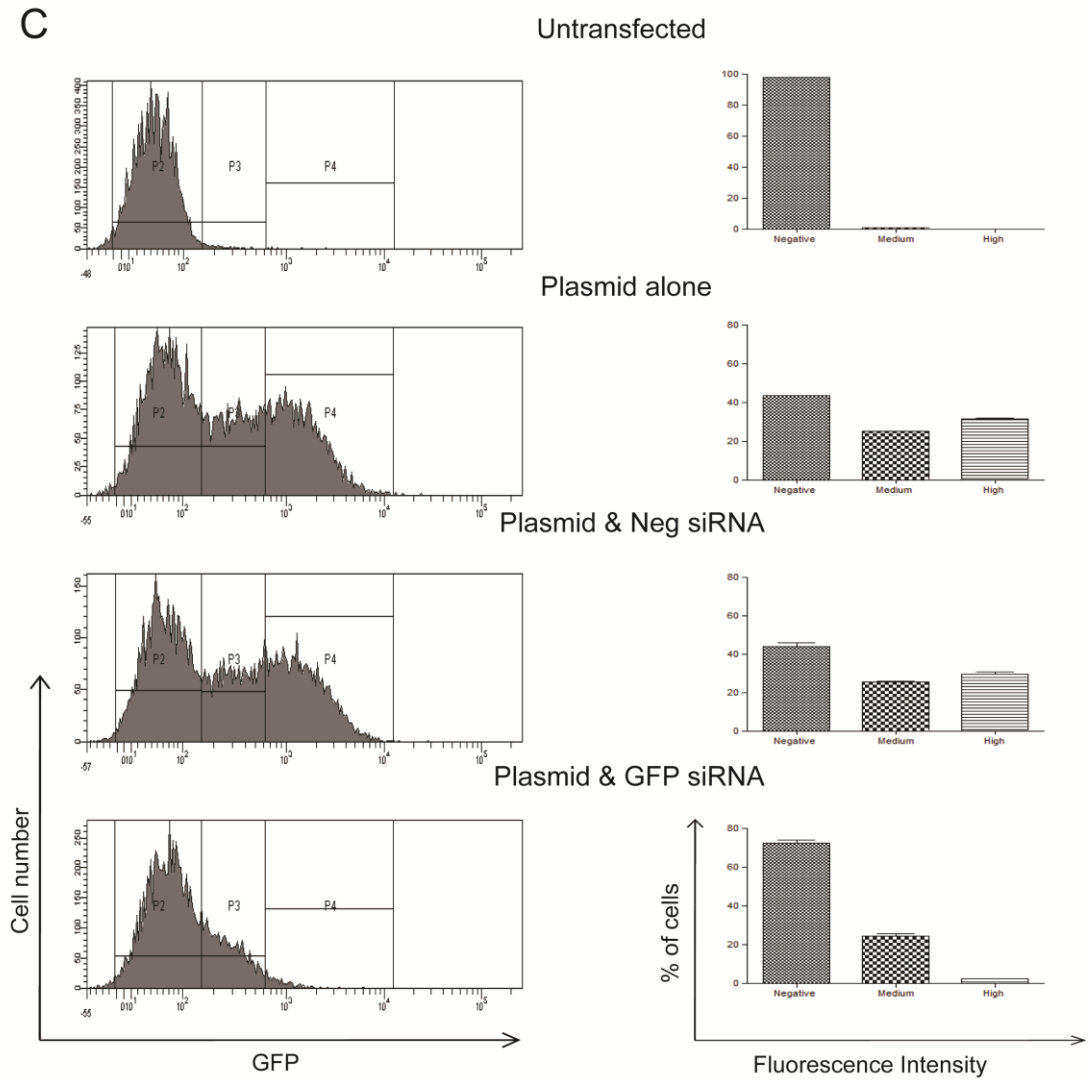

Figure 2.5 Knockdown of EGFP. A) Dot plots from FACS analysis where the numbers indicate the percentage of total cells above the line and hence positive for EGFP expression. Dot plots shown are representative of three independent replicates. **B)** Quantitative output for the number of $EGFP^+$ cells from three replicates presented as the mean +/- SEM (*** $p < 0.001$). **C)** Histograms on the left showing the relative proportion of cells with negative, medium and high fluorescence intensity (P2, P3 and P4 respectively) which correlates with the level of EGFP expression. Each histogram is representative of three independent replicates. The graphs on the right represent the quantitative output from histograms from three independent replicates.

Data presented in Figure 2.5 A and B provide total number of cells positive or negative for the target protein (EGFP), and does not account for changes in level of intracellular expression within positive cells. Since partial knockdown may be sufficient to facilitate a phenotypic change in the cell, it is important to examine all reduction in gene expression. Stratifying the cells according to fluorescence intensity (negative, medium and high) overcomes this issue and accounts for partial knockdown. These data are shown in figure 2.5 C. Comparing a sample that received EGFP plasmid alone, with a sample that received both plasmid and an siRNA targeting EGFP, the percentage of cells with 'high' fluorescence is reduced by 30% (+/- 0.5%; $p < 0.001$) from 32% to 2%. There was no significant change in the 'medium' cell population ($p = 0.592$). This occurs against a backdrop of an increase in the number of negative cells by 30% (+/- 1.3%; $p < 0.001$) from 43% to 73%. This suggests that, following transfection of an siRNA targeting EGFP, cells that highly expressed EGFP now express the protein at an intermediate level, while those previously displaying medium expression are now negative for EGFP.

In this experiment, the proficiency of the *in vitro* assay to assess RNAi was validated by knockdown of the reporter EGFP.

Two 22-base pair chemically synthesised siRNAs (termed mimic #2 and mimic #4) were examined in an *in vitro* assay with mFOXP3-transfected HeLa cells. This assay involved co-transfection of HeLa cells with pFOXP3 and the siRNAs. For this experiment, the plasmid provided the mFOXP3 target gene. mFOXP3 expression was assessed via FACS with anti-mFOXP3 antibody labelling of cells.

Transfection of the target plasmid alone yielded 47% (+/- 2.8%) $mFOXP3^{+}$cells. In terms of 'absolute' silencing efficiency, where cells are either FOXP3 positive or negative, mimic #4 produced a superior knockdown efficiency at 57% compared with 39% for mimic #2. The scrambled, negative control siRNA had an insignificant knockdown effect on mFOXP3 ($p = 0.468$). The knockdown efficiency achieved with both mimics was statistically significant ($p < 0.003$ for mimic #2 and $p < 0.001$ for mimic #4) and the difference in knockdown efficiency between the two mimics was statistically significant ($p = 0.008$) (figure 2.6 A and B). A concordant knockdown to that seen for mFOXP3 was observed by analysing

cells in terms of EGFP expression (data not shown). This validated the integrity of the IRES construct (see section 2.4.9 for further details).

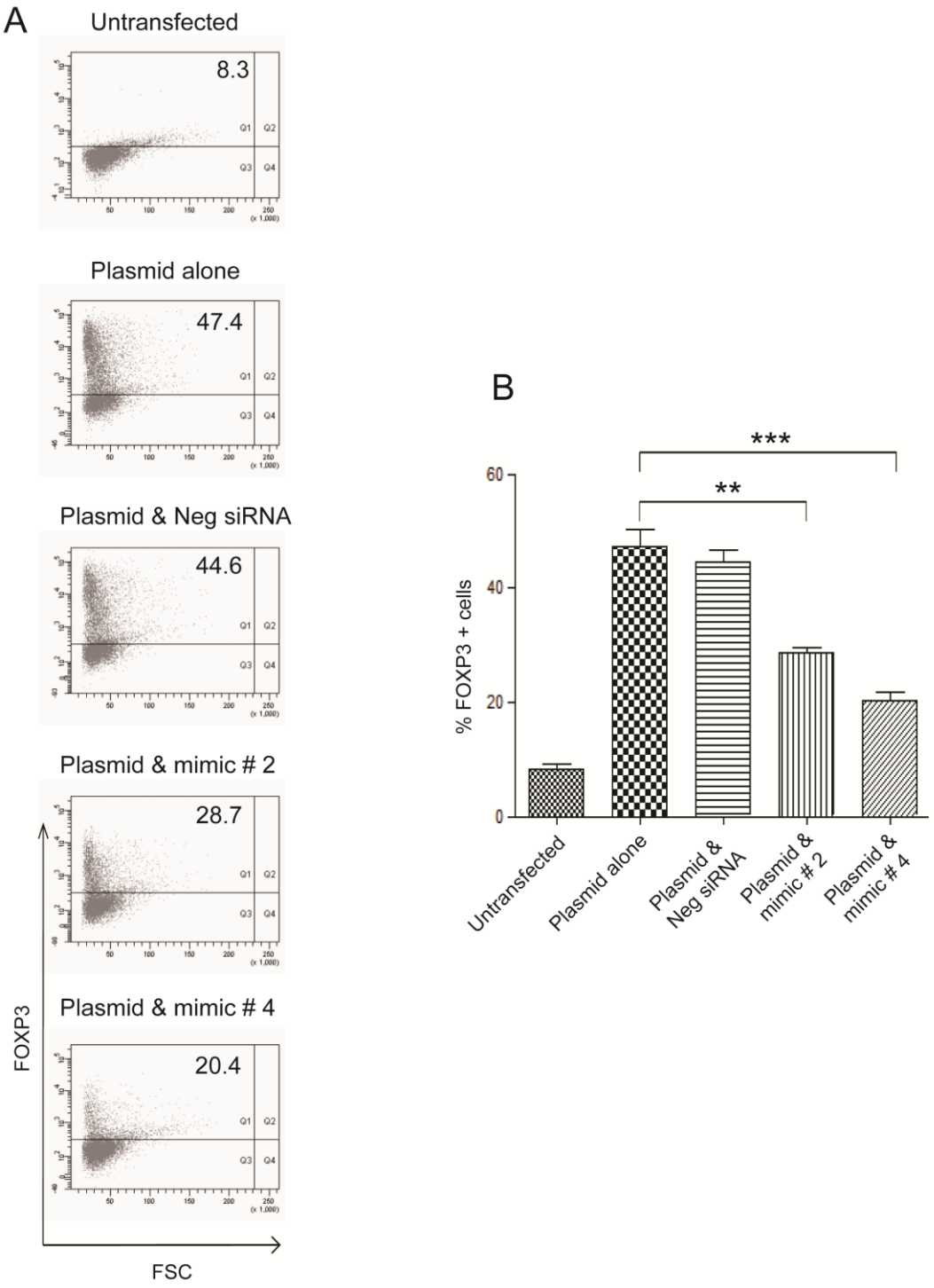
A
Untransfected
8.3
Plasmid alone
47.4
Plasmid & Neg siRNA
44.6
Plasmid & mimic # 2
28.7
Plasmid & mimic # 4
20.4
Q1
Q2
Q3
Q4
FOXP3
FSC
B
% FOXP3 + cells
60
40
20
0
***
**
Untransfected
Plasmid alone
Plasmid & Neg siRNA
Plasmid & mimic # 2
Plasmid & mimic # 4

C

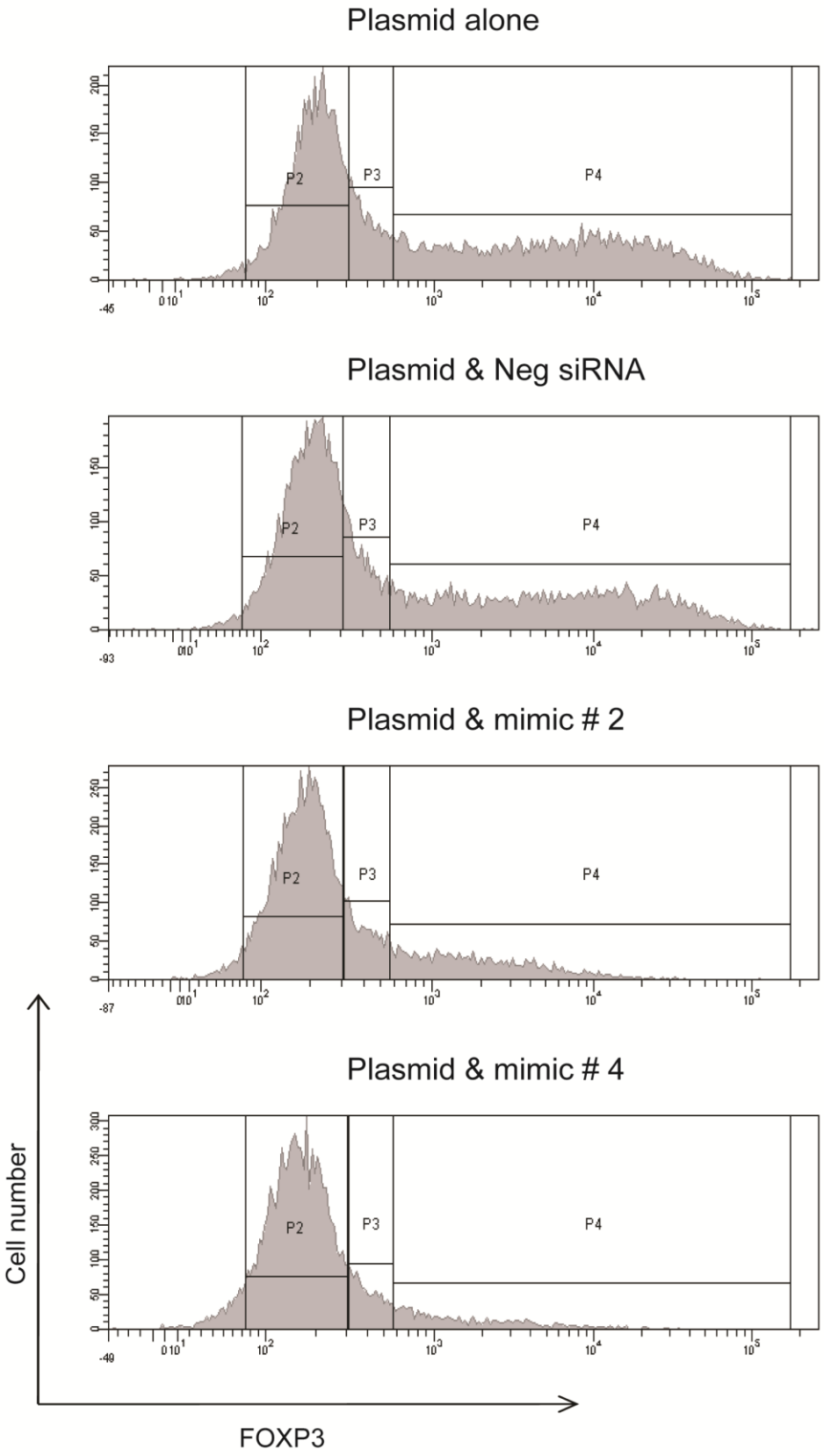
Plasmid alone
P2
P3
P4
Plasmid & Neg siRNA
P2
P3
P4
Plasmid & mimic # 2
P2
P3
P4
Plasmid & mimic # 4
P2
P3
P4
Cell number
FOXP3

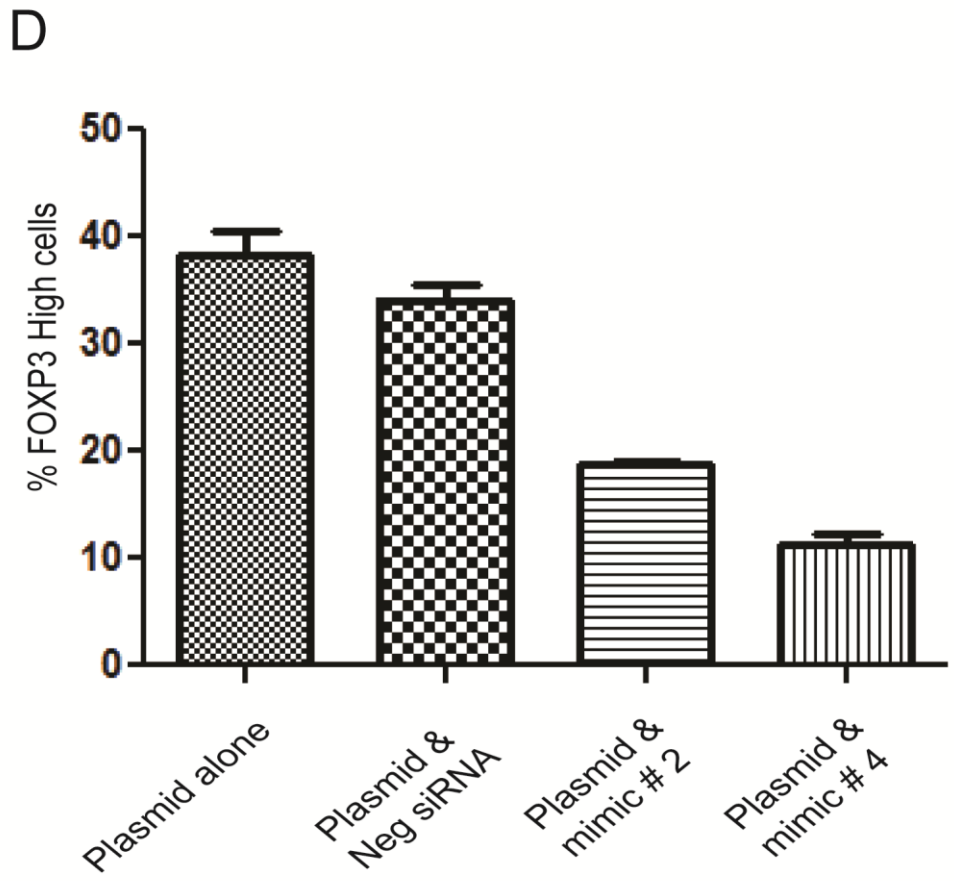

Figure 2.6 siRNA Knockdown of mFOXP3. A) Dot plots from FACS analysis where the numbers indicate the percentage of total cells above the line and hence positive for mFOXP3 expression. Dot plots shown are representative of three independent replicates. **B)** Quantitative output for the number of mFOXP3^{+} cells from three replicates presented as mean +/- SEM (*** $p < 0.001$, ** $p < 0.003$). **C)** Histograms showing the relative proportion of cells with negative, medium and high fluorescence intensity (P2, P3 and P4 respectively) which correlates with the level of mFOXP3 expression. Each histogram is representative of three independent replicates. **D)** The graph represents the quantitative output from histograms from three independent replicates. Only FOXP3 high cells (P4 in the histograms in **C**) are shown on the graph.

As per the knockdown of EGFP, any partial knockdown of mFOXP3 was potentially relevant as even a small reduction in expression of this crucial transcription factor could influence the suppressive capability ofT_{Regs}. Again cell populations were stratified based on fluorescence intensity. Comparing a sample that received mFOXP3 plasmid alone with samples that also received mimic #2 or mimic #4 the percentage of cells with high fluorescence was reduced from 27% to 8% ($p = 0.001$) and 4% ($p < 0.001$) respectively. No significant change was observed in cell populations with medium fluorescence ($p = 0.82$ for mimic #2 and $p = 0.126$ for mimic #4). This occurred against a backdrop of an increase in the number of negative cells from 49% to 63%($p = 0.005$) and 72% ($p < 0.001$) respectively. Representative histograms for these data are shown in figure 2.6 C with quantitative output from three independent replicates shown. As per the EGFP knockdown the data from this experiment suggests that, following transfection mimic #4 and mimic #2, cells that highly expressed mFOXP3 now express the protein at an intermediate level, while those previously displaying medium expression are now negative for mFOXP3

This experiment was crucial to the progression of the overall aim, with two novel RNAi sequences against the target mFOXP3 identified and validated.

Aside from target knockdown efficiency, an important concern when designing an RNAi mediator is to minimise off-target effects. Thus mimic #2 and mimic #4 were tested against EGFP and knockdown efficiency was assessed (figure 2.7 A and B**)**. Neither mimic ($p = 0.051$ for mimic #2 and $p = 0.067$ for mimic #4) nor the negative control siRNA ($p = 0.124$) yielded a statistically significant knockdown of EGFP when compared with a sample that received no siRNA (plasmid alone). As a positive control for the experiment, an siRNA against EGFP reduced the number of $EGFP^+$ cells from 56% to 26% ($p < 0.001$).

In this experiment mimic #2 and mimic #4 failed to silence an irrelevant target (EGFP) suggesting that these RNAi mediators are target specific.

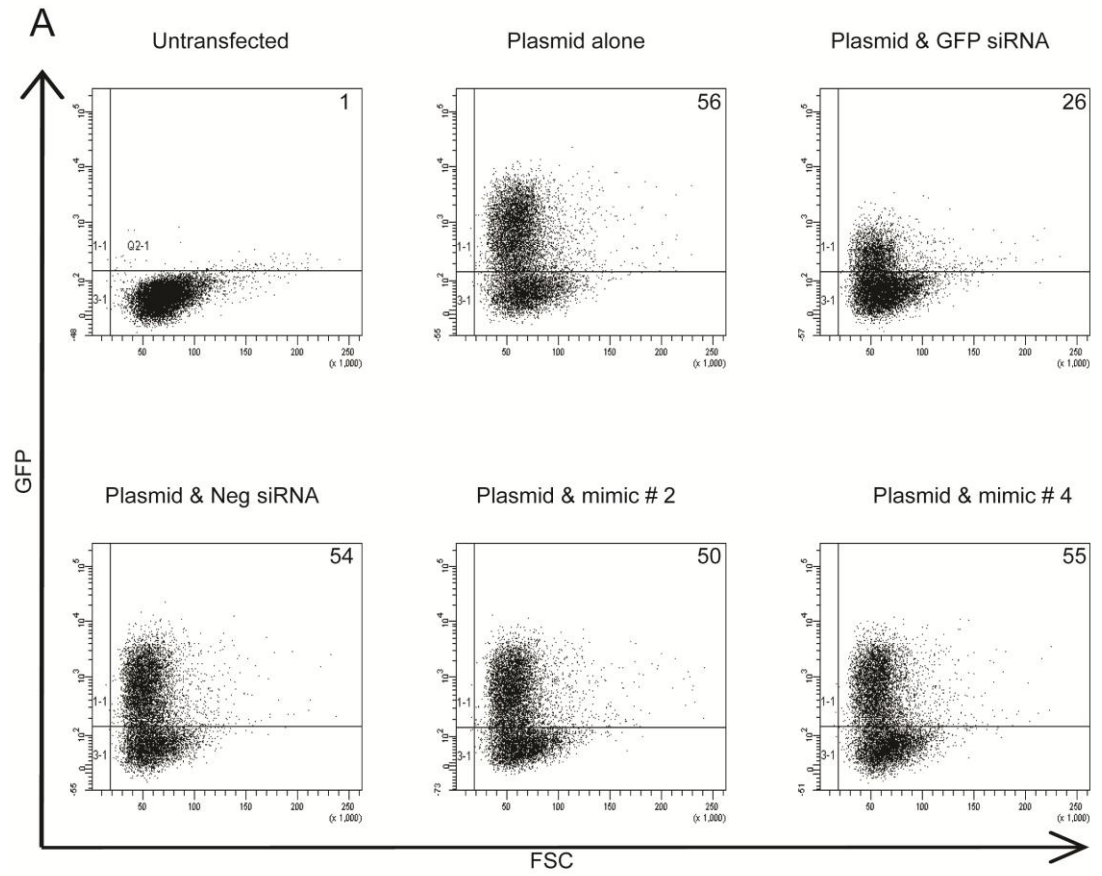
A
Untransfected
Plasmid alone
Plasmid & GFP siRNA
Plasmid & Neg siRNA
Plasmid & mimic # 2
Plasmid & mimic # 4
1
56
26
54
50
55
Q2-1
GFP
FSC

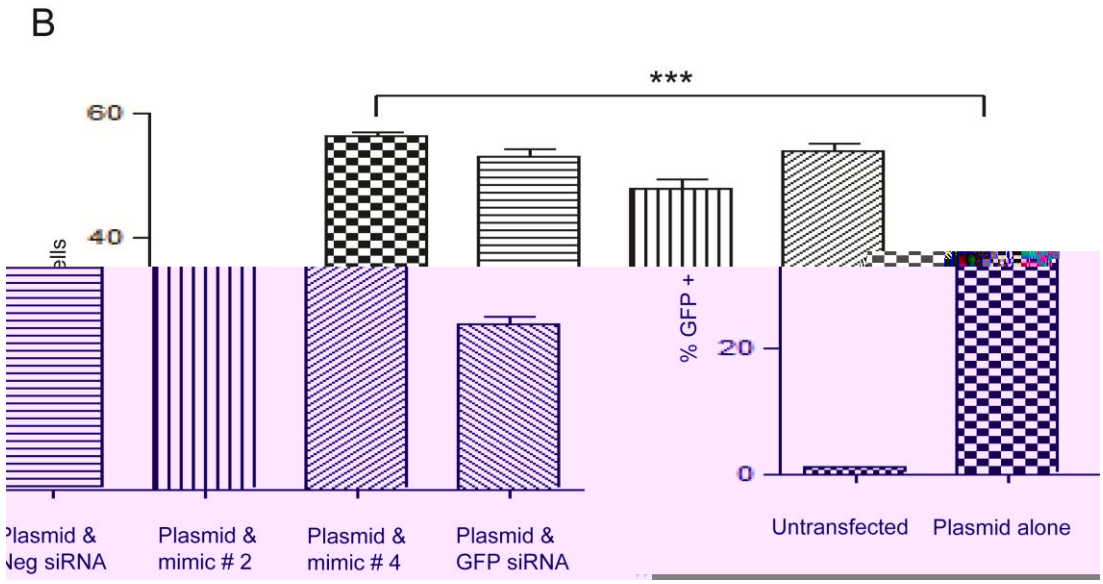
B
***
60
40
20
0
% GFP +
Plasmid & Neg siRNA
Plasmid & mimic # 2
Plasmid & mimic # 4
Plasmid & GFP siRNA
Untransfected
Plasmid alone

Figure 2.7 Mimic # 2 and mimic # 4 are target-specific. A) Dot plots from FACS analysis where the numbers indicate the percentage of total cells above the line and hence positive for EGFP expression. Dot plots shown are representative of three independent replicates. **B)** Quantitative output for the number of EGFP $^{+}$ cells from three replicates presented as the mean +/- SEM (*** $p < 0.001$).

In this chapter endogenous miR-31 was shown to be incapable of silencing mFOXP3. This finding conflicted with the bioinformatic screen. Attention then switched to the design and testing of novel RNAi mediators against mFOXP3. Although designed as pre-microRNA constructs, the mature RNAi duplexes of 22 bps were synthesised independently as siRNAs and tested *in vitro*. Proof of delivery for a fluorescent siRNA was first demonstrated followed by knockdown of a reporter gene. Together these steps validated the *in vitro* model system. Two candidate RNAi molecules were tested against our target gene (mFOXP3) and achieved varying degrees of knockdown. The candidate molecules were furthered tested against a non-target gene. In the absence of knockdown, they were deemed to be target-specific.

Rationale for testing miR-31; miR-31 has been shown to silence hFOXP3 [15]. The initial hypothesis for this study proposed that miR-31 might also silence mFOXP3. The potential benefits of working with a cross-species specific miRNA were many [23] and clearly justified experimentation with miR-31 against mFOXP3; the value of the pre-clinical data would be greatly enhanced as the safety and efficacy data would be reconcilable with human data. If clinical translation of the compound was possible, the process would be greatly expedited and at much lower cost, as a single drug candidate would be conserved from the research stage through to patient administration. The potential for such cross-species reactivity represents a distinct advantage of RNAi therapeutics over small molecule and biological compounds [24].

The sequence of mature miR-31 is conserved between the mouse and human species with the exception of an additional 3' "G" nucleotide on the mouse homolog. However, a miRNA profile of murine T cells did not highlight any distinction in miR-31 levels between T_{Regs} and conventional $CD4^+$ T cells [13]. Furthermore, miRNA target specificity has been shown to fluctuate considerably between organisms due to diversity in RNAi pathways and variations in the components of RISC complexes [16]. However, a bioinformatic screen using the miRanda-mirSVR methodology predicted that miR-31 would silence mFOXP3 (figure 2.1). This bioinformatic tool was deemed to be especially appropriate as the scoring algorithm had been generated based on miRNA transfection data in HeLa cells as per the planned experiments with miR-31 [16]. The mirSVR score of -0.6807 was substantially lower than the cutoff

score of -0.1 where the lower the score the greater the probability of meaningful downregulation; scores of -0.1 or lower have more than a 35% probability of a log expression change of at least -1 and better than 50% probability of a log expression change of at least -0.5. Moreover the mirSVR scores correlate linearly with the extent of downregulation [16].

Limitations of bioinformatic algorithms; The bioinformatic prediction could not be validated at a practical level (figure 2.3) despite successful over-expression and detection of mature miR-31 (figure 2.2). This can most likely be attributed to generation of a false positive result by the miRanda-mirSVR methodology. Despite sequential improvements as newer algorithms have been developed, some limitations remain; the presence of non-specific sequence determinants that influence miRNA-mediated regulation has been muted [25]; RNA-binding proteins and motifs are known to interfere with miRNA regulation [26,27]. Present algorithms are unable to factor these parameters into calculations [16]. While a false positive readout was generated in this experiment perhaps a bigger concern would be false-negative outputs – most current target prediction methods do not consider miRNA target sites within the coding region of genes [16]. However recent data from Argonaute-protein immunoprecipitations suggest that a significant proportion of target sites can be found in the coding regions of mRNAs [28,29].

*Use of siRNAs;*Following on from the demonstration that miR-31 was unsuitable, two novel, alternative candidates were examined and validated, as chemically synthesised siRNAs rather than DNA-based constructs. siRNAs represent an invaluable tool for *in vitro* validation of RNAi mediators at a sequence level [30]. Their small size (generally 22 bp) permits high transfection efficiency using routine chemical transfectants. The researcher need not be concerned with optimising parameters such as plasmid expression and intra-cellular processing. As such, siRNAs represent a more user-friendly method of exploiting RNAi in the early stages of a project. Upon successful validation of RNAi, the siRNA sequence can readily be transposed into DNA-based constructs (detailed in chapter 3).

Target specificity; While it is suggested in this chapter that the two candidate RNAi mediators are target-specific, by their failure to silence an irrelevant EGFP gene (figure 2.7) these data are not definitive. EGFP is not an endogenous gene and a more detailed analysis of the off-target effects would warrant gene expression profiling. This technology is expensive and would not be justified in the absence of any gross abnormality in the cell line used for these experiments. In any case off-target effects in HeLa cells may not be recapitulated in the final target cell population of T_{Regs}.

Conclusion; In conclusion, the exploitation of RNAi as a therapeutic modality is still in its infancy, with currently no RNAi mediator in routine clinical use. RNAi therapeutics promise many benefits but given their potency, rigorous *in vitro* testing accompanied by cautious clinical development would seem prudent. Many of the obstacles, such as saturation toxicity, off-target effects, immune stimulation and delivery are slowly being overcome.

In this chapter, a novel RNAi mediator against mFOXP3 was designed and tested. FOXP3, in its capacity as master regulator of T_{Regs}, has taken on new-found significance as a target protein/gene in recent times in the field of cancer immunology and beyond. The intracellular localisation of this protein/transcription factor lends itself to manipulation by some form of gene therapy such as RNAi. The mouse homolog of FOXP3 was chosen as a target because it provided the potential for *in vivo* experimentation with the putative therapeutic. Such *in vivo* data would have far greater relevance in the context of anti-tumour immunity than any *in vitro* data derived from mixed-leukocyte reactions. The novel RNAi mediators against mFOXP3 did not silence a non-target gene suggesting that they are target-specific.

The 22 bp duplexes utilised in this series of experiments provided a simple and efficient means to test the RNAi mediators at a sequence level. However progressing these siRNAs in their present format to pre-clinical studies and beyond would be very challenging (reviewed in section 1.2.3). A non-viral vector would be required with a resulting drop in delivery efficiency and due to the inherent vulnerability of the siRNAs *in vivo* repeated administration would likely be required. Therefore, subsequent chapters focus on development of optimal methods for delivery of the sequences validated here.

1. Zou W. Regulatory T cells, tumour immunity and immunotherapy. *Nat Rev Immunol* 2006; **6:** 295-307.

2. Byrne WL, Mills KH, Lederer JA, O'Sullivan GC. Targeting regulatory T cells in cancer. *Cancer Res*; **71:** 6915-6920.

3. Colombo MP, Piconese S. Regulatory-T-cell inhibition versus depletion: the right choice in cancer immunotherapy. *Nat Rev Cancer* 2007; **7:** 880-887.

4. Luan YY, Yao YM, Zhang L, Dong N, Zhang QH, Yu Y *et al*. Expression of tumor necrosis factor-alpha induced protein 8 like-2 contributes to the immunosuppressive property of CD4(+)CD25(+) regulatory T cells in mice. *Mol Immunol*; **49:** 219-226.

5. Pan F, Yu H, Dang EV, Barbi J, Pan X, Grosso JF *et al*. Eos mediates Foxp3-dependent gene silencing in CD4+ regulatory T cells. *Science* 2009; **325:** 1142-1146.

6. Fontenot JD, Gavin MA, Rudensky AY. Foxp3 programs the development and function of CD4+CD25+ regulatory T cells. *Nat Immunol* 2003; **4:** 330-336.

7. Hori S, Sakaguchi S. Foxp3: a critical regulator of the development and function of regulatory T cells. *Microbes Infect* 2004; **6:** 745-751.

8. Allan SE, Song-Zhao GX, Abraham T, McMurchy AN, Levings MK. Inducible reprogramming of human T cells into Treg cells by a conditionally active form of FOXP3. *Eur J Immunol* 2008; **38:** 3282-3289.

9. Amendola M, Passerini L, Pucci F, Gentner B, Bacchetta R, Naldini L. Regulated and multiple miRNA and siRNA delivery into primary cells by a lentiviral platform. *Mol Ther* 2009; **17:** 1039-1052.

10. Morse MA, Hobeika AC, Osada T, Serra D, Niedzwiecki D, Lyerly HK *et al*. Depletion of human regulatory T cells specifically enhances antigen-specific immune responses to cancer vaccines. *Blood* 2008; **112:** 610-618.

11. Tsai BY, Suen JL, Chiang BL. Lentiviral-mediated Foxp3 RNAi suppresses tumor growth of regulatory T cell-like leukemia in a murine tumor model. *Gene Ther*; **17:** 972-979.

12. Zhou L, Park JJ, Zheng Q, Dong Z, Mi Q. MicroRNAs are key regulators controlling iNKT and regulatory T-cell development and function. *Cell Mol Immunol*; **8:** 380-387.

13. Cobb BS, Hertweck A, Smith J, O'Connor E, Graf D, Cook T *et al*. A role for Dicer in immune regulation. *J Exp Med* 2006; **203:** 2519-2527.

14. Zhou X, Jeker LT, Fife BT, Zhu S, Anderson MS, McManus MT *et al*. Selective miRNA disruption in T reg cells leads to uncontrolled autoimmunity. *J Exp Med* 2008; **205:** 1983-1991.

15. Rouas R, Fayyad-Kazan H, El Zein N, Lewalle P, Rothe F, Simion A *et al*. Human natural Treg microRNA signature: role of microRNA-31 and microRNA-21 in FOXP3 expression. *Eur J Immunol* 2009; **39:** 1608-1618.

16. Betel D, Koppal A, Agius P, Sander C, Leslie C. Comprehensive modeling of microRNA targets predicts functional non-conserved and non-canonical sites. *Genome Biol*; **11:** R90.

17. Betel D, Wilson M, Gabow A, Marks DS, Sander C. The microRNA.org resource: targets and expression. *Nucleic Acids Res* 2008; **36:** D149-153.

18. Enright AJ, John B, Gaul U, Tuschl T, Sander C, Marks DS. MicroRNA targets in Drosophila. *Genome Biol* 2003; **5:** R1.

19. John B, Enright AJ, Aravin A, Tuschl T, Sander C, Marks DS. Human MicroRNA targets. *PLoS Biol* 2004; **2:** e363.

20. Maragkakis M, Reczko M, Simossis VA, Alexiou P, Papadopoulos GL, Dalamagas T *et al*. DIANA-microT web server: elucidating microRNA functions through target prediction. *Nucleic Acids Res* 2009; **37:** W273-276.

21. Wotschofsky Z, Meyer HA, Jung M, Fendler A, Wagner I, Stephan C *et al*. Reference genes for the relative quantification of microRNAs in renal cell carcinomas and their metastases. *Anal Biochem*; **417:** 233-241.

22. Pfaffl MW. A new mathematical model for relative quantification in real-time RT-PCR. *Nucleic Acids Res* 2001; **29:** e45.

23. de Fougerolles A, Vornlocher HP, Maraganore J, Lieberman J. Interfering with disease: a progress report on siRNA-based therapeutics. *Nat Rev Drug Discov* 2007; **6:** 443-453.

24. Seyhan AA. RNAi: a potential new class of therapeutic for human genetic disease. *Hum Genet*; **130:** 583-605.

25. Didiano D, Hobert O. Molecular architecture of a miRNA-regulated 3' UTR. *RNA* 2008; **14:** 1297-1317.

26. Jacobsen A, Wen J, Marks DS, Krogh A. Signatures of RNA binding proteins globally coupled to effective microRNA target sites. *Genome Res*; **20:** 1010-1019.

27. Kedde M, Strasser MJ, Boldajipour B, Oude Vrielink JA, Slanchev K, le Sage C *et al*. RNA-binding protein Dnd1 inhibits microRNA access to target mRNA. *Cell* 2007; **131:** 1273-1286.

28. Hendrickson DG, Hogan DJ, Herschlag D, Ferrell JE, Brown PO. Systematic identification of mRNAs recruited to argonaute 2 by specific microRNAs and corresponding changes in transcript abundance. *PLoS One* 2008; **3:** e2126.

29. Landthaler M, Gaidatzis D, Rothballer A, Chen PY, Soll SJ, Dinic L *et al*. Molecular characterization of human Argonaute-containing ribonucleoprotein complexes and their bound target mRNAs. *RNA* 2008; **14:** 2580-2596.

30. Whitehead KA, Langer R, Anderson DG. Knocking down barriers: advances in siRNA delivery. *Nat Rev Drug Discov* 2009; **8:** 129-138.

The aim of this study was to develop an *in vivo* delivery strategy for the RNAi mediator developed in Chapter 2. Artificial miRNAs offer many advantages over siRNAs, including the capacity for delivery by viral vectors. Lentiviral vectors offer many desirable features for gene therapy. They mediate high level, long-term expression of the transgene and are lowly immunogenic. Thus, in this chapter the objective was to embed the validated siRNA (mimic #4) from chapter 2 within an artificial miRNA cassette and incorporate this into a lentiviral system.

Functional validation of a lentiviral-mediated artificial miRNA knockdown was achieved against mFOXP3 *in vitro*. Lentiviral-mediated gene delivery to a growing B16OVA melanoma tumour was verified using a *Firefly luciferase* (*FLuc*) reporter gene construct. The optimal time to target T_{Regs} within this tumour model was identified, and B16OVA tumour-bearing mice were intra-tumourally (i.t.) administered lentiviral vector carrying the artificial miRNA. The cytokine and cellular immune responses to treatment were examined but no therapeutic benefit was detected.

FOXP3 is recognised as a master regulator of T_{Regs}[1,2] with a profound effect on their functionality. This prompted the hypothesis that sustained RNA interference would be necessary to functionally inactivate T_{Regs} for a period of sufficient duration to permit development of an altered immune phenotype within the tumour. This mindset encouraged the employment of a DNA-based RNAi mediator delivered via a viral vector; ideally an integrating virus for persistence within the cell. Lentiviral vectors boast many desirable attributes; they are capable of high level, long-term expression of the transgene due to integration into the genome; they are capable of transducing non-dividing cells and relative to other viral vectors, are lowly immunogenic [3,4].

In this study the preferred mediator for RNAi was either a miRNA or an shRNA. Within the context of the proposed therapeutic strategy an siRNA-based approach was deemed unsuitable; delivery via a non-viral vector would be necessary which would undermine delivery efficiency; the short *in vivo* half-life of siRNAs would require repeat administrations, adding a further layer of complexity in terms of optimising posology. In contrast a DNA-based RNAi platform would overcome these issues as the benefits of a lentiviral vector could be harnessed, namely high transduction capability and transgene integration. Furthermore a miRNA, in particular an artificial miRNA, promised distinct advantages over an shRNA; more potent knockdown of the target gene could be expected as embedding the validated siRNA from chapter 1 in the well characterised miR-155 backbone would lead to more efficient handling by the RNAi processing machinery. Moreover the risk of saturating toxicity would be lower as an artificial miRNA would be less likely to overload the RNAi processing machinery [5].

While combining a lentiviral vector with an artificial miRNA seemed like an ideal strategy, some technical concerns have been reported with this combination (reviewed in[6]). For example, although the RNAi mediator used in this study was bioinformatically screened for off-target effects, no mediator is solely functional against the target gene, and it cannot be ruled out that the miRNA sequence could interfere with genes in the 293T producer cells. Self targeting, whereby the miRNA transcript is expressed within the producer cells and then elicits RNAi by targeting

the homologous sequences present in the LV vector genome, is also possible. Although no direct evidence exists for this occurrence with miRNAs, self-targeting has been demonstrated for shRNAs [7]. Given the looser structure of miRNAs (the presence of mismatches) relative to shRNAs, self targeting would seem a legitimate concern. Taken en masse, any RNAi activity mediated by the miRNA of interest in the producer cells is undesirable and could undermine lentiviral vector production.

There is also the possibility of the miRNA-containing vector genome being recognised by Drosha following transcription in the producer cell, leading to its destruction. Increased lentiviral titers secondary to Drosha silencing in the producer cells support this theory [8,9]. Genetic instability in the lentiviral particles as a result of repeat sequences in the artificial miRNA can also be an issue, and duplications and deletions have been found during transduction of target cells [10,11]. Promoter interference is also worth considering – if the promoter driving the transgene is significantly stronger than the promoter driving the full-length vector RNA, abundant transgene but very little vector genome expression manifests [12,13].

Despite these hypothetical concerns about production of lentiviral particles carrying a miRNA, they are unlikely to be significantly relevant if high titre production is achieved, as no significant impact on subsequent delivery or knockdown efficiency would be expected.

The focus of this chapter was the development of a DNA-based version of the siRNA validated in the previous chapter. A secondary goal was to incorporate the DNA-based version in a suitable viral vector.

The aim of this study was to incorporate RNAi mediators into a lentiviral-based system capable of delivery *in vitro* and *in vivo*.

A 21 nucleotide sequence was chosen at random and a 3' "G" derived from the native miR-155 sequence (see below) was added. The sequence was modified according to Invitrogen's guidelines (www.invitrogen.com/rnai): runs of greater than 3 identical nucleotides were avoided and the "GC" content was kept in the range of 30-50% - this ensured that any knockdown failure could be attributed to the nucleotide composition and not any thermodynamic stability issues. The 22 nucleotide sequence was bioinformatically assessed against mFOXP3 using the TargetScan^{TM} software and also run through the Basic Local Alignment Search Tool (BLAST) to confirm the absence of significant homology to any other genes [14]. The reverse complement was generated, yielding a 22 base pair (bp) duplex. This siRNA (designated miR scr) was synthesised by Qiagen and tested *in vitro* against mFOXP3 as previously described (section 2.4.9). The miR scr guide strand had the following sequence; 5' ACGTTCGATTATATCGATCGTG 3'

The 22 bp duplexes of mimic #4 and miR scr were incorporated into pre-microRNA scaffolds (Invitrogen) as shown in figure 3.1 and as described; a 5' overhang (TGCT) was added to the functional siRNA strand (mimic #4 or miR scr) which was then merged with the 3' terminal loop sequence (optimised by Invitrogen); nucleotides 1-8 and 11-21 of the passenger siRNA strand were added to yield a 64 bp single strand top oligo (panel A). The bottom oligo was designed as the reverse complement and both single stranded oligos were synthesised by Invitrogen. The oligos were annealed and ligated into the pcDNA6.2-GW/EmGFP-miR plasmid backbone (Invitrogen) (panel B). Successful insertion of the double stranded oligos was confirmed by *Msc I* restriction digest (which only digests within the terminal loop) and sequencing (Eurofins MWG Operon).

A

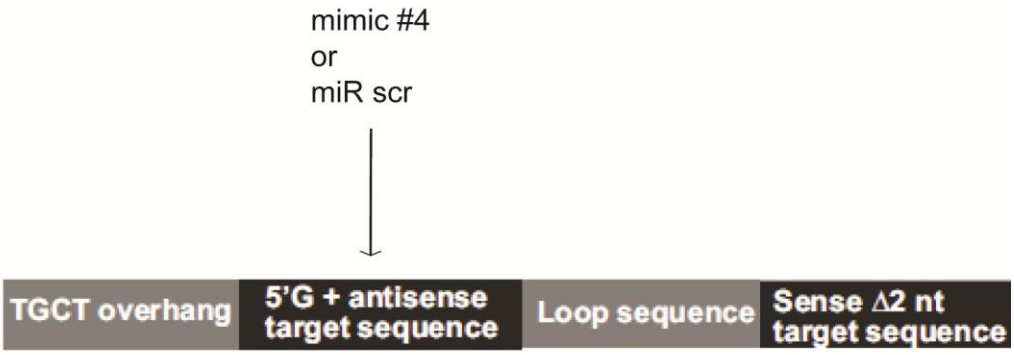
mimic #4
or
miR scr
TGCT overhang
5'G + antisense target sequence
Loop sequence
Sense Δ2 nt target sequence

B

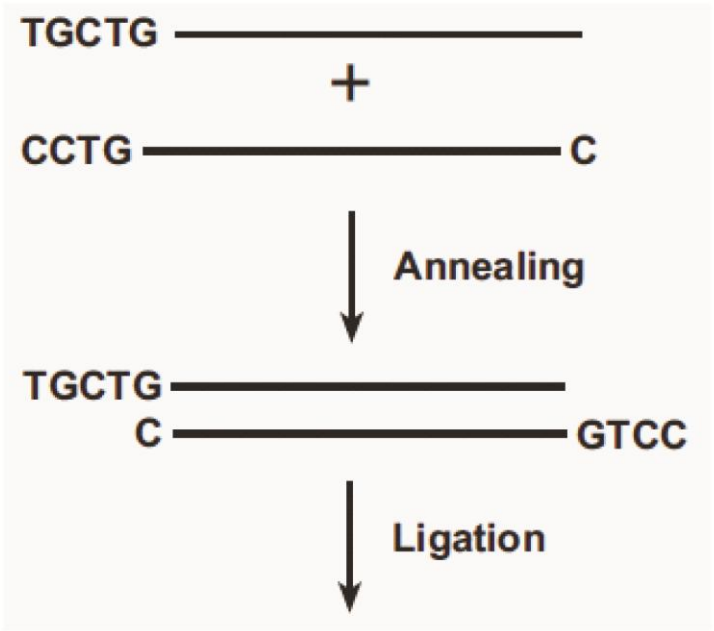
TGCTG
+
CCTG
C
Annealing
TGCTG
C
GTCC
Ligation

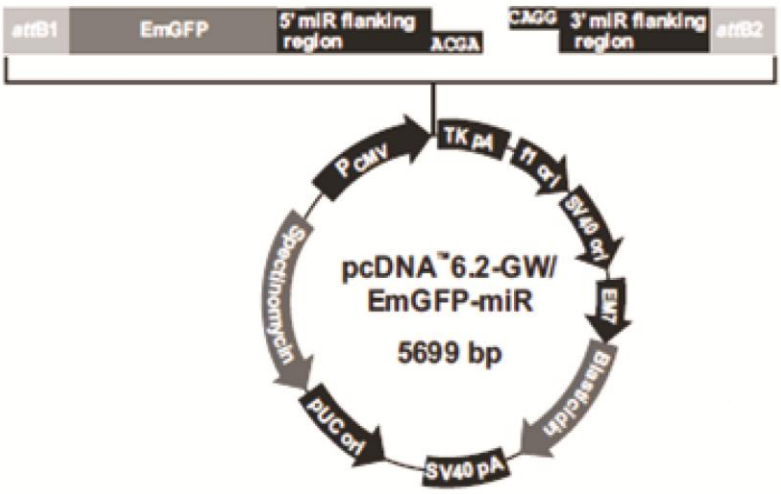
attB1
EmGFP
5' miR flanking region
ACCA
CAGG
3' miR flanking region
attB2
P CMV
TK pA
f1 ori
SV40 ori
EM7
Blasticidin
SV40 pA
pUC ori
Spectinomycin
pcDNA™6.2-GW/
EmGFP-miR
5699 bp

Figure 3.1 Incorporating siRNA sequences into pre-microRNA cassettes. A) Shows how the siRNAs (mimic # 4 and miR scr) were converted into single strand oligos with a hairpin loop. **B)** Shows a simpler representation of the single strand oligo in **A** together with its complementary bottom strand. The two single strand oligos were annealed and ligated into the pre-microRNA expression cassette generated from native miR-155. Further details are provided in the text. Figure adapted from Invitrogen's BLOCK-iT™ Pol II miR RNAi Expression Vector Kit manual.

To facilitate lentiviral vector production the pre-microRNA expression cassettes with their EmGFP reporter genes were transferred to a lentiviral production plasmid. Each EmGFP-pre-microRNA cassette was amplified by PCR using the same 5' SpeI and 3' EcoRI primers. The PCR products were cleaned-up by column purification (Promega) and digested with SpeI and EcoRI. They were then cloned into the pRRL-sin-cPPT-CMV-MCS lentiviral production plasmid that had been digested with the same enzymes. This generated pRRL-303-Lenti-miR scr and pRRL-303-Lenti-miR 4.

Lentivirus vectors (designated Lenti miR 4 and Lenti miR scr) were generated at the UCLA Vector Core by transient co-transfection of 293T cells as described previously, with slight modifications [15]. Briefly, 100 mm dishes of non confluent 293T cells were co-transfected with 6.5 μg of pMDLg/pRRE (encoding HIV gag-pol), 3.5 μg of pMDG (encoding the VSV-G envelope), 2.5 ug of pRSV–REV (encoding HIV rev) and 10 μg of the relevant pRRL-303 plasmid, by the calcium phosphate co-precipitation method [16,17]. The plasmid vectors were kindly provided by Dr Luigi Naldini (University of Torino, Italy). Next day, the medium was adjusted to make a final concentration of 10 mM sodium butyrate and the cells were incubated for 8 h to obtain high-titer virus production as previously described [18]. After the 8 h incubation, cells were washed and incubated in fresh medium without sodium butyrate. Conditioned medium was harvested 16 h later, passed through 0.45 μm filters and concentrated by ultracentrifugation (figure 3.2).

Viral titer was determined by assessing viral p24 antigen concentration by ELISA (Alliance® HIV-I p24 ELISA Kit, Perkin Elmer) and expressed as μg of p24 equivalent units per milliliter. P24 values were related to a previously generated infectious titre standard curve. This standard curve was established by production of reporter particles by substituting the pRRL-303 plasmid with the reporter pLentiLox-DsRed plasmid[19]. Infectious titer was then determined by infection of 293T cells with serial dilutions of the concentrated virus preparation, followed by FACS analysis of DsRed expression 48 h later using an EPICS-XL flow cytometer (Beckman Coulter).

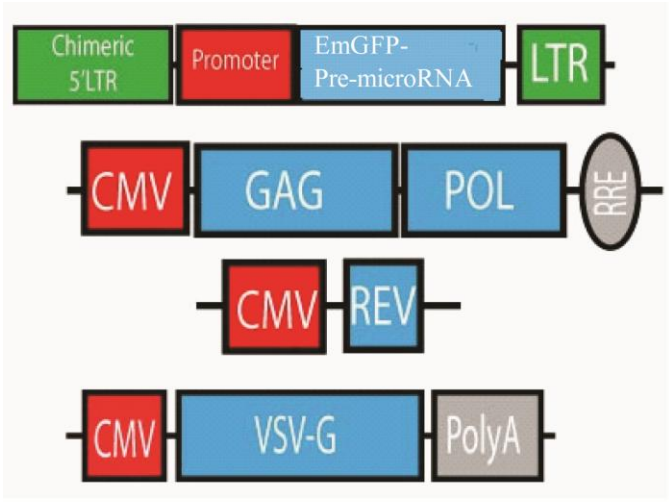

pRRL-303-Lenti-miR scr/
pRRL-303-Lenti-miR 4
10 µg

pMDLg/pRRE
6.5 µg

pRSV–REV
2.5 ug

pMDG
3.5 µg

Calcium phosphate
co-precipitation

293T cells

Sodium butyrate

0.45 µm filter &
ultracentrifugation
& titration

HeLa cells/
In vivo admin.

Figure 3.2 Schematic of lentiviral vector production. Shown are the relevant portions of the four plasmids (and the quantity of each plasmid per plate) used to generate VSV-G pseudotyped lenti miR 4 and lenti miR scr particles (top). These plasmids were co-transfected into 293T cells by the calcium co-precipitation method. Sodium butyrate was utilised to achieve high titer production. 293T cell media was passed through a 0.45 μm filter and the particles were concentrated by ultracentrifugation. Following titration lentiviral particles were tested on HeLa cells in culture or *in vivo*. Further details are provided in the text.

$1x10^5$ HeLa cells were seeded per well of a 24-well plate in 1 ml media and grown to approximately 80% confluency. Lentiviral particles were thawed, diluted in serum free media and the appropriate multiplicity of infection (MOI) added per well in a 100 µl volume. For knockdown experiments pFOXP3 was transfected 6 h later as previously described (section 2.4.5). FACS analysis was carried out directly for GFP expression or following permeabilisation and staining with an anti-mFOXP3 antibody as previously described.

7 week old female C57 Bl/6 mice were anaesthetised and their right flanks shaved. $1x10^6$ B16OVA cells in a 200 µl volume were injected subcutaneously into the right flank of each mouse. Tumour volume was determined from measurements of the tumour in two dimensions using a callipers and the formula $V=ab^2\pi/6$, where a is the longest diameter of the tumour and b is the longest diameter perpendicular to diameter a. Measurements were taken on alternate days from when the tumour first emerged until death of the animal. They were also taken immediately prior to culling the animal for T_{Reg} quantification.

In vivo

9 days post tumour induction (based on the T_{Reg} infiltration data) lentiviral particles were administered directly into the tumour. Three different injection sites were used to deliver a total dose of $5x10^7$ infectious units in a 100µl volume using a 32 gauge needle. For the proof of delivery experiment lenti-luc2 particles were used. Lenti miR 4 particles and control, lenti miR scr particles, were used for the treatment experiment.

Mice were anaesthetised, re-shaved around the tumour site and injected with 200 µl luciferin solution (3mg/ml) i.t. and a further 200 µl into the peritoneal cavity. Five

mins waiting was observed before mice were imaged on an IVIS imager (Perkin Elmer).

The entire tumour was recovered and divided into equal and representative portions for FACS and cytokine analysis. The samples for FACS were processed into a single cell suspension as follows; the tumour mass was incubated in 1ml collagenase (Sigma) and dispase (Sigma) buffer (3 mg/ml of each) at 37^0C in a shaking incubator for 10 mins. The sample was then mixed further by pipetting through 10 ml and then 5 ml pipettes, before passing through a mesh filter in a physical extrusion technique. The cells were pelleted by centrifugation (1500 rpm for 5mins at 4^0C), washed twice in PBS and resuspended in 2mls red cell lysis buffer (Sigma) with 5 minutes incubation at room temperature. 30 mls media with serum was added to stop the lysis process. Cells were recovered by centrifugation again, washed once in PBS and counted – both viable and non-viable. $1x10^6$ viable cells were aliquoted per sample to be analysed and cells were fixed and stained as previously described (section 2.4.11).

Tumours were harvested and processed into a single cell suspension as above. The following antibodies were used for staining; CD4-PerCP Cy5.5 (clone RM4-5), CD8-APC H7 (clone 53-6.7) (both 0.2 µg/test from Biolegend); CD25-APC (clone PC61.5) (0.1 µg/test, eBioscience) and FOXP3-PE (clone FJK-16a) (0.5 µg/test, eBioscience). For quantification of T_{Reg} infiltration cells were gated first on viability and then distinguished based on CD4 or CD8 positivity and analysed in terms of CD25 and FOXP3 expression. This gave the following two populations of T_{Regs}; $CD4^+$, $CD25^+$, $FOXP3^{high}$ and $CD8^+$, $CD25^+$, $FOXP3^{high}$ and the following populations of activated $CD4^+$ helper T cells ($CD4^+$, $CD25^+$, $FOXP3^{low}$) and activated $CD8^+$ cytotoxic T cells ($CD8^+$, $CD25^+$, $FOXP3^{low}$). For determining T cell subsets post lentiviral vector administration cells were gated first on viability and then stratified according to the level of FOXP3 expression. Using this stratification cells were then analysed in terms of CD25 and either CD4 or CD8 expression.

in vivo

A representative portion of tumour (approximately one third) was harvested from animals, flash frozen and stored at -80^{0}C. Cytokine analysis was performed on a mouse pro-inflammatory multi-plex plate (Meso Scale Discovery) as per the manufacturer's instructions. Seven cytokines were assayed for: Interferon (IFN) γ, Interleukin (IL) 12 (p70 subunit), IL-1β, IL-6, mKC, IL-10 and tumour necrosis factor (TNF) α.

The following preparatory work was performed on tumour samples; samples were thawed on ice and a 300 mg specimen was isolated. The appropriate volume of homogenisation buffer (PBS with protease inhibitor cocktail [Roche] and 10% FCS) was added to each specimen to yield a concentration of 100 mg of tissue per ml and a uniform solution was achieved using a tissue homogeniser. 500 µl of this solution was centrifuged at 1000*g* and the supernatant recovered.

The cytokine assay was run as follows; 25µl of Blocker D-B (containing blocker and stabilisation agents) was added to each well, the plate was sealed and placed on a plate shaker for 30 min. Following incubation, the plate was washed (x1) in PBS + 0.05% Tween (Sigma) and blotted on tissue paper. Each sample supernatant was diluted 1 in 20 and 50 µl (equivalent to 250 µg of tissue) added per well. The standards were diluted to create a standard curve, as per protocol, in the homogenisation buffer and 50 µl was added to each well of the 96-well MSD plate. The plate was sealed and placed on a plate shaker for 1.5-2 h at 800rpm. The detection antibody solution mix (1µg/ml), from kit, was added to each well (25µl/well). The plate was sealed, covered with tinfoil, and placed on a plate shaker for 1.5 h. Following incubation, the plate was washed (x3) in PBS + 0.05% Tween (Sigma) and blotted on tissue paper. MSD Read buffer (2X), from kit, was added to each well (150µl/well) using reverse pipetting to prevent bubbles. The plate was read using an electro-chemiluminescent multiplex system Sector 2400 imager (Meso Scale Discovery). This system has a CCD camera that measures the output signal from the wells in units of counts of light. Using the standard curve (signal versus concentration [pg/ml]) the concentration of analyte in the unknown samples was derived from the output signals from the samples with known levels of the analyte of interest.

In vitro experiments were performed with a minimum of 3 replicates per group. *In vivo* experiments were performed with a minimum of 3 mice per group. Results were tested for significance using an unpaired Student's *t* test with GraphPad Prism Version 5.0 software.

Although the negative control siRNA tested in chapter 2 fulfilled its function in validating the specificity of the test siRNA against mFOXP3, its sequence was proprietary and did not lend itself to incorporation into a plasmid construct. Thus, a new scrambled siRNA sequence (miR scr) was designed and examined in a mFOXP3 expression assay as before.

Results are displayed in figure 3.3. miR scr had a statistically greater effect on the number of $FOXP3^+$ cells than Neg siRNA ($p = 0.01$). However the knockdown efficiency induced by the test RNAi mediator (mimic #4) on $FOXP3^+$ cells of 45% was still significantly greater than that induced by miR scr (17%). This difference which represented genuine RNA interference equated to 28% (+/- 1.8%, $p < 0.001$) and provided the confidence to go forward and incorporate both duplexes into lentiviral constructs.

In conclusion, a novel negative control RNAi molecule amenable to incorporation into a DNA-based construct was generated here and validated for the purpose of testing the experimental RNAi therapeutic.

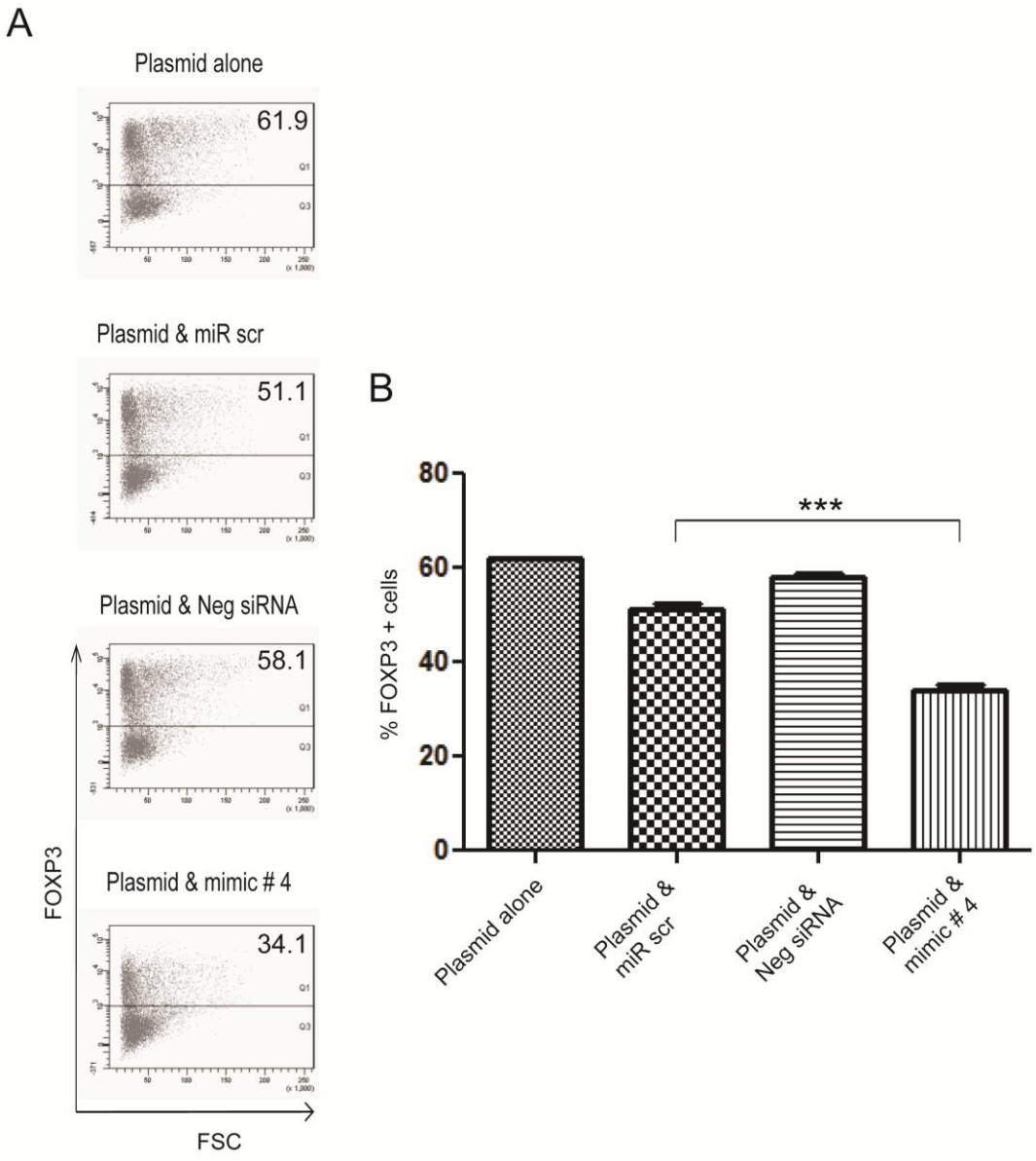

Figure 3.3 mFOXP3 expression assay with new scrambled siRNA. A) Dot plots from FACS analysis representing the percentage of $FOXP3^{+}$ cells following transfection of pFOXP3 and various siRNA duplexes into HeLa cells. The dot plots shown are representative of three independent experiments. **B)** Quantitative output for the data shown in A. Data are represented as mean +/- SEM of $n = 3$. (*** $p < 0.001$).

in vitro

The data above and in chapter 2 confirmed that the mimic #4 sequence was capable of silencing mFOXP3. To facilitate *in vivo* therapy, delivery of the RNAi mediator DNA would be required. In this series of experiments, we sought to optimise the parameters required to achieve maximum lentiviral vector-based delivery and expression *in vitro* and thus induce maximal knockdown efficiency with the test miR. A GFP-encoding version of the lentiviral vector was employed for *in vitro* assays to examine the kinetics of transgene expression post transduction.

The time at which maximum expression was achieved post transduction was first determined. An arbitrary MOI of 10 was chosen and the average GFP brightness per cell (mean fluorescence intensity [MFI]) quantified at different time points. Results are displayed in figure 3.4. Within the limitations of this assay, MFI was observed to be highest at 72 h post transduction, although not significantly higher than at 48 h ($p = 0.168$). Consequently 72 h was chosen as the time of maximum expression for all further *in vitro* experiments.

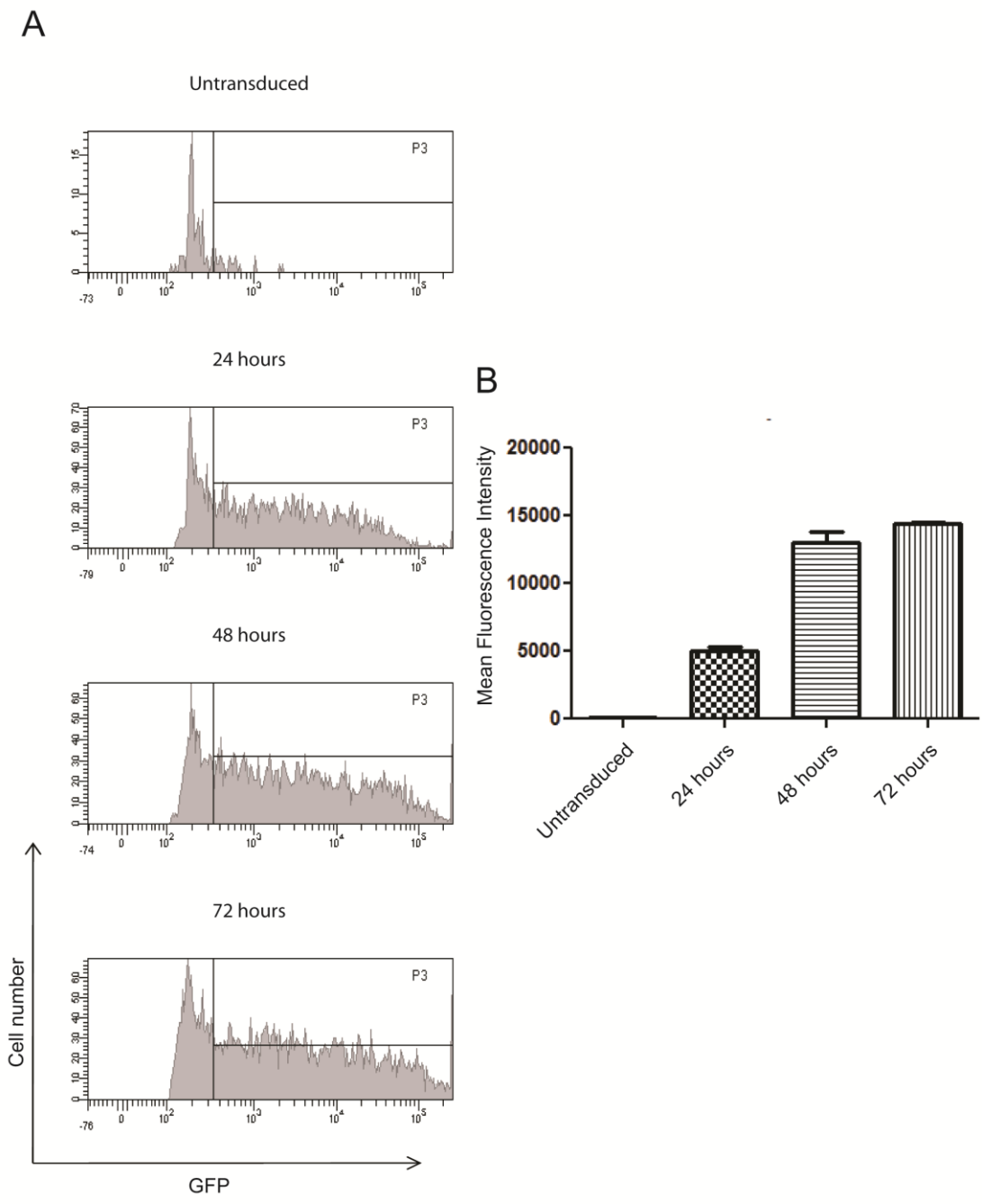

Figure 3.4 Determination of the time for maximal lentiviral expression *in vitro*. HeLa cells were transduced in culture with lentiviral particles carrying a GFP transgene at an MOI of 10. FACS analysis was carried out at the designated time points post-transduction. **A)** Histograms plotting the mean fluorescence intensity (MFI) against the number of cells. Histograms are representative of three independent experiments. **B)** Quantitative output from three replicates presented as the mean +/- SEM.

The optimal MOI for lentiviral vector on HeLa cells was then determined. This information would help achieve transduction of the maximum number of cells and hence the best knockdown possible. A range of MOIs from 5 to 20 was tested. Results are displayed in figure 3.5. An MOI of 20 was found to provide the highest transduction as evidenced by GFP expression by FACS. No reduction in cell viability (as measured by FACS analysis using propidium iodide) was observed with increasing MOI (data not shown). Although not statistically superior to an MOI of 15 ($p = 0.439$), an MOI of 20 was used for future *in vitro* experiments.

The above two experiments identified the optimal parameters for *in vitro* lentiviral vector transduction with the goal of facilitating maximum knockdown efficiency in subsequent assays.

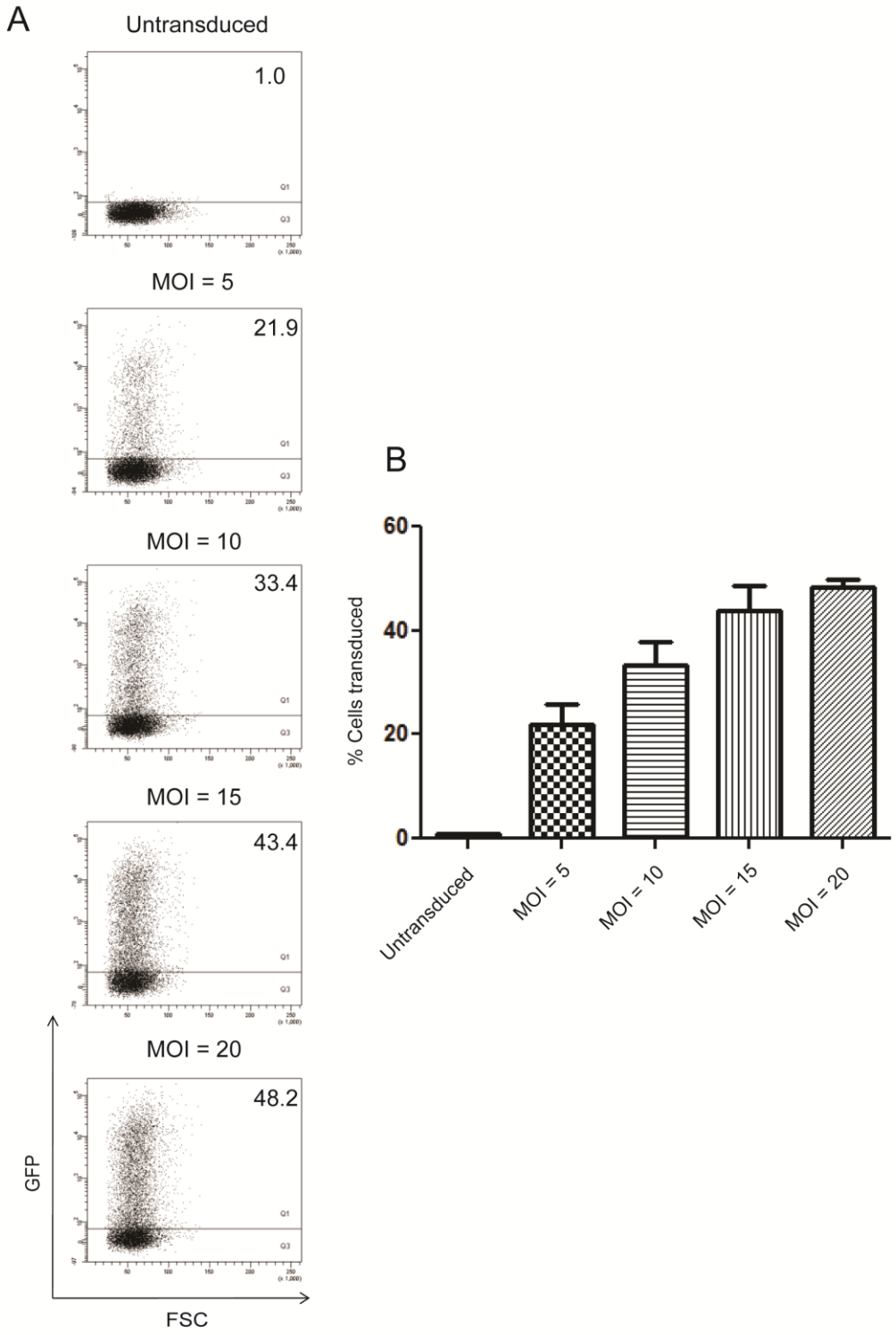
A
Untransduced
1.0
MOI = 5
21.9
MOI = 10
33.4
MOI = 15
43.4
MOI = 20
48.2
GFP
FSC
B
% Cells transduced
60
40
20
0
Untransduced
MOI = 5
MOI = 10
MOI = 15
MOI = 20

Figure 3.5 Determination of optimal MOI for lentiviral transduction of HeLa cells *in vitro*. HeLa cells were transduced in culture with lentiviral particles carrying a GFP transgene at various MOI. The transduction efficiency as indicated by the number of GFP^+ cells was determined by FACS at 72 h. **A)** Dot plots from FACS analysis representing the percentage of GFP positive cells. The dot plots shown are representative of three independent replicates. **B)** Quantitative output from three replicates presented as the mean +/- SEM.

The validated lentiviral vector system was utilised for delivery of DNA cassettes corresponding to miR 4 (Lenti miR 4) or miR scr (Lenti miR scr) in *in vitro* assays. The effect of transduction of these constructs on mFOXP3 expression was examined by FACS in *in vitro* assays. Results are displayed in figure 3.6. A global picture of silencing efficiency can be obtained by looking at the percentage of cells that were mFOXP3 positive in the various samples (figure 3.6 A & B). Lenti-miR 4 significantly reduced the number of $FOXP3^{+}$ cells compared with lenti miR scr (11% +/- 1.5%, $p < 0.002$) and an untransduced control (8.4% +/- 1.4%, $p = 0.004$).

However as outlined in Chapter 2, assessment of knockdown efficiency in terms of positive or negative cells may not reveal intracellular reductions in expression. Partial knockdown may be overlooked, although it may be sufficient for a phenotypic change in the cell. Thus, the FOXP3 status of cells was stratified according to fluorescence intensity (negative, medium and high) (figure 3.6 C). The graphs show a reduction in the number of highly positive FOXP3 cells following lenti miR4 transduction in comparison with lenti miR scr (5.8% +/- 1.8%,$p = 0.033$). The reduction in the number of cells highly expressing FOXP3 is accounted for by increases in the number of cells with medium expression (1.5% +/- 4%) and no expression at all (4% +/- 5.4%), although neither increase is statistically significant ($p= 0.745$ and $p = 0.479$ respectively). This suggests that, following lenti miR 4 transduction, cells that highly expressed FOXP3 now express the protein at an intermediate level, while those previously displaying medium expression are now negative for FOXP3.

This experiment validated lentiviral vector as an *in vitro* delivery vehicle for artificial miRNAs and confirmed that the mimic #4 sequence mediates RNAi against mFOXP3.

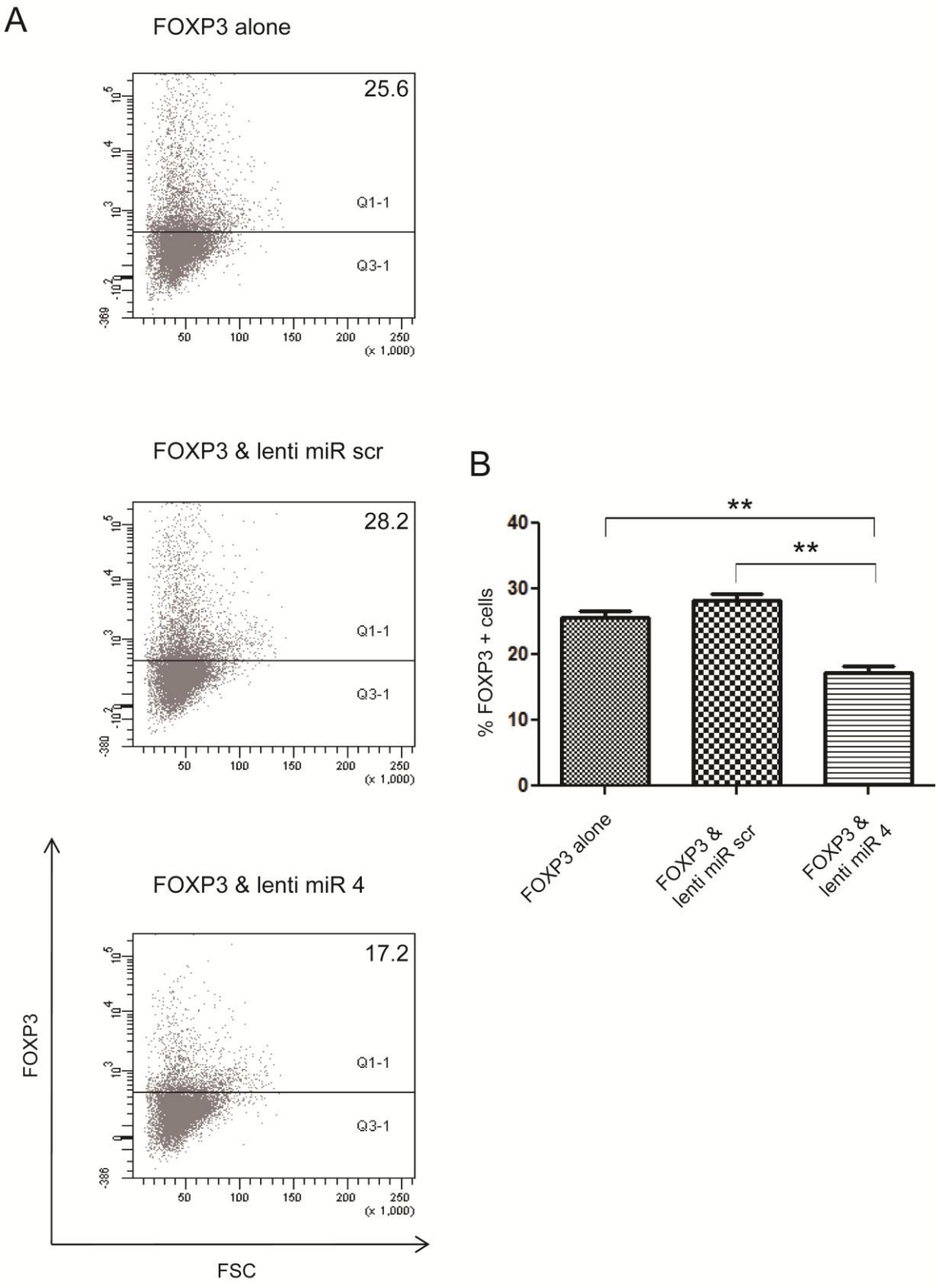
A
FOXP3 alone
25.6
Q1-1
Q3-1
FOXP3 & lenti miR scr
28.2
Q1-1
Q3-1
FOXP3 & lenti miR 4
17.2
Q1-1
Q3-1
FOXP3
FSC
(x 1,000)
B
% FOXP3 + cells
**
**
FOXP3 alone
FOXP3 & lenti miR scr
FOXP3 & lenti miR 4

C

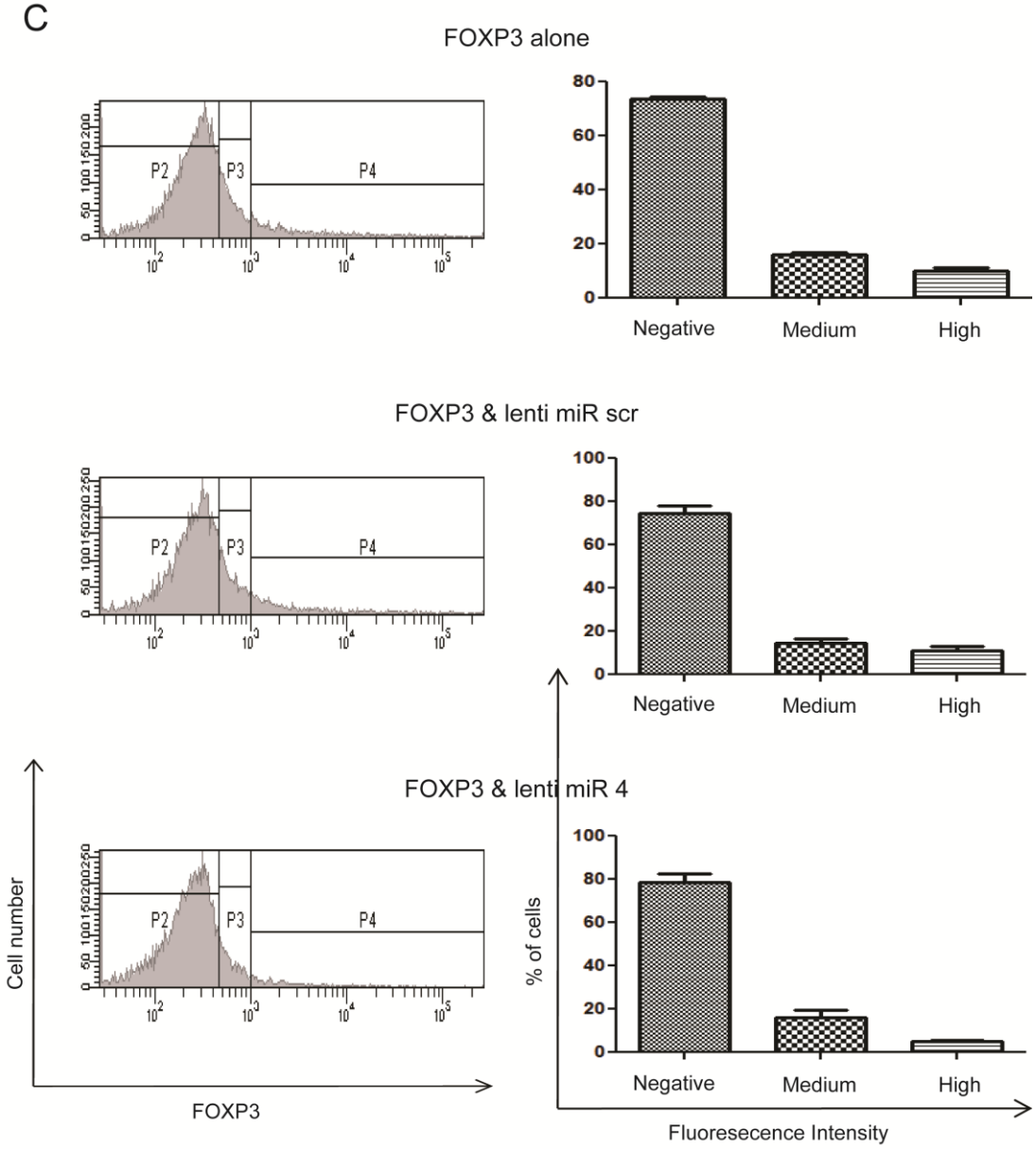
FOXP3 alone
P2
P3
P4
80
60
40
20
0
Negative
Medium
High
FOXP3 & lenti miR scr
P2
P3
P4
100
80
60
40
20
0
Negative
Medium
High
FOXP3 & lenti miR 4
P2
P3
P4
100
80
60
40
20
0
Negative
Medium
High
Cell number
FOXP3
% of cells
Fluoresecence Intensity

Figure 3.6 Effects on FOXP3 expression following transduction with lentiviral vector-microRNA particles *in vitro*. HeLa cells were transduced in culture with lentiviral particles carrying miR scr or miR 4 at an MOI of 20. 6 h later, cells were transfected with pFOXP3. After 72 h, cells were analysed for mFOXP3 expression by FACS. **A)** Dot plots representing the percentage of $FOXP3^+$ cells. The dot plots shown are representative of three independent replicates. **B)** Quantitative output from three replicates presented as the mean +/- SEM. (** indicates $p < 0.005$). **C)** A more detailed analysis of the changes in mFOXP3 expression following lentiviral vector-mediated RNAi. Histograms (left panel) show the relative proportion of cells with negative, medium and high fluorescence intensity (P2, P3, P4 respectively) which correlates with the level of mFOXP3 expression. Each histogram is representative of three independent replicates. The graphs represent the quantitative output from three replicates presented as the mean +/- SEM.

in vivo

Before attempting RNAi *in vivo* the first step was to confirm lentiviral vector-mediated gene delivery to murine tumours. Reporter lentiviral particles carrying the *luc2* gene were injected directly into s.c. B16OVA tumours. After four days, animals were imaged by IVIS whole body luminescence imaging. A 2 log-fold increase in luminescence could be detected specifically in tumours, compared with untreated control mice. Given the broad host range of the lentiviral vector employed, and the heterogenous nature of cell types within tumours, all cell types (T cells, other immune cells, tumour cells, fibroblasts etc) were expected to be transduced. While the specific cell types within the tumour which were transduced was not examined here, this experiment confirmed the ability of i.t. injection of the lentivirus particles to mediate *in vivo* transduction and expression of their transgene.

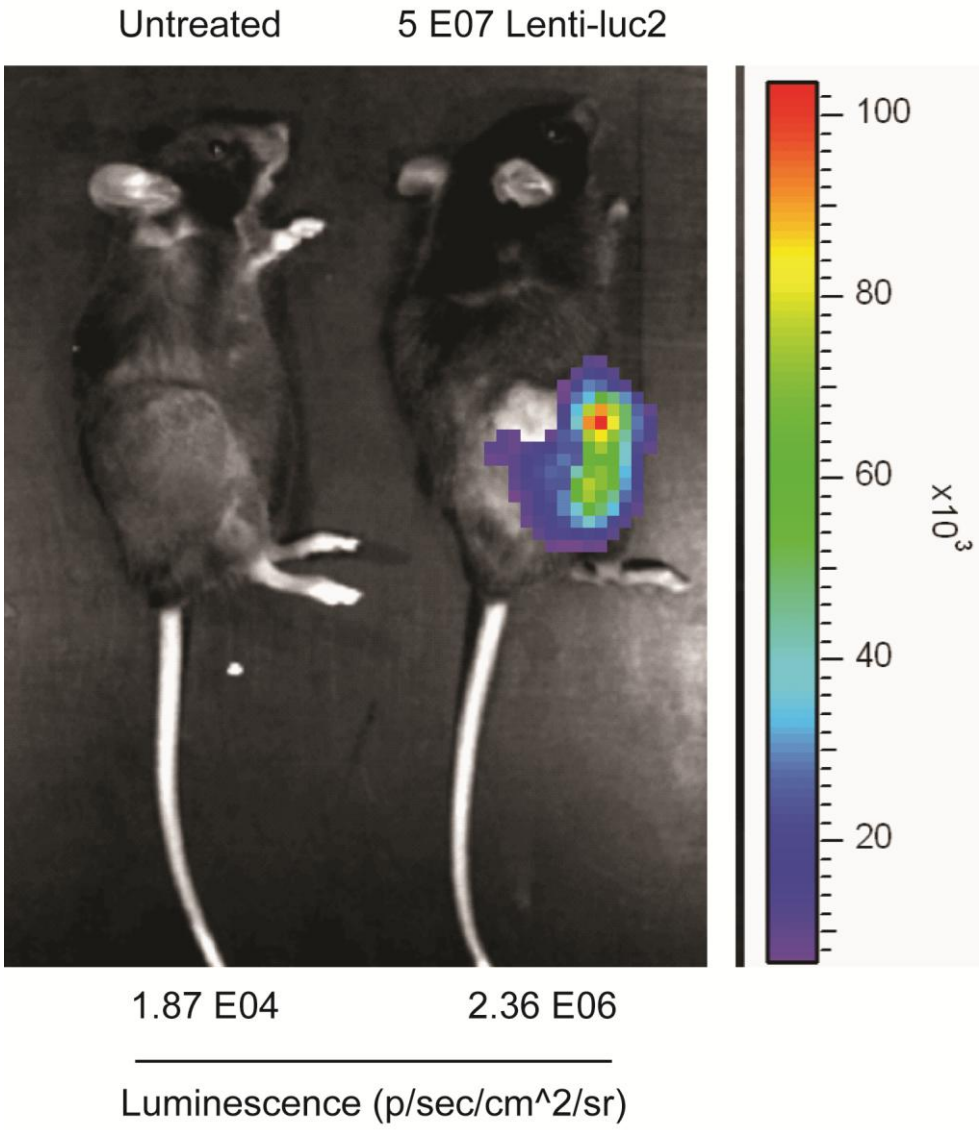

Figure 3.7 Lentiviral vector transduction *in vivo*. Murine xenograft tumours (flank) were i.t. injected with lentiviral particles carrying the *luc2* transgene or PBS. Four days later, mice were subjected to whole body imaging. Bioluminescence is presented as a pseudocolour scale (right-hand side): red, the highest photon flux; blue, the lowest photon flux. Luminescence was detected specifically in the tumour region. A quantitative readout is also supplied below the image.

As a forerunner to *in vivo* experimentation with miR particles, the optimal time for tumour treatment was examined. Since intra-tumoural T_{Reg} numbers differ at various stages of xenograft growth, the aim was to establish the optimum therapeutic window to manipulate T_{Regs} within the context of a growing tumour and so maximise therapeutic response. The ideal setting would require T_{Reg} infiltration prior to treatment but not too late in the course of the disease to ensure that tumour immune escape had not already taken place.

In the absence of a non-terminal assay to determine T_{Reg} infiltration numbers, a reference curve of T_{Reg} number versus tumour volume for the s.c. B16OVA xenograft model was generated (figure 3.8).

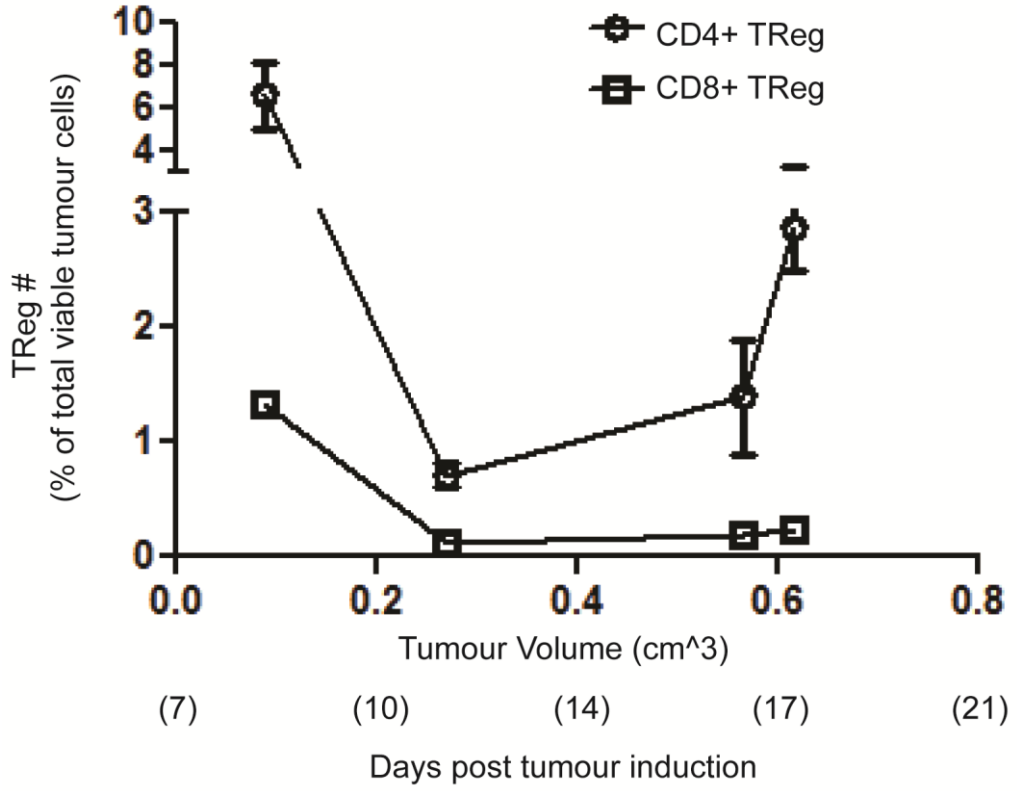

Figure 3.8 Temporal analysis of intra-tumoural T_{Reg} numbers in B16OVA tumours. $CD4^+$ and $CD8^+$ T_{Regs} are graphed independently. T_{Reg} numbers as a percentage of total viable tumour cells were established by FACS analysis at various time points post induction of B16OVA tumours. These data were plotted against the average tumour volume for mice culled at that time point and the time post tumour induction. T_{Reg} numbers are plotted as the mean of 5 mice per time point +/- SEM.

A similar pattern was observed with $CD4^+$ and $CD8^+T_{Regs}$ albeit $CD8^+T_{Regs}$ were generally present at a lower level (range 0.1 to 1.3% versus 0.7 to 6.6%). While tumour volume increased over time, the relative proportion of T_{Regs} varied widely throughout the course of xenograft growth. Following an initial peak of T_{Reg} infiltration, numbers then declined followed by a trend towards increasing number again at the terminal stages of the disease.

Since tumour volume could readily be established without the need to sacrifice the animal, this curve permitted estimation of the number of T_{Regs} within a given tumour at a given time and hence at what tumour volume to treat. Based on the curve the optimal time to treat was determined to be at or before the tumour volume reached 0.1 cm^3or day 8/9 post tumour induction. Identification of the optimal time at which to manipulate T_{Regs} within the growing tumour provided the best chance of therapeutic success.

Following identification of the optimal time to manipulate T_{Regs} within the growing tumour mice were then treated with lentiviral particles carrying miR 4. Untreated tumour-bearing mice and mice treated with lenti miR scr served as controls. The hypothesis was that, following therapeutic intervention, the first detectable alteration would be a change in cytokine profile. 9 days post tumour induction (based on the T_{Reg} infiltration data) lentiviral particles were administered i.t. 4 days later all mice were culled at a single time point. Tumours were harvested and processed for cytokine analysis. The content of interferon-γ, IL-12p70, IL-1β, IL-6, mKC, IL-10 and TNF-α was determined for each experimental tumour. Levels were quantified in supernatant derived from tumour homogenate using mouse pro-inflammatory multiplex plates. Results are displayed in figure 3.9. With the exception of a significant reduction in IL-1β levels ($p = 0.029$), administration of lenti miR 4 failed to invoke a globally significant change in cytokine profile relative to control animals. Indeed this reduction in IL-1β is contrary to the expected outcome – if mFOXP3 knockdown had been successful one would expect a pro-inflammatory response which might be evidenced by an increase in IL-1β levels. Of note lenti miR scr failed

to invoke any detectable, significant change in cytokine profile compared with untreated animals. This is suggestive of the low immunogenicity of the vector itself.

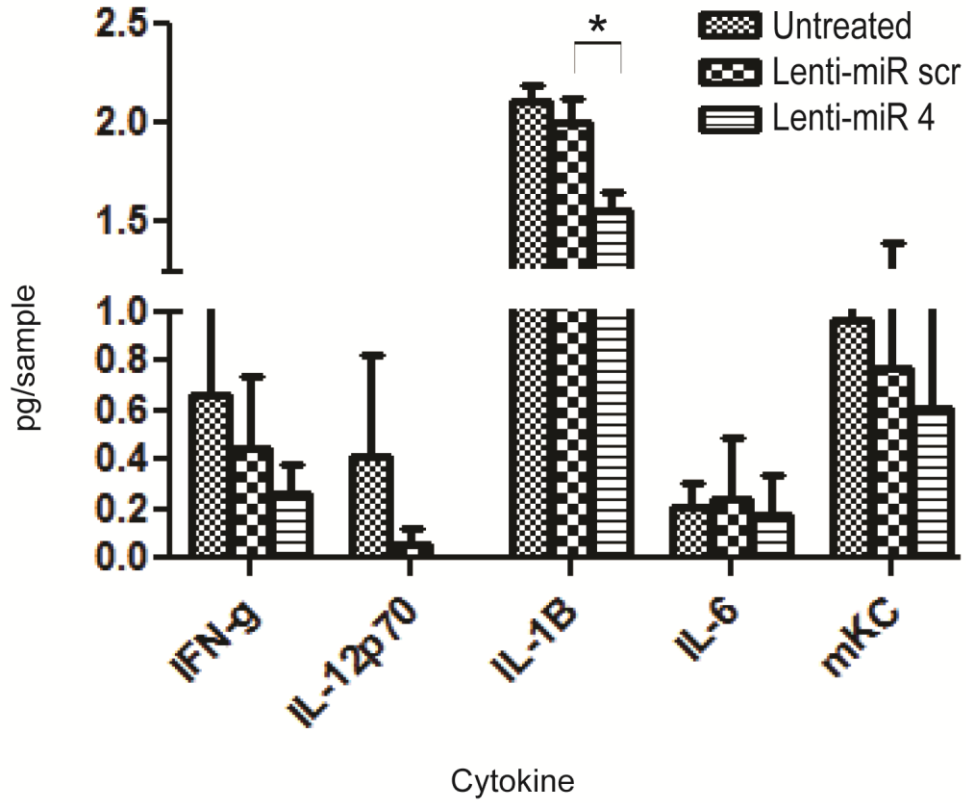

Figure 3.9 The intra-tumoural cytokine profile following lenti miR 4 treatment

C57 Bl/6 mice bearing s.c. B16OVA tumours were treated with lenti miR 4 or lenti miR scr. The cytokine profile of tumours 4 days post treatment was determined using a mouse pro-inflammatory multiplex plate. Levels are shown only for cytokines above the limit of detection and expressed as the mean +/- SEM for three mice per group. Statistics compare the two lentiviral treatment groups where one group received miR 4 and the other received miR scr. * indicates p = 0.029. Sample in this context refers to a representative portion of each tumour corresponding to 250 µg of tissue.

Had there been a cytokine change as a result of functional inhibition of T_{Regs} a decrease in the number of detectable T_{Regs} along with a concomitant increase in immune effector populations (e.g. $CD8^+$ cytotoxic T cells) would be expected [20]. Nonetheless, both these T cell subsets were characterised by FACS analysis (figure 3.10). However, as expected, no distinction in their relative abundance could be detected. The cytokine and T cell profiles presented confirm that further optimisation of the putative therapeutic and/or the experimental design are required to achieve a therapeutic response.

Lenti-miR scr

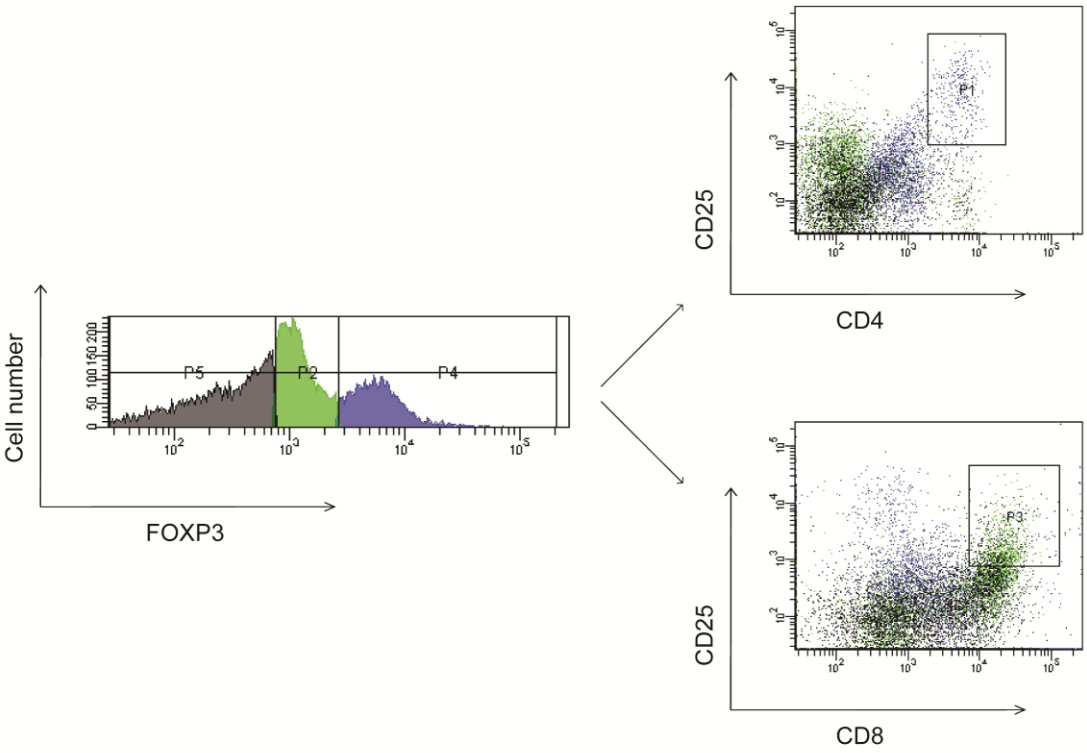

Lenti-miR 4

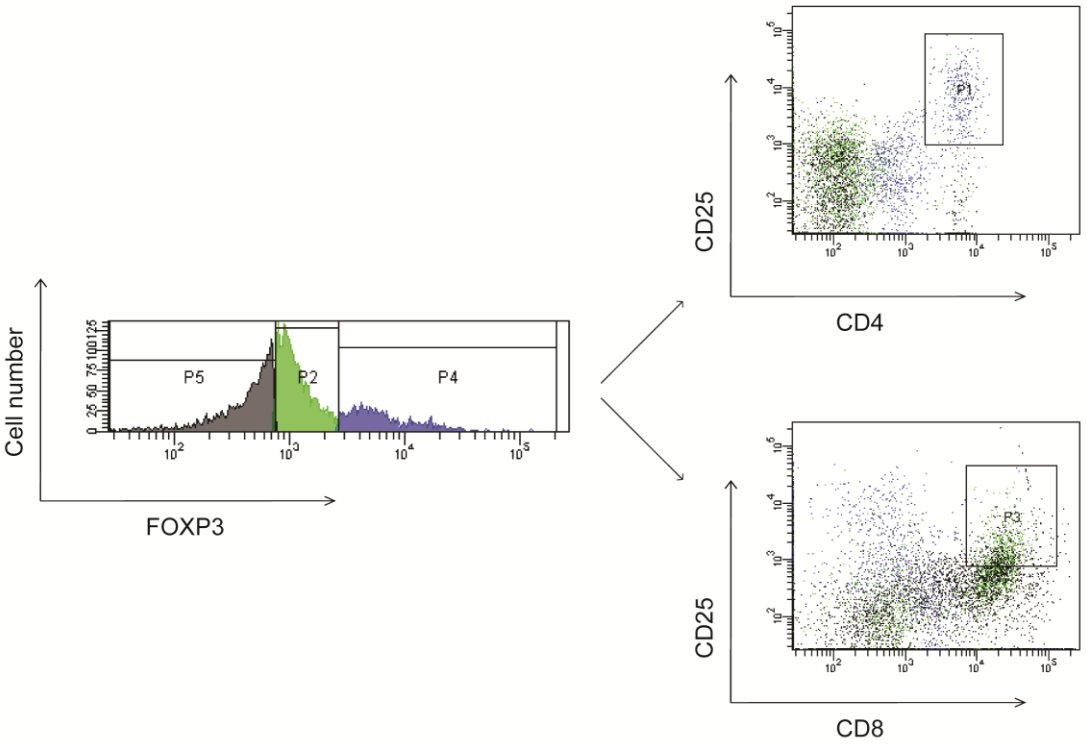

Figure 3.10 Intra-tumoural T cell subsets following lenti miR treatment. The relative abundance of different T cell subsets in tumour samples was determined by FACS analysis. Representative T cell populations from a mouse treated with lenti miR scr and a mouse treated with lenti miR 4 are compared from groups of 3 mice. Cells were stratified according to FOXP3 expression (left) and then analysed in terms of CD25 and either CD4 or CD8 expression (right). P1 identifies $CD4^{+}$, $CD25^{High}$, $FOXP3^{High}$ cells and represents $CD4^{+}$ T_{Regs}. P3 identifies $CD8^{+}$, $CD25^{High}$, $FOXP3^{Low}$ cells and represents $CD8^{+}$ cytotoxic T cells.

In this chapter the goal was to advance our validated RNAi mediator from an experimental tool towards an *in vivo* therapy by combining it with a lentiviral vector system. This clinically relevant vector was demonstrated to be capable of delivery and induction of gene silencing in an *in vitro* system. Moreover, transduction was validated in an *in vivo* tumour model. The optimum stage in tumour progression at which to intervene with this and other similar therapeutic approaches was identified. However, within the limitations of the experimental model, no therapeutic benefit could be demonstrated following lentiviral delivery of an artificial miRNA targeting mFOXP3 in a pilot study. Further modifications of the therapeutic such as cell-specific delivery capability coupled with improvements in experimental design should enhance the likelihood of success.

Limitations of in vitro experimental setup: mFOXP3 was successfully silenced using a lentivirus vector to deliver an artificial miRNA in an *in vitro* system (figure 3.6). However the knockdown efficiency was only 37% with lenti miR 4 in contrast to 57% with mimic #4 delivered with Lipofectamine® (figure 2.6). This could in part be explained by the poor transduction efficiency achieved with the lentiviral particles (48% - figure 3.5) in contrast to the 70 % efficiency achieved with siRNA delivered using Lipofectamine® (figure 2.4).

The poor knockdown efficiency could be further explained by the experimental setup for the *in vitro* knockdown assay (figure 3.6). In the absence of a cell line that stably expressed mFOXP3 it was necessary to transfect cells with a plasmid carrying the target gene and also transduce cells with lentivirus carrying the relevant miR. The transduction and transfection of the same cells *in vitro* is not an ideal system, as one process likely interferes with the other and it requires a compromise between optimal conditions for both processes to succeed; for lentivirus transduction the optimal protocol involved seeding the cells 24 h in advance of transduction with maximum expression achieved after 72 h (figure 3.4); in contrast, maximum expression was achieved 48 h post transfection with Turbofect®, again allowing a 24 hour window after seeding (data not shown).

We attempted to combine these protocols without modification (transduction followed by transfection 24 hours later), but this proved unsatisfactory due to the

inability to transfect overly-confluent cells 48 h post seeding. Overall, cell viability was not significantly reduced however. We compromised by proceeding with transfection 6 h rather than 24 h post transduction. This improved transfection efficiency albeit not to the levels achieved under optimal conditions; transfection alone, under optimal conditions reached 47% of cells (figure 2.6) while transfection under the modified conditions and in the presence of lentivirus reached only 25.6% of cells (figure 3.6). Generation of HeLa cells stably expressing the miRNAs of interest using the lentiviral particles may have circumvented this problem as the optimal transfection protocol could have been followed.

The above notwithstanding, the experimental strategy served to permit validation of the optimal miR from the various hypothetical sequences outlined in Chapter 2.

In vivo transduction: Lentiviral transduction *in vivo* was confirmed using the *luc2* reporter gene and whole body imaging (figure 3.7). This assay did not provide any information as to which particular cell types within the tumour had been transduced however. Efforts were made to characterise which cell types had been transduced by FACS analysis through antibody detection of the delivered luciferase protein and a panel of cell-specific markers (data not shown). The absence of a robust, high affinity antibody against the luciferase protein made this work unachieveable however. Thus, we can only speculate as to what cells received lentimiR 4; Given that the lentiviral particles had been pseudotyped with VSV-G one would expect quite a broad, indiscriminate tropism[21].

miR activity: The effects of miR 4 expression within non-target (i.e. non-T_{Reg}) cells is largely unpredictable, but is likely to be heavily influenced by the level of FOXP3 expression within a given cell type. Worthy of note, is that all human cancer cell lines tested in one study expressed detectable levels of FOXP3 [22]. It is hypothesised that cells expressing high levels of FOXP3 would be most responsive to miR4 over-expression, but that FOXP3 knockdown may result in widely varying phenotypes for different cell types. Of concern would be the possibility that FOXP3 knockdown in cancer cells may be detrimental – recent reports suggest that FOXP3 acts as a tumour suppressor gene in breast [23,24] and prostate cancer[25].

Limitations of xenograft model: From figure 3.8 the optimal time to treat was determined to be at or before the tumour volume reached 0.1 cm^3. In practical terms, this related to tumour dimensions of approximately 0.6 cm x 0.6 cm. While it was possible to measure tumour volumes smaller than this, no samples were taken to determine T_{Reg} infiltration numbers as tumours were too small for FACS processing. It could be concluded that a day or two prior to the tumour volume reaching 0.1 cm^3 (Day 8 or 9 post tumour induction) there were sufficient T_{Regs} *in situ* for treatment and tumour immune evasion had not yet occurred. Intervention at this early/intermediate stage of disease progression is consistent with a previous study using diphtheria toxin to deplete T_{Regs} in transgenic DEREG (*de*pletion of *reg*ulatory T cells) mice[20]. This study also confirmed that intervention at a later time point in the disease had no effect on tumour volumes. Based on this, it was deduced that following the initial peak in T_{Reg} number within the s.c. B16OVA tumour model, immune control has been circumvented and therapies aimed at abrogating the suppressive component of the immune system would be insufficient to surmount anergy.

Suggested reasons for therapeutic failure: Despite validation of *in vivo* transduction and optimisation of the time to target T_{Regs} within the B16OVA tumour model, no therapeutic benefit could be detected at a cytokine or cellular level (figures 3.9 and 3.10). A number of explanations for the apparent failure of the therapy *in vivo* can be proposed;

i) The experimental setup only included one sampling point – 4 days post lentiviral delivery directly to the tumour. Based on the whole body imaging data (figure 3.7) it is likely that the therapeutic artificial miRNA was expressed and most likely processed into the mature miR at this stage. However, it is unclear if an appropriate window of time was allowed for a response to FOXP3 silencing to manifest as an altered cytokine profile. Perhaps more pronounced alterations in individual cytokine levels may have been detectable earlier than day 4. The time lag for a cytokine response to translate into a cellular immune response is also difficult to predict and thus cellular changes may also have been missed by the single

sampling time point. Larger-scale trials including multiple sampling time points were beyond the practicalities of this thesis work. Future work might also look beyond lymphocytes and include a full immune cell profile of the tumour microenvironment.

ii) The suitability of the tumour model may also need to be revisited. The B16OVA melanoma model was chosen as it represents an antigenically defined tumour. Thus any immune response raised against the tumour would be directed predominantly against a single antigen (the OVA peptide) and more readily detectable. However, the B16 tumour represents an aggressive model whose growth rate quickly outstrips its neovascularisation. This leads to a solid, vascularised outer tumour surrounding highly necrotic more central regions. Consequently distribution of lentiviral particles within the tumour and cytokine secretion throughout the tumour mass are highly variable and unpredictable.

iii) As outlined above, it is unclear which particular cell types within the tumour mass were transduced. The potential exists for FOXP3 knockdown in non-T_{Reg} cells to nullify any potential therapeutic benefit. It is more likely that an insufficient number of T_{Regs} were transduced to achieve a detectable alteration in cytokines. Targeted lentiviral transduction of T cells or more specifically T_{Regs} would be one solution; such targeted particles promise improved efficiency of delivery to T_{Regs} while simultaneously reducing off-target effects through their enhanced selectivity. A number of versatile platforms exist to redirect lentiviral particles (reviewed in section 1.3.3). Moreover the literature provides robust examples of lentivirus targeted to T cell surface receptors; Wang et al., have targeted the CD3 receptor [26] while the Chen lab have demonstrated receptor-specific delivery via CD4 [27]. Perhaps the most appropriate surface receptor for targeting T_{Regs} would be CD25 as it is constitutively expressed at a high level but only expressed on other T cell subsets following activation by antigen. Support for this receptor target comes from the myriad of T_{Reg} depletion studies using antibodies directed against CD25 (reviewed in [28]).

iv) It is possible that the RNAi mediator was not potent enough i.e. that the level of FOXP3 knockdown within each cell was not sufficient to alter the T_{Reg} phenotype. While this was not determined for the *in vivo* experiment, the *in vitro* data would suggest that following lenti miR 4 delivery up to 15% of cells retain a medium level of FOXP3 expression (figure 3.6). It is unclear if such a level of FOXP3 expression can maintain the suppressive nature of $T_{Regs.}$ That said, if the knockdown achieved *in vitro* were to be recapitulated *in vivo* (with approximately 80% FOXP3 negative T_{Regs}) one could predict that any immunosuppressive threshold had been overcome and an anti-tumour immune response would soon follow.

Conclusion Conceptually the idea of treating cancer by manipulating immune cells (especially suppressive immune cells) is relatively novel [29,30]. Immune-based therapies promise significant advantages over existing treatment modalities – through the generation of immunological memory distant secondaries and disease reoccurrences can be eradicated. The altered immune microenvironment that exists and indeed is fostered within a developing tumour, affords a therapeutic niche over the unflustered systemic immune system. In this chapter, we sought to exploit this niche - we present an exciting therapeutic strategy to harness the immune system to fight cancer by combining lentiviral vectors with an artificial miRNA. We developed a novel RNAi mediator against mFOXP3 but further improvements in delivery efficiency and specificity may be warranted.

1. Fontenot JD, Gavin MA, Rudensky AY. Foxp3 programs the development and function of CD4+CD25+ regulatory T cells. *Nat Immunol* 2003; **4:** 330-336.

2. Hori S, Sakaguchi S. Foxp3: a critical regulator of the development and function of regulatory T cells. *Microbes Infect* 2004; **6:** 745-751.

3. Quinonez R, Sutton RE. Lentiviral vectors for gene delivery into cells. *DNA Cell Biol* 2002; **21:** 937-951.

4. Collins SA, Guinn BA, Harrison PT, Scallan MF, O'Sullivan GC, Tangney M. Viral vectors in cancer immunotherapy: which vector for which strategy? *Curr Gene Ther* 2008; **8:** 66-78.

5. McBride JL, Boudreau RL, Harper SQ, Staber PD, Monteys AM, Martins I *et al*. Artificial miRNAs mitigate shRNA-mediated toxicity in the brain: implications for the therapeutic development of RNAi. *Proc Natl Acad Sci U S A* 2008; **105:** 5868-5873.

6. Liu YP, Berkhout B. miRNA cassettes in viral vectors: problems and solutions. *Biochim Biophys Acta*; **1809:** 732-745.

7. Poluri A, Sutton RE. Titers of HIV-based vectors encoding shRNAs are reduced by a dicer-dependent mechanism. *Mol Ther* 2008; **16:** 378-386.

8. Liu YP, Vink MA, Westerink JT, Ramirez de Arellano E, Konstantinova P, Ter Brake O *et al*. Titers of lentiviral vectors encoding shRNAs and miRNAs are reduced by different mechanisms that require distinct repair strategies. *RNA*; **16:** 1328-1339.

9. Brandl A, Wittmann J, Jack HM. A facile method to increase titers of miRNA-encoding retroviruses by inhibition of the RNaseIII enzyme Drosha. *Eur J Immunol*; **41:** 549-551.

10. An W, Telesnitsky A. Frequency of direct repeat deletion in a human immunodeficiency virus type 1 vector during reverse transcription in human cells. *Virology* 2001; **286:** 475-482.

11. Zhuang J, Jetzt AE, Sun G, Yu H, Klarmann G, Ron Y *et al*. Human immunodeficiency virus type 1 recombination: rate, fidelity, and putative hot spots. *J Virol* 2002; **76:** 11273-11282.

12. Lee AH, Suh YS, Sung JH, Yang SH, Sung YC. Comparison of various expression plasmids for the induction of immune response by DNA immunization. *Mol Cells* 1997; **7:** 495-501.

13. Xu ZL, Mizuguchi H, Ishii-Watabe A, Uchida E, Mayumi T, Hayakawa T. Optimization of transcriptional regulatory elements for constructing plasmid vectors. *Gene* 2001; **272:** 149-156.

14. Altschul SF, Gish W, Miller W, Myers EW, Lipman DJ. Basic local alignment search tool. *J Mol Biol* 1990; **215:** 403-410.

15. Naldini L, Blomer U, Gage FH, Trono D, Verma IM. Efficient transfer, integration, and sustained long-term expression of the transgene in adult rat brains injected with a lentiviral vector. *Proc Natl Acad Sci U S A* 1996; **93:** 11382-11388.

16. Chen C, Okayama H. High-efficiency transformation of mammalian cells by plasmid DNA. *Mol Cell Biol* 1987; **7:** 2745-2752.

17. Sakoda T, Kaibuchi K, Kishi K, Kishida S, Doi K, Hoshino M *et al*. smg/rap1/Krev-1 p21s inhibit the signal pathway to the c-fos promoter/enhancer from c-Ki-ras p21 but not from c-raf-1 kinase in NIH3T3 cells. *Oncogene* 1992; **7:** 1705-1711.

18. Sakoda T, Kasahara N, Hamamori Y, Kedes L. A high-titer lentiviral production system mediates efficient transduction of differentiated cells including beating cardiac myocytes. *J Mol Cell Cardiol* 1999; **31:** 2037-2047.

19. Dull T, Zufferey R, Kelly M, Mandel RJ, Nguyen M, Trono D *et al*. A third-generation lentivirus vector with a conditional packaging system. *J Virol* 1998; **72:** 8463-8471.

20. Klages K, Mayer CT, Lahl K, Loddenkemper C, Teng MW, Ngiow SF *et al*. Selective depletion of Foxp3+ regulatory T cells improves effective therapeutic vaccination against established melanoma. *Cancer Res*; **70:** 7788-7799.

21. Cronin J, Zhang XY, Reiser J. Altering the tropism of lentiviral vectors through pseudotyping. *Curr Gene Ther* 2005; **5:** 387-398.

22. Karanikas V, Speletas M, Zamanakou M, Kalala F, Loules G, Kerenidi T *et al*. Foxp3 expression in human cancer cells. *J Transl Med* 2008; **6:** 19.

23. Zuo T, Liu R, Zhang H, Chang X, Liu Y, Wang L *et al*. FOXP3 is a novel transcriptional repressor for the breast cancer oncogene SKP2. *J Clin Invest* 2007; **117:** 3765-3773.

24. Zuo T, Wang L, Morrison C, Chang X, Zhang H, Li W *et al*. FOXP3 is an X-linked breast cancer suppressor gene and an important repressor of the HER-2/ErbB2 oncogene. *Cell* 2007; **129:** 1275-1286.

25. Wang L, Liu R, Li W, Chen C, Katoh H, Chen GY *et al*. Somatic single hits inactivate the X-linked tumor suppressor FOXP3 in the prostate. *Cancer Cell* 2009; **16:** 336-346.

26. Yang H, Joo KI, Ziegler L, Wang P. Cell type-specific targeting with surface-engineered lentiviral vectors co-displaying OKT3 antibody and fusogenic molecule. *Pharm Res* 2009; **26:** 1432-1445.

27. Morizono K, Bristol G, Xie YM, Kung SK, Chen IS. Antibody-directed targeting of retroviral vectors via cell surface antigens. *J Virol* 2001; **75:** 8016-8020.

28. Rech AJ, Vonderheide RH. Clinical use of anti-CD25 antibody daclizumab to enhance immune responses to tumor antigen vaccination by targeting regulatory T cells. *Ann N Y Acad Sci* 2009; **1174:** 99-106.

29. Finn OJ. Cancer immunology. *N Engl J Med* 2008; **358:** 2704-2715.

30. Weiner LM. Cancer immunotherapy--the endgame begins. *N Engl J Med* 2008; **358:** 2664-2665.

The majority of human and mouse solid tumours feature an abundant macrophage population. However, despite the direct tumouricidal ability of macrophages and their ability to mobilise anti-tumoural immune responses through antigen presentation, a lack of these activities within tumours is apparent. The primary reason suggested for this phenomenon is the tumour-driven polarisation of macrophages to an M2-like phenotype, which is pro-tumourigenic. Thus, efforts to re-educate or re-programme the abundant tumour-associated macrophages (TAMs) to an anti-tumour M1 phenotype would seem meritorious, and has recently been validated in preclinical studies.

NFκB signalling is central to maintaining the M2 phenotype. Inhibition of this transcription factor has been shown to re-educate TAMs. Targeting of IKK2, the major activator of NFκB, has been shown to induce significant antitumour responses preclinically. To date, only *ex vivo* transfection strategies related to this have been explored, and while validating this therapeutic target, possess only limited potential for clinical translation. This study sought to develop a more universally applicable strategy that could modify TAMs *in situ*, involving TAM-specific transfection *in vivo*.

It was hypothesised that intra-tumoural non-invasive bacteria would serve as effective and specific delivery agents to TAMs. A non-pathogenic *E. coli* strain carrying a plasmid for mammalian cell expression of an IKK2 dominant negative protein (IKK2-DN) was designed and generated. The ability of this vector to mediate gene delivery to macrophages was validated *in vitro* in a human macrophage cell line using FACS analysis. I.t. administration of the therapeutic vector to growing s.c. tumours was examined in *in vivo* murine trials. TAM transfection was demonstrated by FACS. Cytokine profile analyses of tumours demonstrated induction of intra-tumoural pro-inflammatory cytokines following treatment (compared with controls), suggesting re-education of M2 TAMs.

This study demonstrates the utility of non-invasive bacteria as a novel class of TAM-specific gene delivery vector, as well as the potential for *in vivo* targeting of the NFκB pathway to re-programme TAMs, thereby switching their phenotype from pro- to anti-tumour.

TAMs generally follow an "M2" phenotype and play a detrimental role in cancer pathophysiology (section 1.1.3 above). They are found in distinct microenvironments within the tumour where they are co-opted by the presence or absence of various locally-derived signals for tumour gain; areas of invasion where they promote cancer cell motility, stromal and perivascular regions where they encourage metastasis, and in hypoxic regions where they stimulate angiogenesis [1]. Moreover, TAMs resident within hypoxic tumour regions have been shown to increase production of matrix metalloproteinase-7 [2]. This protein cleaves Fas ligand on tumour cells rendering them less sensitive to chemotherapy and immune-mediated cellular cytotoxicity [3,4]. The behaviour of M2 macrophages within a growing tumour is totally at odds with that of M1 macrophages that are capable of tumour cell lysis, antigen presentation and stimulation of anti-tumour T and natural killer cell responses [1]. Thus, re-programming macrophages to an M1 phenotype represented a justifiable therapeutic endeavour.

Recent evidence from Hagemann *et al* suggested that the NFκB pathway was central to macrophage phenotype and that manipulation of this pathway could re-programme macrophages [5]. Activation of NFκB is regulated by the inhibitor of kappa B (IκB) kinase (IKK) complex of which the β-kinase (IKKβ or IKK2) is dominant. Following phosphorylation, IKK2 then phosphorylates IκB which is then degraded in the proteosome. The p65/p50 NFκB heterodimer is released, enabling translocation to the nucleus and inflammatory gene transcription [6]. This signalling cascade can be blocked by introduction of a kinase-deficient, dominant negative IKK2 protein (IKK2-DN)[7,8]. This decoy protein competes with the unmodified, endogenous protein for binding to IκB. When IKK2-DN binds to its target, it is unable to phosphorylate it and the pathway is halted. In the absence of a robust protein delivery platform, the most robust means of delivering IKK2-DN is at a nucleic acid level via a genetic construct.

Introduction of IKK2-DN into TAMs *ex vivo* followed by transfer of the modified macrophages has been shown to be effective in inducing anti-tumour responses.[5]. However such *ex vivo* manipulation lacks clinical translatability. Thus, we sought to combine IKK2-DN with a vector capable of *in situ* manipulation of

macrophages. Given the widespread expression of NFκB in different cell types a degree of selective delivery is required to mitigate off-target effects.

The concept of bacteria-mediated gene therapy is not novel, and bacteria are known to localise to solid tumours following systemic administration[9,10]. Traditionally, invasive species of bacteria are used to non-specifically invade host tumour cells for 'hand-over' of plasmid DNA for host cell expression of a therapeutic. This process (termed 'Bactofection') is also used in vaccination strategies for various diseases, most commonly with oral administration of bacteria for the purpose of transfecting mucosal phagocytic cells to induce antigen presentation and antigen immune induction.

We hypothesised that, in the context of intra-tumoural bacteria, use of non-invasive bacteria would permit specific transfection of phagocytic cells, representing a novel strategy for cell type-specific targeting of tumour-related immune cells. The use of non-invasive bacteria promised to restrict the cell types that received IKK2-DN to phagocytic cells such as macrophages.

The aim of this study was to assess the potential of *MG1655*, a non-invasive *E. coli* strain, to mediate bacterial gene therapy to tumour-associated macrophages. A second, dependent aim was to re-educate tumour-associated macrophages by inhibition of the NFκB pathway through non-invasive bacterial delivery of IKK2-DN.

THP-1 cells were maintained in RPMI 1640 medium (Sigma-Aldrich) supplemented with 10% v/v foetal bovine serum (Sigma-Aldrich) and 2mM L-glutamine in the absence of antibiotics in a 37^0C incubator with 5% CO_2.

THP-1 cells were differentiated using a protocol modified from that previously published by Takashiba *et al* [11]. Briefly $2x10^5$ cells were seeded per well of a 24-well plate in 1 ml media. PMA (eBioscience) diluted in DMSO was added to a final concentration of 200nM. Cell adherence and a spreading morphology were confirmed using a light microscope. After 24 h the media was changed and cells were allowed to recover for 48 h before further experimentation.

E.coli K12 MG1655 was used in all experiments (UCC culture collection). For *in vitro* work a GFP plasmid (pMAX-GFP, Amaxa, USA) under the control of a eukaryotic promoter was introduced into this strain by electro-transformation.

For optimal transfection efficiency, hlyA-expressing bacteria are commonly employed; the *hlyA* gene derived from *Listeria monocytogenes* encodes the pore-forming listeriolysin O protein, which facilitates phagosome escape, and has been previously shown to significantly increase bacterial vector mediated transfection efficiency[12].For all *in vivo* work, a *hlyA*-expressing *E. coli* MG1655 strain (referred to as *E. coli* hereafter) was employed; MG1655 was transformed with a *hlyA* plasmid (pNZ44 - generated by Dr. Joanne Cummins, Cork Cancer Research Centre).

E. coli was transformed with the therapeutic plasmid carrying a kinase-negative mutant of IKK2 (IKK2-DN) – a kind gift from Dr. Rainer de Martin[7].

GFP and IKK2-DN genes were driven by eukaryotic promoters. Presence of the *hlyA* and therapeutic plasmid in the bacteria was confirmed by colony PCR to detect the *hlyA* and ampicillin resistance genes respectively.

in vitro *in vivo*

The appropriate bacterial stock was inoculated into 10 ml LB-broth with antibiotic selection and grown overnight (~16 h) at 37^{o}C, shaking at 200 rpm. The optical density of the culture was measured at a wavelength of 600 nm (OD_{600}) and the culture then diluted to an OD_{600} = 0.1. The culture was grown for a further 2-3 h at 37^{o}C, shaking at 200 rpm and the bacteria harvested when the OD_{600} reached 0.8-1.0. 1ml of the culture was then pelleted by centrifugation (13500 rpm for 1 min), the pellet was washed twice in PBS and resuspended in 1ml PBS. The concentration of this solution had previously been determined to be approximately $1x10^{9}$ CFU/ml. This stock solution was then diluted in PBS to the appropriate concentration.

Bacteria carrying pMAX-GFP were prepared as above and added directly to the differentiated THP-1 cells at different multiplicities of infection (MOI). In all experiments, cells and bacteria were co-incubated overnight for 16 h.

The efficacy of gene delivery was indicated by the number of GFP^{+} cells as determined by FACS analysis. FACS was performed as previously outlined (section 2.4.11) with some modifications to the cell preparation steps; the adherence of the cells to the plate was broken by incubating in PBS with 5mM EDTA for 10-20 mins and pipetting up and down vigorously. Cells were resuspended in PBS with 10% FBS to prevent clumping.

The time window after bacterial exposure and before FACS analysis was deemed an important parameter for maximal detection of GFP expression. Thus, two different time windows were explored; in one strand of the experiment, the culture media was changed following overnight incubation with the bacteria and the cells were rested for 8 h prior to analysis. In a second strand of the experiment, cells were rested for 24 h before analysis. In this latter experiment, extracellular bacteria were killed with gentamicin (20mg/ml for 2 h) in an effort to preserve the viability of the macrophage cells.

in vivo

6 week old female Balb/C mice (an immuno-competent strain) were anaesthetised and their right flanks shaved. The minimum tumourigenic dose ($1x10^5$ cells) were injected s.c. into the right flank to induce the mouse CT26 colon tumour model. 18 days post tumour induction mice were injected intra-tumourally at three different sites with a total dose of $1x10^6$ CFU of bacteria in a 100µl volume using a 32 gauge needle.

$1x10^6$ CFU of *E. coli* MG1655 with an integrated *lux* cassette (driven by a bacterial promoter) were injected into growing CT26 tumours in a 100µl volume using a 32 gauge needle. At various time points mice were anaesthetised and subjected to whole body imaging using an IVIS imaging system (Perkin Elmer).

The therapeutic IKK2-DN protein was FLAG-tagged which permitted detection with an antibody and FACS analysis to determine which cells had been reached. A single cell suspension was derived from the tumour as outlined previously (section 3.4.8) and intracellular FACS staining carried out as per section 2.4.11. The following antibodies and test concentrations were used; F4/80-PE (clone BM8) (eBioscience, 0.2 µg/test), anti-CD68-PerCP/Cy5.5 (clone FA-11) (Biolegend, 0.25 µg/test) and anti-FLAG Alexa Fluor 647 (Cell signalling, 1 in 450 dilution).

As per section 3.4.10.

As per section 3.4.5**.**

As per section 3.4.11.

E. coli MG1655 *in vitro*

To demonstrate proof of principle for non-invasive bacterial gene delivery to macrophages *in vitro*, the human THP-1 monocyte cell line was differentiated into macrophages and exposed to a bacterial strain carrying a plasmid encoding GFP under the control of a eukaryotic promoter. Transfection was assessed by FACS analysis for detection of GFP^+ cells.

Results shown in figure 4.1 demonstrate close to 100% transfection efficiency on viable cells following bacterial exposure at an MOI of 2.5 to 10, regardless of the time window between bacterial exposure and FACS analysis (see Materials and Methods 4.4.5 above). Cytotoxicity was clearly detectable under a light microscope at higher MOIs of 20 and 30 (data not shown) and, despite gating on viable cells, transfection efficiency was diminished by 90% (figure 4.1 A).

A longer time window of 24 h after bacterial exposure and before FACS analysis resulted in greater macrophage cell death (data not shown).In an attempt to reduce macrophage cell death caused by bacterial replication, an antibiotic strategy for elimination of live bacteria was assessed. However, the use of gentamicin in this context was ineffective and did not influence the number of dying macrophages (data not shown). It is likely that cell death pathways had already been engaged in the macrophage cells.

Overall, these data demonstrated the ability of this non-invasive bacterial vector to mediate efficient transfection of macrophages.

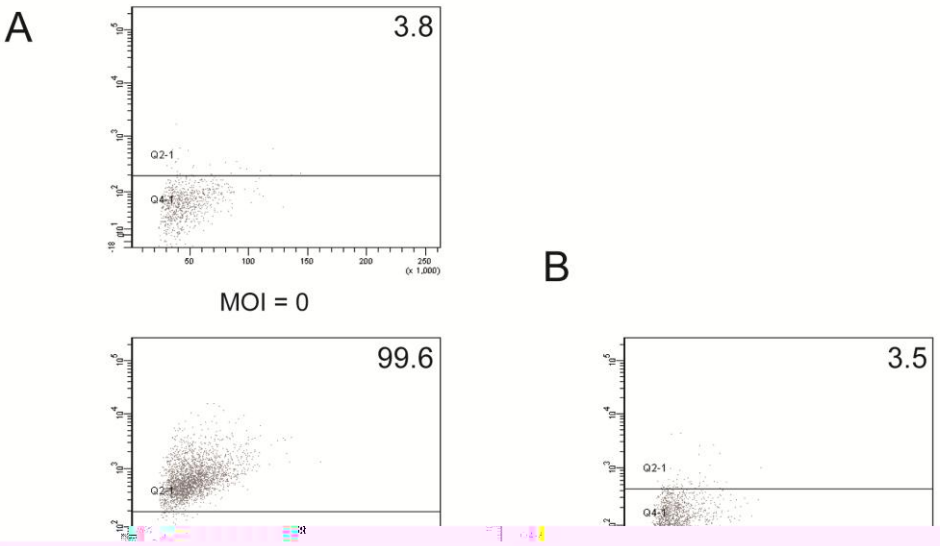
A
3.8
Q2-1
Q4-1
MOI = 0
B
99.6
Q2-1
3.5
Q2-1
Q4-1

Figure 4.1 Bacterial-mediated transfection *in vitro*. The THP-1 monocyte cell line was differentiated into a macrophage-like phenotype and exposed to *E.coli MG1655* carrying a GFP plasmid at different multiplicities of infection. Macrophages were allowed to recover for 8 h (A) or 24 h with gentamicin treatment (B). FACS analysis on viable cells was used to determine the number of GFP^+ cells. Data presented are representative of three independent replicates.

in vivo

Prior to initiating murine therapeutic trials, the fate of bacterial vector following i.t. injection to s.c. tumour xenografts was examined. It would be expected that a portion of the administered bacteria would i) be scavenged by phagocytic cells within the tumour, ii) leave the tumour and disseminate throughout the animal and/or iii) colonise the tumour microenvironment.

To provide data towards answering these questions, 1 x10^6 CFU *MG1655* carrying the *lux* cassette were injected into s.c. CT26 tumours in mice and monitored *in vivo* using whole animal imaging (figure 4.2). Since in this case expression of the *lux* reporter cassette was driven by a bacterial promoter, luminescence was indicative of live bacteria, rather than transfected cells. Thus detection of luminescence did not indicate whether the bacteria were intra- or extra-cellular. Figure 4.2 indicates that administered bacteria specifically colonised the tumour over time and continued to survive/grow within this microenvironment. This indicated that not all administered bacteria were phagocytosed. (Transfection was examined in subsequent experiments). No bacterial luminescence was detected elsewhere in the body, suggesting no significant spread of the vector. The reduction in luminescence detected at day one was interpreted as initial death of bacteria post injection. Thereafter bacterial replication commenced and luminescence increased accordingly.

A

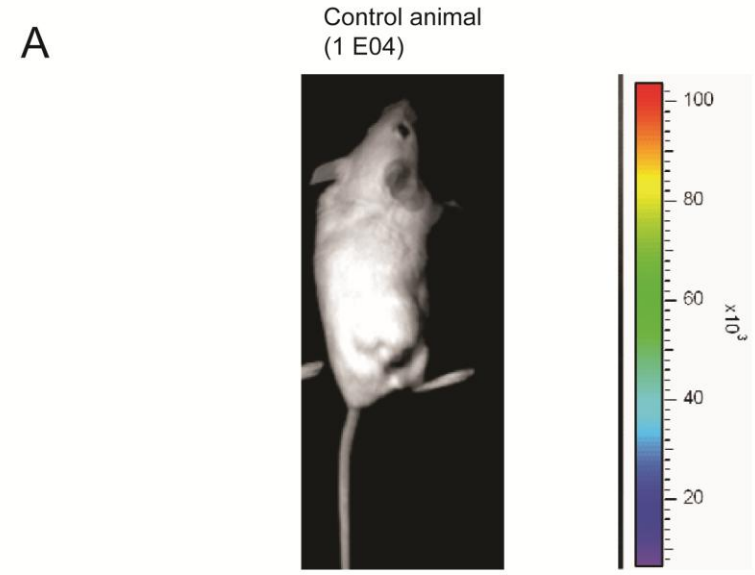
Control animal
(1 E04)
100
80
60
40
20
x10³
Day 0 (2.2 E06)
Day 1 (1.5 E05)
Day 2 (1.3 E06)
Day 5 (1.2 E07)

B

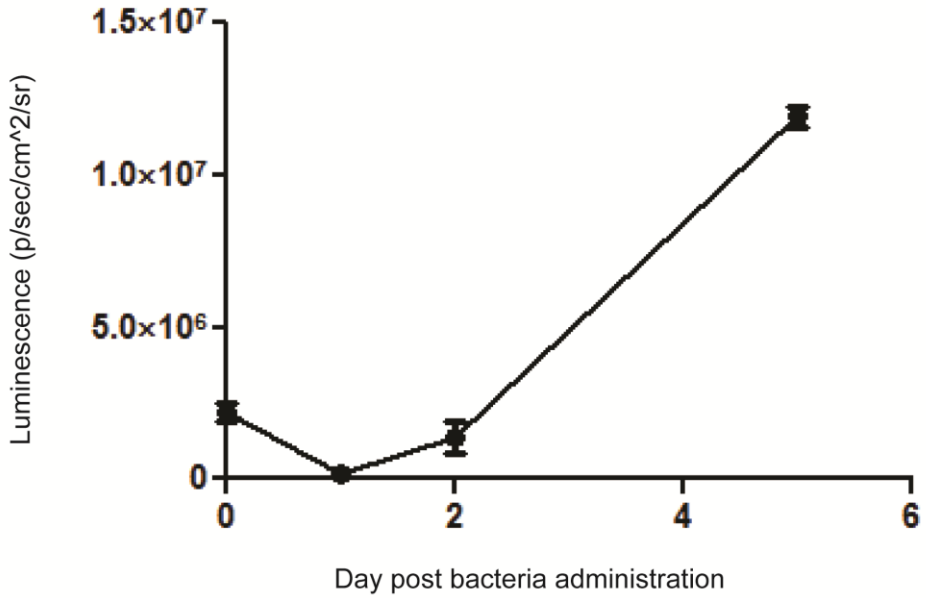

Figure 4.2 Fate of i.t. administered bacteria in mice. 1x10^6 *MG1655* bacteria carrying the *lux* cassette were administered directly into growing CT26 tumours. Viable, luminescent bacteria were detected at various time points specifically in the tumour using whole body imaging. Bioluminescence is presented as a pseudocolour scale (top, right): red, the highest photon flux; blue, the lowest photon flux. **A)** Average luminescence in p/sec/cm^2/sr is shown in parentheses. An untreated, tumour-bearing animal was imaged at each time point and is shown as a control. **B)** Graphical representation of tumour luminescence over time plotted as the mean +/- SEM for three mice.

in vivo

To provide evidence of gene delivery *in vivo,* bacteria bearing a plasmid encoding a FLAG-tagged protein under the control of a mammalian promoter were i.t. administered to s.c. CT26 tumours. FLAG expression was possible only following uptake of the bacteria by a mammalian cell and detection of FLAG by FACS was taken to be indicative of hand-over of the plasmid-borne gene from bacterial vector to, and expression by host mammalian cells. The cell type transfected was examined using antibody markers specific for macrophages.

Tumours were harvested two days post treatment and a single cell suspension generated. Cells were labelled with appropriate antibodies. FACS analysis is displayed in figure 4.3. The TAM population was selected for analysis through gating on both CD68 and F4/80. Having gated on double positive macrophages the number that were $FLAG^+$ (transfected) cells was determined. Compared with the control animal where the bacteria did not carry FLAG plasmid, approximately 20% of TAMs were $FLAG^+$ (66 versus 46.4) (figure 4.3A, right). Further characterisation of bacteria as *in vivo* gene therapy vectors might involve assessment of their capability to recruit phagocytic cells to the tumour. This extra information could be readily extracted from the above experimental setup by inclusion of a third group which did not receive any bacteria.

As the goal was to specifically transfect TAMs it was also important to determine how selective the bacteria were as a delivery vector. For this, all cells were gated in terms of FLAG positivity (figure 4.3B, left) and then analysed through macrophage markers (figure 4.3B, right). Within the confines of this pilot study 17% of all cells in the tumour were deemed to be transfected by the bacteria. Of these, 20% were definitely macrophages (stained double positive) while another 10% (Q1 and Q4) could also be of macrophage origin. 68% of $FLAG^+$ cells (Q3) were not positive for either macrophage marker however. The $FLAG^+$ cells were detected at day two only. No $FLAG^+$ cells could be detected at day four or beyond (figure 4.3 and data not shown).

This experiment demonstrated the ability of non-invasive bacteria to transfect TAMs *in vivo* and provided further information as to the cell-specificity of this delivery strategy.

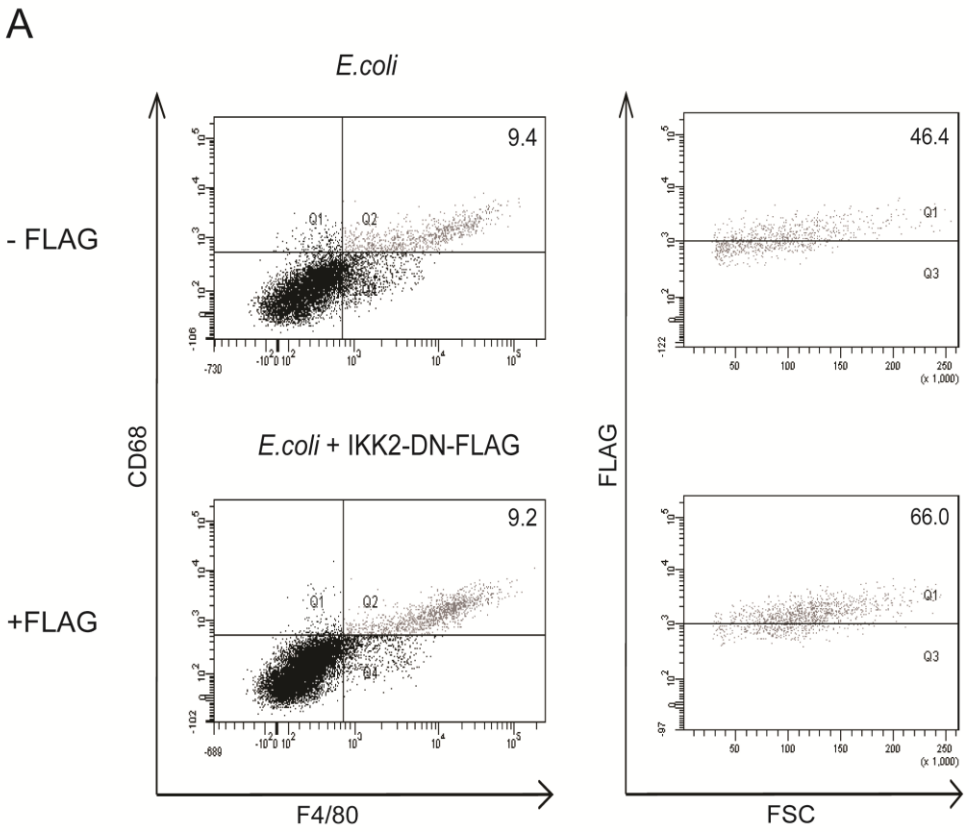
A
E.coli
- FLAG
+FLAG
E.coli + IKK2-DN-FLAG
9.4
46.4
9.2
66.0
Q1
Q2
Q3
Q4
CD68
F4/80
FLAG
FSC

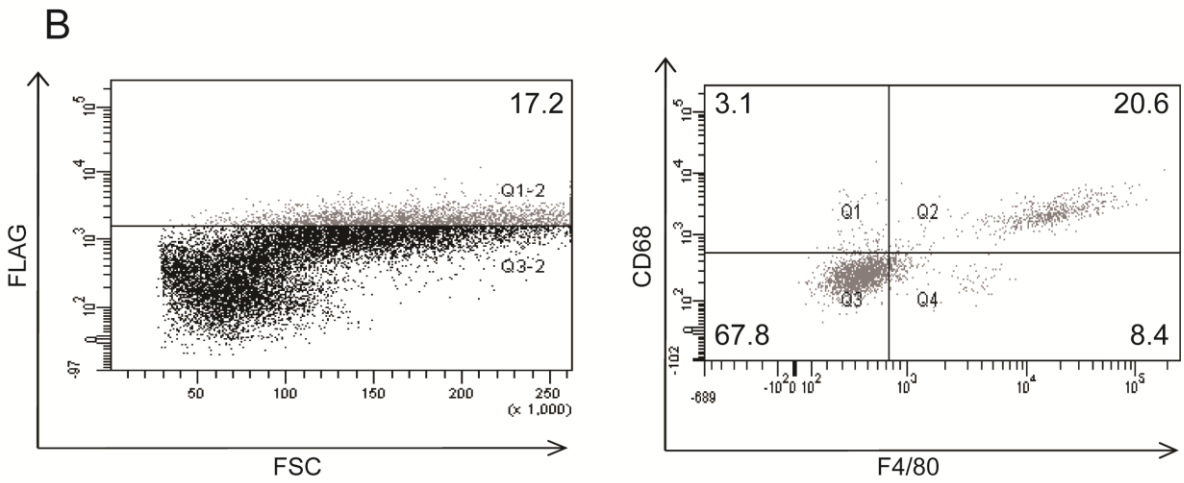
B
17.2
Q1-2
Q3-2
FLAG
FSC
3.1
20.6
67.8
8.4
Q1
Q2
Q3
Q4
CD68
F4/80

Figure 4.3 Bacterial-mediated gene delivery *in vivo*. *E.coli* +/- FLAG-tagged plasmid were i.t. administered directly to CT26 tumours. Two days later, tumours were harvested and individual cells analysed for TAM transfection by FACS detection of FLAG. **A) % FLAG$^+$ TAM:** CD68$^+$F4/80$^+$ TAMs (left) were gated on FLAG positivity (right). **B) % FLAG$^+$ which are TAM**; FLAG$^+$ cells (left) were gated on macrophage markers (CD68 and F4/80) (right). Each panel shows data from a single representative animal.

Confident that the bacteria were capable of transfecting 20% of TAMs in the tumour, it was then examined if the therapeutic strategy could alter the immune phenotype within the tumour. *E.coli* +/- the IKK2-DN encoding plasmid, or PBS was i.t. injected to growing CT26 tumours. The cytokine profile within the tumour was assessed at three time points post treatment. Results are displayed in figure 4.4.

Greatest differences overall were observed four days post treatment, and statistics for this time point are displayed in figure 4.4 (right panel). At day four, a significant change in cytokine levels could be attributed to the IKK2-DN gene. Cytokine changes invoked within the tumour involved significantly increased ($p<0.05$) IL-12, IL-1β, IL-6 and mKC, which is consistent with a pro-inflammatory response.

The possibility that administration of *E.coli* without the IKK2-DN gene could also induce a change in cytokine profile was also explored (figure 4.4.). The effect of the bacterial vector alone was assessed by comparing the *E.coli* treatment group with mice that received PBS. The cytokine levels in the bacterial vector group varied widely across the different time points. For clarity each cytokine was interpreted individually; for IFN-γ the decrease at day 4 and the increase at day 7 were insignificant ($p = 0.091$ and $p = 0.145$ respectively). For IL-12p70 the decrease at day 7 was not significant ($p = 0.234$). The increase seen at day 7 for IL-1β was not significant ($p = 0.102$).

The increases in IL-6 levels between PBS and *E.coli* groups at day 2 and day 7 were not statistically significant ($p = 0.245$ and $p = 0.05$ respectively). Notably however, the further increases seen in IL-6 at these time points due to the IKK2-DN plasmid were not significant either ($p = 0.509$ and $p = 0.796$ respectively) and thus the change in IL-6 was attributed solely to the vector. This contrasts with IL-6 levels on day 4 where an increase can be attributed directly to the IKK2-DN plasmid (see above).

The increases in mKC (PBS compared with *E.coli*) at day 2 and day 7 were statistically significant ($p = 0.033$ and $p = 0.036$ respectively). However inclusion of the IKK2-DN plasmid (PBS compared with *E.coli* + IKK2-DN) was not significant

at day 2 ($p = 0.135$) but significant at day 7 ($p = 0.027$). however on closer inspection the change attributable to IKK2-DN compared with the vector alone at day 7 was not significant however ($p = 0.731$). Therefore the changes in mKC at day 2 and day 7 were attributed solely to the vector. This contrasts with mKC levels on day 4 where an increase can be attributed directly to the IKK2-DN plasmid (see above). The increase in mKC due to the bacterial vector alone on day 4 was not significant ($p = 0.114$).

Overall, these data demonstrate that, with the exception of an increase in mKC at day 2 and day 7, the bacterial vector had a minimal effect on the intra-tumoural cytokine profile. In contrast the bacterial vector carrying IKK2-DN induced a significant change in the cytokine profile ($p < 0.05$) within the tumour.

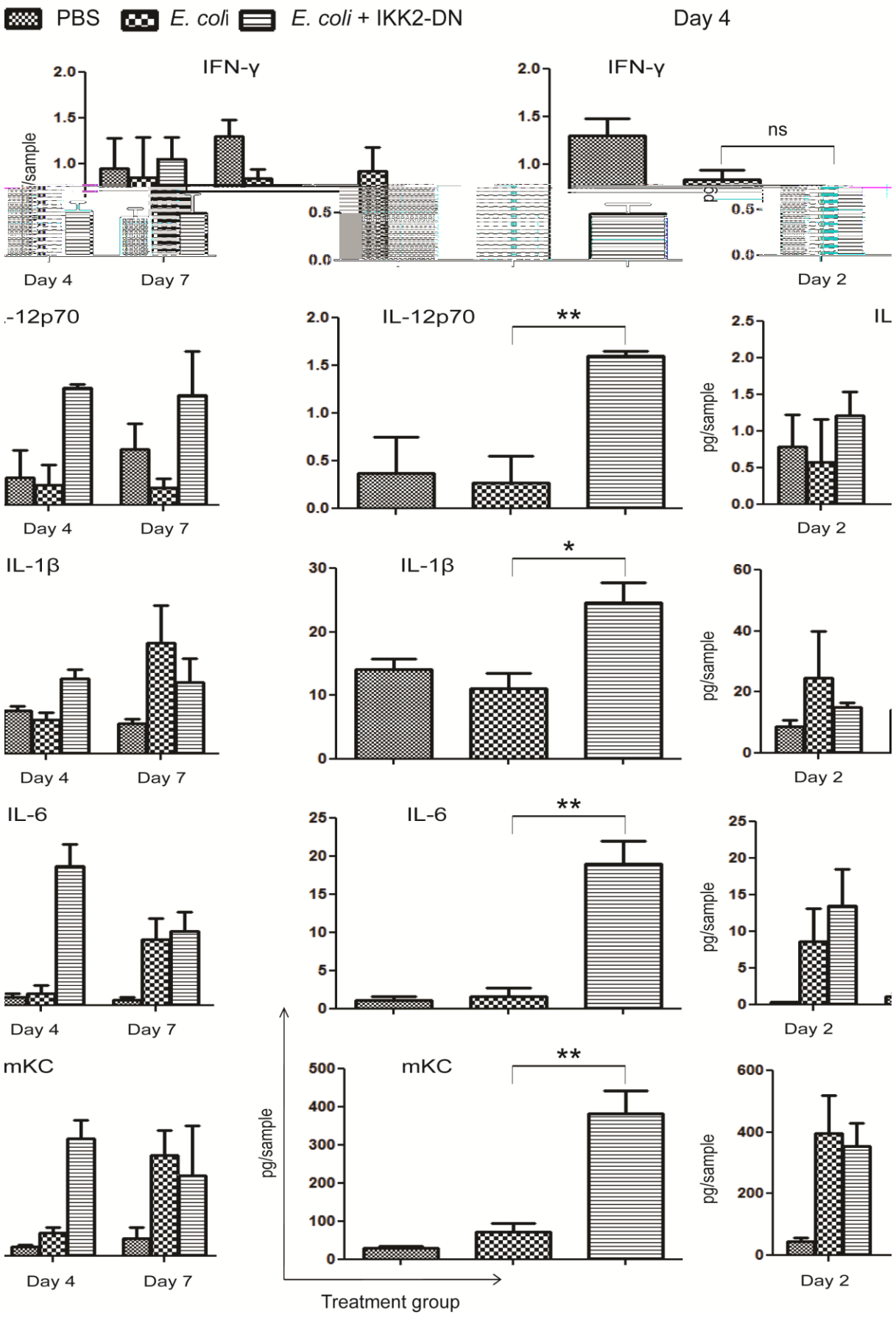
PBS
E. coli
E. coli + IKK2-DN
Day 4
IFN-γ
IFN-γ
ns
pg/sample
Day 4
Day 7
Day 2
-12p70
IL-12p70
**
IL
IL-1β
IL-1β
*
IL-6
IL-6
**
mKC
mKC
**
Treatment group

Figure 4.4 Cytokine profile following bacterial delivery of IKK2-DN. Balb/c mice bearing s.c. CT26 tumours were treated with PBS, *E.coli* or *E.coli* + IKK2-DN plasmid. The cytokine profile within the tumour was determined using a mouse pro-inflammatory multiplex plate. Levels are expressed as the mean +/- SEM for 3 mice per group. The left panel displays individual cytokine profiles at three distinct time points post bacterial administration. The right panel focuses on day four where the greatest change in cytokine levels was detected. Statistics compare the two bacterial treated groups where one group received the therapeutic IKK2-DN gene and the other did not. *indicates $p< 0.05$. **indicates $p< 0.005$. Sample in this context refers to a representative portion of each tumour corresponding to 250 μg of tissue.

in vivo

To determine if this immune response translated to a gross tumour growth response, tumour volume was monitored for 14 days following bacterial administration. No change in tumour volume could be detected between the different groups. At any time point a significant difference in average tumour volume could not be detected between PBS and *E. coli* groups ($p > 0.257$) or between *E. coli* and IKK2-DN groups ($p > 0.327$) (figure 4.5).

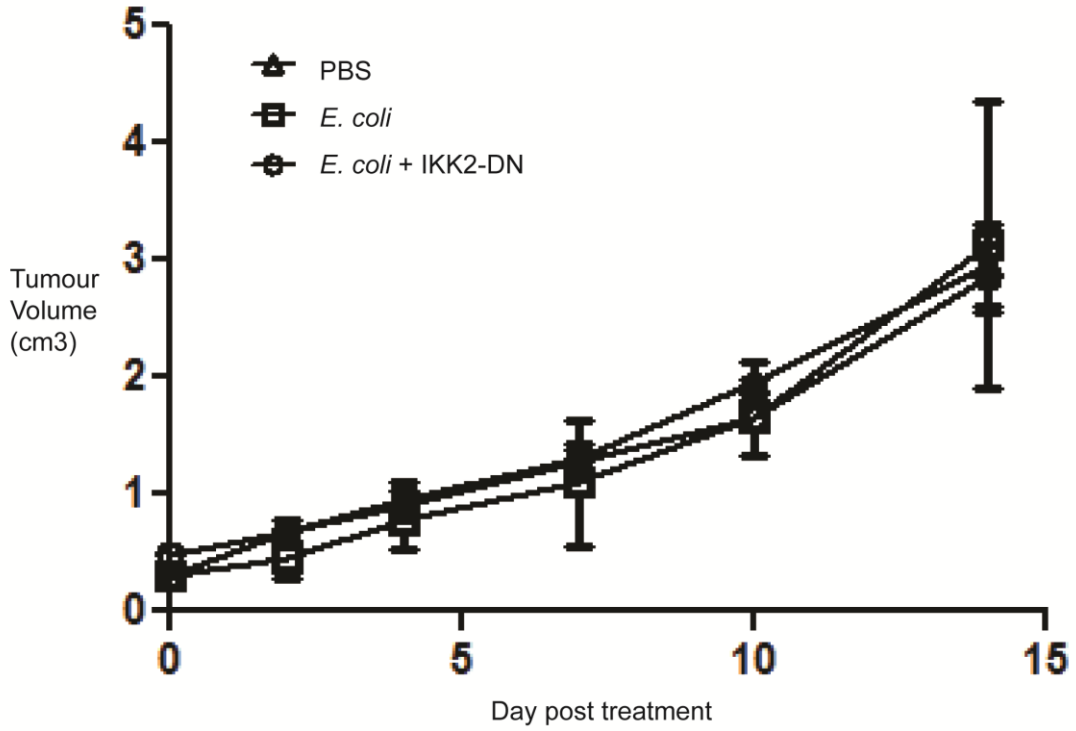

Figure 4.5 The effect of NFκB pathway modulation on tumour growth. Balb/c mice bearing s.c. CT26 tumours were treated with PBS, *E.coli* or *E.coli* carrying an IKK2 dominant negative plasmid. Tumour volumes were determined at various time points and expressed as the mean +/- SEM (n=3 mice per group).

In this study proof of principle was demonstrated for the use of non-invasive bacteria as gene delivery vectors to immune cells. Delivery capability was initially validated *in vitro* using a differentiated human monocyte cell line and this could be replicated *in vivo* using a subcutaneous tumour model. Evidence was also supplied of an enhanced anti-tumour immune response secondary to bacterial delivery of a therapeutic gene – this response can most likely be attributed to an altered macrophage phenotype due to manipulation of the NFkB pathway. It is anticipated that further improvements to this therapeutic approach will pave the way for reduced cancer morbidity and extended survival in pre-clinical models and beyond.

Bacterial vector colonises the tumour; The hypothesis that non-invasive bacteria could be used as gene delivery vehicles to reach phagocytic cells was tested. Proof of principle was demonstrated *in vitro* but before *in vivo* validation the behaviour of non-invasive and non-pathogenic bacteria following intra-tumoural injection was characterised. It was important to know if the bacteria would survive in this environment and if so would they colonise? Figure 4.2 confirmed that the bacteria colonised the tumour. This represented an important issue in designing the therapeutic protocol; colonisation implied that a steady supply of the bacteria and hence the therapeutic would be available to phagocytic cells in the tumour. This suggested that a single bacterial administration would be sufficient and that re-treatment would not be required. That said whole animal imaging did not provide any information as to which regions of the tumour (e.g. viable or non-viable) had been colonised. This represents an important question for further development of a therapeutic protocol (see below). Such a question could be readily answered using immuno-histochemical techniques.

TAM modulation in situ; The work in this study is predicated upon a previous study where the phenotype of macrophages was manipulated *ex vivo* by two different methods[5]; bone marrow-derived macrophages (BMDMs) were harvested from mice carrying a “floxed” *IKK2* allele and transduced with adenovirus carrying a Cre

recombinase to generate IKK2-null macrophages. Alternatively BMDMs or TAMs were infected with adenovirus carrying a dominant-negative inhibitor of IKK2 (IKK2-DN). The therapeutic potential of NFκB manipulation in macrophages was demonstrated in the ability to induce regression of existing tumours. However their approach depended on *ex vivo* transduction of sorted macrophages as no *in vivo* cell-specific delivery mechanism was furthered. Recovery of TAMs from the majority of patient tumours is not feasible but interestingly the same therapeutic benefit could be achieved using syngeneic bone marrow-derived macrophages (BMDMs). It is important to note that IKK2 targeting in BMDMs most likely did not represent re-education as these macrophages are unlikely to be polarised – rather IKK2 targeting prevents their polarisation when they reach the tumour. That said, autologous transplants of *ex-vivo*-modified BMDMs are laborious and technically-demanding and may not be financially feasible.

Hence a strategy to reprogramme TAMs from an M2 to an M1 phenotype *in situ* was devised. This strategy was successful to a certain extent, although only 20% of TAMs were reached. The reason for this relatively low transfection efficiency of the target population may rest in the dissimilar localisation patterns of macrophages and bacteria within the tumour; although still a contentious topic, bacteria are thought to localise to hypoxic regions (reviewed in section 1.3.4); macrophages on the other hand are widely disseminated throughout the tumour mass although TAMs have been found within the hypoxic regions of a wide array of human tumours and experimental models [1]. However if the bacteria localise only to hypoxic regions the remaining non-hypoxic macrophages will remain untransfected.

Selectivity of delivery strategy; Perhaps of greater concern than the low transfection of macrophages is the knowledge that of the 17% of $FLAG^+$ cells only 20% were macrophages. Enumerating a further 10% as macrophages due to non-concordance between the CD68 and F4/80 markers 70% of the cells transfected can still be defined as non-target cells (figure 4.3B). This could be anticipated however; choosing a non-invasive strain of bacteria was predicted to substantially restrict expression of the transgene. Only phagocytic cells which scavenged the bacteria would receive the transgene and large populations of tumour cells and lymphocytes for example would be exempt. However no means to limit phagocytosis or

expression to one particular phagocytic cell type were included. Other phagocytes such as dendritic cells are predicted to constitute the majority of the remaining 70% of $FLAG^+$ cells. How these other phagocytes respond to NFκB pathway modulation remains to be fully elucidated. In the broader sense however it should be noted that reaching these other non-target phagocytic cells may be beneficial in the context of a non-specific activation the immune system within the tumour microenvironment.

Interpretation of the cytokine response; Regardless of the cellular origin, the cytokine profile achieved of increased IL-12, IL-1β, IL-6 and mKC was consistent with a pro-inflammatory phenotype and could be expected to invoke an anti-tumour immune response. IL-12 provokes a T helper 1 immune response and is known to increase the proliferation and cytotoxicity of T and natural killer cells [13]. Indeed over-expression of IL-12 from macrophages introduced with human prostate cancer cells into mice enhanced MHC expression in TAMs with subsequent increased T cell infiltrate and anti-tumour immune response [14]. The IL-1 cytokines, of which IL-1β greatly predominates, upregulate adhesion molecules on vascular endothelial cells and stimulate production of chemotactic cytokines such as IL-8 [15]. This aids in the attachment of lymphocytes to the endothelium where they extravasate and migrate into the tumour mass. IL-1β is also a significant stimulator of IL-6 production by other cells. Although IL-6 is considered a T-helper 2 cytokine it can be involved in tumour rejection by augmenting eosinophil function and promoting B cell antibody production[16]. mKC, also known as CXCL1, is thought to play a role in tumourigenesis and tumour progression[17]. Thus the elevated levels are difficult to rationalise in the context of increased levels of the other anti-tumour cytokines.

Taken together, this cytokine milieu would be expected to promote tumour regression. Indeed induction of a similar pro-inflammatory cytokine response (IL-12^{high} and IL-10^{low}) invoked solely by modulation of the NFκB pathway in macrophages inhibited tumour growth as detected by luminescence in an ID8-luc ovarian model [5]. This benefit could not be rationalised by the transient elevation in nitric oxide production and compelling evidence was advanced to support an IL-12-mediated increase in natural killer cell recruitment.

Demonstration of reduced IL-10 (or indeed TNF-α) levels within the tumour following IKK2-DN delivery would further support a change in immune response.

However, even in the untreated animals IL-10 was below the level of detection (0.3 pg/µl). Therapeutic success would be expected to further reduce IL-10 levels rendering it more difficult to detect IL-10 in treated animals. Inclusion and detection of spiked controls (purified IL-10 protein with tumour homogenate) in the assay protocol rules out the possibility of anything in the tumour homogenate masking and hence blocking the detection of IL-10. Thus the inability to detect IL-10 was not attributable to a technical issue with the assay. Rather it would seem the levels were genuinely low within the tumour. Indeed levels lower than 0.3 pg/µl could be deemed inconsequential in terms of the global immune response.

Limitations of this experimental strategy; While inhibition of tumour growth was observed in the aforementioned study, no change in tumour growth was detected in this study. Explanations for this include the different tumour models employed, the different strategies for monitoring therapeutic responses and the persistence of the different therapeutic strategies investigated;

i) This study used the CT26 s.c. xenograft model which displays a rapid growth rate, providing only a short window of opportunity for therapeutic intervention and monitoring of responses (< 2 weeks). This is in stark contrast to the slow growing ID8 model employed by Hagemann *et al* where this window stretches to nearly 8 weeks.

ii) While an altered cytokine profile was detected tumour volume was the only parameter employed to assess the consequences of this in terms of a global tumour response. This parameter represents a poor indicator of cell viability as live and dying/metabolically inactive cells are measured indiscriminately. FACS analysis of apoptotic markers would be useful to indicate if the therapeutic strategy had invoked cell death. Alternatively measurements of tumour density such as those undertaken clinically by MRI may provide evidence of therapeutic success at a whole tumour level. Furthermore an expanded study, incorporating a survival curve may generate further evidence of therapeutic benefit. Moreover tumour volume was determined rather subjectively using a callipers to measure externally in two dimensions. This approach does not account for subtle changes in tumour depth.

In contrast Hagemann *et al* used the ID8-luc ovarian cancer model where tumour progression/regression was indicated by changes in luminescence. Non-

viable cells were omitted as they were incapable of expressing the *luciferase* gene necessary for light and hence the resolution was likely far superior. Indeed with the advent of newer, more powerful optical imaging technologies as few as 3 luminescent cells can be detected in the live mouse [18]. In the absence of a luminescent CT26 model, the intervening steps in the therapeutic response (between cytokine changes and a macroscopic tumour response) could be followed; as reported an IL-12-driven increase in natural killer cell recruitment could be detected by FACS [5].

iii) Hagemann *et al* introduced genetically manipulated macrophages into the tumour microenvironment. One could reasonably expect that large numbers of these macrophages would remain viable and this is borne out by the cytokine profile which is still skewed towards an M1 phenotype 14 days later. This sustained alteration in the cytokine balance is likely to lead to the recruitment of other immune cells (such as natural killer cells) with a subsequent macroscopic tumour response (as observed). In contrast bacteria were directly administered to the tumour microenvironment to be scavenged by phagocytic cells in this study. Although the bacteria colonised the tumour (figure 4.2) expression of the therapeutic plasmid was short-lived following delivery in this fashion as the FLAG-tagged protein could be detected in macrophages at day 2 but not day 4 after bacterial administration. This is supported by the cytokine data, where, allowing for a time lag between IKK2-DN expression and a cytokine response, a pro-inflammatory response could be detected at day 4 but had subsided by day 7. Thus the transient interruption of NFκB signalling and cytokine alteration may have been insufficient to induce a global tumour response. It is also likely that manipulation of just 20% of TAMs was insufficient to achieve a global tumour response.

The transient expression of the FLAG-tagged IKK2-DN protein and short-term cytokine alteration appears to contradict the colonisation data. However this phenomenon may be rationalised by the contrasting localisation patterns of the bacteria and TAMs – TAMs are predominantly found within viable, well-vascularised compartments while the bacteria are thought to prefer hypoxic regions in the tumour. The bacteria and TAMs may well have been co-localised in a viable region following initial intra-tumoural introduction of the bacteria and this would explain the initial FLAG expression and detection. However it is likely that the

bacteria did not survive long term and/or were scavenged by phagocytic cells in these viable regions and their number was significantly depleted. In contrast bacteria within hypoxic regions thrived and were unhindered by phagocytic cells such as macrophages. It is these bacteria that are likely represented by the colonisation data at later time points (e.g. day 5 in figure 4.2).

Therapeutic improvements; Improvement upon this therapeutic approach could be attempted from many angles. Although not justified based on the colonisation evidence one way of dealing with the transient nature of the intervention would be to retreat perhaps two or three days later with the hope of targeting viable tumour regions and maintaining the altered cytokine profile. As alluded to earlier, the indiscriminate delivery to many phagocytic cell types could prove problematic – this could be overcome by use of a macrophage-specific promoter such as the proximal part of the CD68 promoter [19]. Increasing the potency with which the therapy blocks the NFκB signalling pathway could enhance the pro-inflammatory response and hence the disease outcome. Potency might be improved by use of an RNAi mediator against IKK2 for example.

Conclusion; In summary, the concept presented in this study represents a paradigm shift in the approach to gene therapy. Since its inception as an experimental therapy, gene therapy has exclusively focused on delivery vectors as active agents and explored methodologies to enhance both their efficacy and specificity of delivery to target cells [20]. Although the vector employed in this study has the capability to actively seek out the target organ, once within the hypoxic tumour microenvironment, it can be viewed as a passive delivery agent, prey waiting to be scavenged by predatory phagocytic cells. The stereotypical vector-target cell interaction is reversed with the target cell instigating the engagement. The immune response to a bacterial infection is hijacked for therapeutic gain. To our knowledge,this is the first employment of non-invasive bacteria for gene delivery to cells within tumours. A credible path for clinical translation of therapeutics targeting NFκB signalling in macrophages is offered. Moreover the data presented here support this gene therapy approach for macrophage manipulation in cancer, yet the

approach could easily be extended to other settings such as infectious disease or autoimmune conditions.

1. Lewis CE, Pollard JW. Distinct role of macrophages in different tumor microenvironments. *Cancer Res* 2006; **66:** 605-612.

2. Burke B, Giannoudis A, Corke KP, Gill D, Wells M, Ziegler-Heitbrock L *et al*. Hypoxia-induced gene expression in human macrophages: implications for ischemic tissues and hypoxia-regulated gene therapy. *Am J Pathol* 2003; **163:** 1233-1243.

3. Mitsiades N, Yu WH, Poulaki V, Tsokos M, Stamenkovic I. Matrix metalloproteinase-7-mediated cleavage of Fas ligand protects tumor cells from chemotherapeutic drug cytotoxicity. *Cancer Res* 2001; **61:** 577-581.

4. Fingleton B, Vargo-Gogola T, Crawford HC, Matrisian LM. Matrilysin [MMP-7] expression selects for cells with reduced sensitivity to apoptosis. *Neoplasia* 2001; **3:** 459-468.

5. Hagemann T, Lawrence T, McNeish I, Charles KA, Kulbe H, Thompson RG *et al*. "Re-educating" tumor-associated macrophages by targeting NF-kappaB. *J Exp Med* 2008; **205:** 1261-1268.

6. Hagemann T, Biswas SK, Lawrence T, Sica A, Lewis CE. Regulation of macrophage function in tumors: the multifaceted role of NF-kappaB. *Blood* 2009; **113:** 3139-3146.

7. Oitzinger W, Hofer-Warbinek R, Schmid JA, Koshelnick Y, Binder BR, de Martin R. Adenovirus-mediated expression of a mutant IkappaB kinase 2 inhibits the response of endothelial cells to inflammatory stimuli. *Blood* 2001; **97:** 1611-1617.

8. Perkins ND. Integrating cell-signalling pathways with NF-kappaB and IKK function. *Nat Rev Mol Cell Biol* 2007; **8:** 49-62.

9. Grillot-Courvalin C, Goussard S, Huetz F, Ojcius DM, Courvalin P. Functional gene transfer from intracellular bacteria to mammalian cells. *Nat Biotechnol* 1998; **16:** 862-866.

10. Nauts HC, Fowler GA, Bogatko FH. A review of the influence of bacterial infection and of bacterial products (Coley's toxins) on malignant tumors in man; a critical analysis of 30 inoperable cases treated by Coley's mixed toxins, in which diagnosis was confirmed by microscopic examination selected for special study. *Acta Med Scand Suppl* 1953; **276:** 1-103.

11. Takashiba S, Van Dyke TE, Amar S, Murayama Y, Soskolne AW, Shapira L. Differentiation of monocytes to macrophages primes cells for

lipopolysaccharide stimulation via accumulation of cytoplasmic nuclear factor kappaB. *Infect Immun* 1999; **67:** 5573-5578.

12. Guo H, Zhang J, Inal C, Nguyen T, Fruehauf JH, Keates AC *et al*. Targeting tumor gene by shRNA-expressing Salmonella-mediated RNAi. *Gene therapy* 2011; **18:** 95-105.

13. Trinchieri G. Interleukin-12 and the regulation of innate resistance and adaptive immunity. *Nat Rev Immunol* 2003; **3:** 133-146.

14. Satoh T, Saika T, Ebara S, Kusaka N, Timme TL, Yang G *et al*. Macrophages transduced with an adenoviral vector expressing interleukin 12 suppress tumor growth and metastasis in a preclinical metastatic prostate cancer model. *Cancer Res* 2003; **63:** 7853-7860.

15. Feldmann M. Proinflammatory cytokines. *Cytokine Ref* 2001**:** 291-305.

16. Dranoff G. Cytokines in cancer pathogenesis and cancer therapy. *Nat Rev Cancer* 2004; **4:** 11-22.

17. Dhawan P, Richmond A. Role of CXCL1 in tumorigenesis of melanoma. *J Leukoc Biol* 2002; **72:** 9-18.

18. Rabinovich BA, Ye Y, Etto T, Chen JQ, Levitsky HI, Overwijk WW *et al*. Visualizing fewer than 10 mouse T cells with an enhanced firefly luciferase in immunocompetent mouse models of cancer. *Proc Natl Acad Sci U S A* 2008; **105:** 14342-14346.

19. Levin MC, Lidberg U, Jirholt P, Adiels M, Wramstedt A, Gustafsson K *et al*. Evaluation of macrophage-specific promoters using lentiviral delivery in mice. *Gene Ther*; **19:** 1041-1047.

20. Kay MA. State-of-the-art gene-based therapies: the road ahead. *Nat Rev Genet*; **12:** 316-328.

Overall, the work presented here describes two novel approaches to abrogating the tumour-induced immune suppression that constrains the immune response to a tumour. The work can be subdivided based on the target cell population - regulatory T cells or tumour-associated macrophages;

1) Targeting regulatory T cells

- An *in vitro* mFOXP3 expression assay was developed and optimised
- An endogenous miRNA (miR-31) wasinvestigated as a potential RNAi mediator against mFOXP3 and confirmed to be incapable of silencing this target, in contrast to its human homologue
- Novel RNAi mediators were designed and tested, and two candidates were confirmed to significantly silence mFOXP3
- The best candidate RNAi mediator, in addition to a novel, validated scrambled siRNA, were embedded within DNA-based artificial miRNA cassettes
- The artificial miRNA cassettes were incorporated into lentiviral vector particles
- Lentiviral vector gene delivery parameters were optimised *in vitro*
- Lentiviral-mediated artificial miRNA knockdown was achieved against mFOXP3 *in vitro*
- Lentiviral-mediated gene delivery to a growing B16OVA tumour was established using an *FLuc* reporter gene construct
- The optimal time to target T_{Regs} within this tumour model was identified
- Mice were treated intra-tumourally with lentiviral vector carrying the artificial miRNA and therapeutic responses analysed. However, no significant therapeutic response was observed.

2) Targeting tumour-associated macrophages

- Non-invasive bacteria were shown to mediate ‘spontaneous’ gene delivery to macrophages *in vitro*
- Following intra-tumoural injection, non-invasive bacteria were confirmed to colonise the tumour

- *In vivo* transfection of tumour-associated macrophages by non-invasive bacteria was established and the selectivity of this delivery strategy investigated
- A pro-inflammatory cytokine response was invoked within the tumour following bacterial delivery of a gene targeting the NFκB pathway suggesting 're-education' oftumour-associated macrophages

The outputs from this project provide much justification for continuation of this work. With regard the Treg targeting approach, while no therapeutic response was observed within the limitations of the model utilised, the data generated suggest value in the strategy. The RNAi mediator identified was shown to be highly effective *in vitro,* and it was successfully incorporated into a robust artificial miRNA system. This system minimises any potential issues with intra-cellular processing by the endogenous RNAi machinery. ,It seems likely that the success of the putative therapeutic *in vivo* was undermined at the delivery stage, in terms of insufficient numbers of transduced target cells. Future work might involve utilisation of modified or indeed alternative vector systems. The artificial miRNA system confers flexibility such that the RNAi mediator can readily be incorporated into most vector systems. The future deployment of a targeted lentiviral vector system would improve both the efficiency and specificity with which the RNAi mediator is delivered to the target, regulatory T cell population and would seem especially justified.

Similarly, the targeting of tumour-associated macrophagesfor therapeutic benefit appears very promising. The use of non-invasive bacteria as a delivery vector to reach this population represents a novel concept in gene therapy whereby the vector is passive rather than active. Proof of delivery was demonstrated and an immunological response was identified following delivery of a validated therapeutic gene. Thus, future work would involve refinements to this therapeutic strategy; other bacterial strains could be explored with a view to improving delivery efficiency, a more potent therapeutic could be employed, while incorporation of a macrophage-specific promoter would improve selectivity of gene expression. Any future work would benefit from a more sensitive *in vivo* tumour model such as the ovarian ID8-luc2 model, which features an abundance of TAM. While a cytokine response was

readily detectable using the CT26 tumour model, macroscopic tumour improvements were difficult to discern. A more sensitive model would better guide therapy optimisation. Moreover, the advent of transgenic "reporter mice" coupled to improvements in optical imaging technology promise more powerful *in vivo* models of cancer and its treatment. Of relevance to this work is the emergence of NFκB reporter mice. Adoptive transfer of sorted macrophages from these mice to "non-reporter" animals with growing ID8-luc2 tumours would provide aformidable tool for assessment of the therapeutic response at both the gene (NFκB) and macroscopic tumour level (luminescence) simultaneously.

Another future project might involve combining aspects of both therapeutic strategies explored in this thesis. The recent identification of a population of $FOXP3^{+}$ macrophages within the tumour microenvironment presents this opportunity. Although the contribution of this population to the dynamic interplay between cancer and the immune system is still being characterised, it is suggested that silencing FOXP3 expression would also be beneficial. Thus combining the validated RNAi mediator with the bacterial vector system would seem rational.

Published Abstract:

- **Targeting Regulatory T Cells in Cancer by Selective Delivery of RNA Interference.** Byrne WL, Forde PF, O'Sullivan GC. *Mol Ther* 19 (7) ; 1384 (July 2011)

Poster Presentations:

- **Lentiviral-mediated cell-specific RNA interference in Regulatory T cells.** Byrne WL, Forde PF, O'Sullivan GC. AACR Conference Chicago April 2012
- **Targeting Regulatory T Cells in Cancer.** Byrne WL, Forde PF, O'Sullivan GC. ASGCT Conference Seattle May 2011